C.P. No. 857

ROYAL A...
BEDrОкu.

MINISTRY OF AVIATION

AERONAUTICAL RESEARCH COUNCIL

CURRENT PAPERS

Laminar Boundary Layers with Uniform Fluid Properties Similar Solutions to the Velocity Equations involving Mass Transfer

By

HL. Evans

ROYAL A...
BEDFORD.

Laminar Boundary Layers with Uniform Fluid Properties.
Similar Solutions to the Velocity Equation
involving Mass Transfer*

- By -

H. L. Evans,
Department of Mechanical Engineering,
Imperial College.

SUMMARY

The report discusses solutions to the equation:

$$f''' + ff'' + \beta(1-f'^2) = 0$$

subject to the boundary conditions $f = f_0$, $f' = 0$ at $\eta = 0$ and $f' \to 1$ as $\eta \to \infty$. Numerical solutions are tabulated for wide ranges in the pressure gradient parameter β and mass transfer parameter f_0. Some related topics discussed are (i) the asymptotic behaviour of solutions for intensive mass transfer, (ii) the ranges of β and f_0 for which acceptable solutions exist and (iii) the application of these "similar" solutions to problems involving non-similar flows.

CONTENTS

6./

NOTATION

Where the quantities in the following list possess dimensions, typical units are given in brackets after the definitions.

A quantity occurring in equation (84) but later assumed to be infinite

a_1, a_2, a_3 ..... a_r coefficients in equation (134)

b_1, b_2, b_3 ..... b_r coefficients in equation (136)

C constant occurring in equation (6)

c_1, c_2, c_3 ..... c_r coefficients in equation (137)

d_1, d_2, d_3 ..... d_r coefficients in equation (139)

E_2 correction to a straight-line approximation to relationship between F_2 and λ_2 with zero mass transfer [see equation (121)]

e_1, e_2, e_3 ..... e_r coefficients in equation (141), [see also equation (142)]

f dimensionless stream function defined by equation (10)

f_0 value of f in the fluid at the wall; a measure of the velocity with which mass flows through the wall and called "the mass transfer parameter"; related to the velocity v_0 by equation (14)

f_0'' second derivative of f with respect to η evaluated at the wall; a measure of the shear stress at the wall; also equals $1/\delta_4^*$

$\bar{f}$ real form of f when variables are pure imaginary [see equation (15)]

$\bar{f}_0/$

$\bar{f}_0$ value of $\bar{f}$ at the wall; the mass transfer parameter when variables are pure imaginary and β is small

F_1 rate of growth function for the displacement thickness δ_1, defined by equation (41) with $n = 1$

F_2 rate of growth function for the momentum thickness δ_2, defined in equation (36)

F_4 rate of growth function for the shear thickness δ_4; occurs in equation (44)

g dimensionless stream function for intensive suction defined by equation (128)

g_1, g_2, g_3 .... functions occurring in equation (131)

h dimensionless stream function for intensive blowing defined in equation (143)

h_1, h_2, h_3 .... functions occurring in equation (146)

H_{12} ratio of the displacement thickness to the momentum thickness, equation (33)

H_{21} reciprocal of H_{12}

H_{24} ratio of the momentum thickness to the shear thickness, equation (33)

H_{14} ratio of the displacement thickness to the shear thickness, equation (33)

J function defined by equation (75)

j_1, j_2 quantities occurring in equation (126)

k_0 mass transfer parameter when β is large, related to the velocity v_0 by equation (18)

$\bar{k}_0$ real form of k_0 when variables are pure imaginary, [see equation (28)]

M constant of integration occurring in equation (77) given by equation (79)

Q function defined by equation (65)

q function defined by equation (107)

q_1, q_2, q_3 ..... q_r coefficients occurring in equation (148); note that q_1 in equations (109) and (110) has a different meaning, as it is the value of q at $\phi = 1$

R the quantity $-k_0 y$ occurring in equation (99)

s/

S — function defined by equation (117)

$s_1, s_2, s_3 \ldots s_r$ — coefficients occurring in equation (149); see also equation (150)

t_0, t_k — quantities occurring in equation (151)

$t_1, t_2, t_3 \ldots t_r$ — coefficients in equation (152) whose numerical values are given shortly after that equation

u — component of fluid velocity in the x-direction (ft/h)

u_G — value of u in the main stream (ft/h)

v — component of fluid velocity in the y-direction, taken to be positive when directed outwards, (ft/h)

v_0 — value of v at the wall boundary; the velocity at which mass flows through the wall, (ft/h)

w — dependent variable used in Section 9, equation (154)

x — distance parallel to the wall measured from the start of the boundary layer, (ft)

y — distance perpendicular to the wall measured from the wall towards the main stream

z — independent variable used in Section 9, equation (153).

Greek Symbols

α — independent co-ordinate for intensive suction, equation (127)

β — parameter occurring in equations (6), (12) and (19) related to the magnitude of the main-stream pressure gradient

γ — local dimensionless shear stress used as dependent variable when β is infinite, equation (21)

γ_0 — value of γ at the wall

$\bar{\gamma}$ — real form of γ when variables are pure imaginary, equation (25)

δ — denotes any boundary layer thickness of the velocity layer (ft)

δ_1 — displacement thickness, $= \int_0^\infty \left(1 - \frac{u}{u_G} \right) dy$, (ft)

$\delta_1^*/$

δ_1^* displacement thickness in the similar co-ordinates (η, f), equation (29)

δ_1^{**} displacement thickness in the similar co-ordinates (ξ, θ),

$$= \int_0^\infty (1 - \theta') \, d\xi \ ;$$

δ_2 momentum thickness, $= \displaystyle\int_0^\infty \frac{u}{u_G} \left(1 - \frac{u}{u_G} \right) dy, \quad (ft)$

δ_2^* momentum thickness in the similar co-ordinates (η, f), equation (30)

δ_2^{**} momentum thickness in the similar co-ordinates (ξ, θ),

$$= \int_0^\infty \theta'(1 - \theta') \, d\xi$$

δ_4 shear thickness, $= u_G/(\partial u/\partial y)_0$, (ft)

δ_4^* shear thickness in the similar co-ordinates (η, f), equation (31)

δ_4^{**} shear thickness in the similar co-ordinates (ξ, θ), $= 1/\theta_0''$

ζ independent variable used in Section 5.2, equation (74)

η length co-ordinate used as independent variable when β is small, equation (9)

$\bar{\eta}$ real form of η when variables are pure imaginary, equation (15)

θ stream function used as dependent variable when β is large, equation (17)

$\bar{\theta}$ real form of θ when the variables are pure imaginary

λ_1 pressure gradient parameter relating to the displacement thickness, equation (39)

λ_2 pressure gradient parameter relating to the momentum thickness, equation (35)

λ_4 pressure gradient parameter relating to the shear thickness, equation (43)

ν kinematic viscosity of the fluid, (ft^2/h)

ξ length co-ordinate used as independent variable when β is large, equation (16)

$\bar{\xi}/$

$\bar{\xi}$ real form of ξ when variables are pure imaginary

ϕ dimensionless fluid velocity used as independent variable when β is infinite, equation (21)

$\bar{\phi}$ real form of ϕ when variables are pure imaginary, equation (25)

χ independent co-ordinate for intensive blowing, equation (143)

ψ stream function defined by equation (4)

Subscripts

o   denotes conditions in the fluid close to the wall

i   denotes conditions in the main stream

G   denotes conditions in the main stream

a,b   denote values at two arbitrary points in the fluid

Superscripts

'   denotes differentiation with respect to the independent variable in question, which may be η, ξ, ϕ or one of several others

*   denotes quantities expressed in terms of the similar co-ordinates (η, f)

**   denotes quantities expressed in terms of the similar co-ordinates (ξ, θ).

---

1. Introduction

1.1 The interest in "similar" solutions to the boundary-layer equations

The monograph is concerned with "similar" solutions to the velocity equation of the two-dimensional, laminar boundary layer when the properties of the fluid are uniform throughout the field of flow. Solutions are given for wide ranges in the two parameters which represent the variables:

(i) The pressure gradient in the free stream in a direction parallel to the wall on which the boundary layer exists, and

(ii) The velocity with which some component of the fluid passes through the wall. This velocity may be directed either inwards or outwards and determines the rate of mass transfer through the boundary layer.

The literature contains many discussions of the velocity equation for similar boundary layers, namely equation (12) below, so some justification must be provided for devoting yet another long publication to it. Such justification will be given in various parts of Section 1, which starts here with a brief resumé of the various ways in which the solutions may be applied. In what follows it will be convenient to abbreviate the name of the above two variables simply to "pressure gradient" and "mass transfer rate".

Practical engineering problems requiring the estimation of rates of heat or mass transfer in forced convection frequently cover wide ranges in pressure gradient and mass transfer rate. In order to carry out such calculations, therefore, solutions to the boundary-layer equations must be known for wide ranges in these variables. Yet the similar solutions are the only accurate solutions which are known both at sufficiently small intervals and over sufficiently wide ranges in the variables to be useful for this purpose.

Quite apart from such important practical considerations, however, the study of the similar solutions in the past has contributed greatly to our understanding of the mechanisms which govern the processes of heat, mass and momentum transfer through laminar boundary layers, and this continues to be true today.

It is of interest to note that the similar solutions are also required in several exact series solutions to the partial differential equations of the boundary layer, where they usually appear as the first term; solutions of this kind have been given by Howarth[1], Görtler[2] and Hahnemann[3].

The solutions may, of course, be directly applied in the calculation of rates of heat or mass transfer for fluid flows which satisfy the conditions for similarity. The cases of fluids flowing over wedges form one important group of such flows, although the name "wedge flows" frequently used in this connection is avoided here because it is too restrictive. The name "similar flows" is preferred because it covers a wider range of pressure gradient and includes the wedge flows.

The importance of the similar solutions has greatly increased in recent years because they serve as the foundation for a number of more general methods of boundary-layer analysis used for estimating transfer rates for both

similar and non-similar boundary layers. Although approximate by nature, such general methods can, with due care, give results which are sufficiently accurate for many practical purposes.

1.2 The need for solutions of high accuracy

There has therefore been a considerable and growing interest in the similar solutions, but even so, comparatively few were found in the literature which were accurate and for which the mass transfer parameter was not zero. The solutions known up to a few years ago were collected and summarised by Spalding and Evans[4], although more have appeared since then. A number of solutions of moderate accuracy were known at that time and with the use of interpolation procedures given in that paper, others could be obtained to within a few percent for wide ranges of pressure gradient and mass transfer. The main conclusion, however, was that many more solutions of high accuracy were needed.

Similar solutions to the velocity equation are obtained not only for use in their own right in the ways outlined in Section 1.1, but also so as to solve the b-equation, Spalding and Evans[8], which governs other conserved fluid properties just as the velocity equation governs fluid momentum. Solutions to the b-equation are also required for use in general methods of boundary-layer analysis.

Experience during recent years has amply demonstrated that, in order to make the use of computers worthwhile when solving the b-equation, the accuracy of solutions to the velocity equation which are used must be considerably better than is obtained by interpolation.

On the other hand, there may be objections that the accuracy of the solutions in the present monograph is excessive in view of the fact that the boundary-layer equations are themselves only an approximation to the complete equations of motion of the fluid. While being in some respects sympathetic to this point of view, the author has found from experience that, within reasonable limits, the final digits in any quantity, which have been used during computation and which are known to be correct, should be retained. Even if the author himself has no call to do so, a reader may at some future date wish to apply some mathematical process to the data which requires high accuracy. To cite just one such process, a considerable loss of accuracy would occur, for example, if further solutions were obtained from those in the present monograph by numerical interpolation; the loss of accuracy would be even more severe if an extrapolation process were necessary.

1.3 Accurate solutions already available

Solutions are regarded as accurate in the present context when they are correct to about six digits, an accuracy which is readily achieved with a reasonably advanced digital computer. However, relatively few solutions were known to this accuracy at the time of the survey by Spalding and Evans[4], which included work up to mid 1959.

The case of zero pressure gradient had been adequately treated by Emmons and Leigh[11], including both inward and outward mass transfer; their results were subsequently used to solve the b-equation, Evans[12]. Accurate solutions were also known for zero mass transfer covering a wide, but not the whole, range in pressure gradient; these too were applied to the b-equation, Evans[9]. Because few other solutions of the required accuracy were known, work on the b-equation had to be discontinued at that stage.

Some/

Some other solutions for scattered values of the pressure gradient and mass transfer parameters were also known, but in general these were only accurate to four or five digits. Asymptotic solutions for very intensive suction were also known and the accuracy of these solutions improved with increasing rate of suction.

Discussion of the present state of our knowledge of similar solutions is best left until the end of the monograph. If reference is made to Fig. 29 in Section 9, which shows the known solutions marked on the $F_2 - \lambda_2$ plane (for definitions see notation list), the accurate solutions known when the present programme of work was initiated were therefore as follows:

1. Solutions were known for $\beta = 0$; these lie along the ordinate $\lambda_2 = 0$.

2. The line $(v_0 \delta_2 / \nu) = 0$ was known from its intercept with the separation line up to the line $\beta = 2 \cdot 0$; its intercept with the line $\beta = \pm \infty$ was also known because that point is obtained from an exact analytical solution.

3. The asymptotic solutions for intensive suction were known; on the scale of Fig. 29, however, these were confined to a very small region close to the point $F_2 = \lambda_2 = 0$.

4. Some other isolated points on Fig. 29 were also known; these were largely confined to the quadrant lying between the lines marked $\beta = 0$ and $\beta = 1 \cdot 0$.

1.4 How the report came to be written

To overcome the shortage of accurate similar solutions, therefore, the task of computing others was undertaken and some of the first results were duly published, Evans[1]. Others were obtained in groups at various times using a number of different methods and these too were submitted for publication. When several papers had been accepted, however, it became clear that, since they treated various aspects of a single subject, some advantage would be gained for the reader if they were published together. It was therefore decided to prepare the work for publication in the form of the present report.

While this decision meant that the whole work had to be rearranged, and indeed several sections had to be completely rewritten, it gave a welcome opportunity for clearing up a number of obscurities in the original versions of the papers and for showing more clearly how the various sections are related to each other.

It will be seen in the concluding discussion of the report that there still remain large gaps in the available accurate solutions. However, the preparation of the report is the end of a phase in the work because, for various reasons, further solutions are not likely to be obtained for some time to come.

1.5 Outline of the report

The forms of the velocity equation for similar boundary layers with which the report is concerned are given in Section 2. The pressure gradient parameter β occurs in this equation. In the monograph, the form of the

equation/

equation most frequently given in the literature is used when $|\beta| < 1\cdot0$ but an alternative form is adopted whenever $|\beta| > 1\cdot0$; for $|\beta| = 1$ either form can be used. For the particular case when $|\beta|$ is infinite a simpler form of the equation is deduced and this is found to yield solutions fairly readily.

Section 3 contains formulae which relate the various functions of the velocity layer to each other. They have been used, among other things, to evaluate the required boundary-layer functions from quantities given by the computer.

The variation of the shear stress near the main stream is discussed in Section 4. By examination of the differential equation it is shown that when the dimensionless fluid velocity is close to unity, so that the stream function is virtually a linear function of distance, the local shear stress should diminish rapidly with increasing distance from the wall, although computed solutions frequently do not behave in this way.

A few analytical solutions known to the author are given in Section 5.

The numerical solutions which are the main contribution of the present report are discussed in Section 6. These are divided into several groups, but only brief remarks are made about the first two groups, the first with accelerated flows when β is small and positive, and the second for decelerated flows when β is small and negative. However, more attention is paid to the solutions with separation as well as to those for infinite $|\beta|$.

Section 7 is devoted to a general method of boundary-layer analysis based on the displacement thickness, akin to that based on the momentum thickness by Spalding[5]. For some problems, those involving decelerated flows for example, this method may possess some advantages over others because of the way in which the boundary-layer functions vary under such conditions.

The work described in Section 8 was carried out in co-operation with Miss Joan D. Hayhurst formerly of the Division of Food Preservation, C.S.I.R.O., Australia, and is concerned with conditions of intensive mass transfer and with conditions of no mass transfer when the parameter β is large. For intensive mass transfer, analytical solutions are given in the form of asymptotic series in inverse powers of the mass transfer parameter. The solutions for intensive suction, first given by Watson[6], are complete in the sense that it is possible to evaluate all the boundary-layer functions of interest in the present work. For intensive blowing, however, only a series for the dimensionless wall shear is given. For no mass transfer and large $|\beta|$ a polynomial expansion in inverse powers of β is given; this can be used for positive and negative β, namely for both the real and the imaginary domains relating to equation (12).

In the concluding discussion in Section 9, the present state of our knowledge of similar solutions is summarized and suggestions are made about how the work should be continued. Solutions which can be related to boundary layers exist only as far as certain limiting values in the pressure gradient and mass transfer parameters; with solutions for values beyond these limits the displacement thickness may not be finite or the local shear may not decrease to zero at large distances from the wall. However, there are some unexpected features about the behaviour of solutions near the limiting values for decelerated flows.

2. The Velocity Equation for Similar Boundary Layers

2.1 The partial differential equations

The transformation of the partial differential equations of the uniform-property, laminar boundary layer to similar co-ordinates is given in many places in the literature. Only a brief account is needed here; a more detailed discussion may be found in a recent paper, Evans[7], which also contains references to many earlier papers in the field.

The velocity equation in similar co-ordinates contains a parameter β which may take any real value, positive or negative. Equation (12) below is the form of this equation most frequently encountered in the literature and this can be used, for example to obtain numerical solutions, whenever $|\beta|$ is not large. When $|\beta|$ approaches infinity, however, a different form of the equation must be used, see Evans[7].

These alternative forms of the equation are identical for $\beta = 1$ and it has been realized recently that some advantages are gained by using the more familiar form of the equation only when $|\beta| \leqslant 1$, and adopting the second form, in which the parameter is $1/\beta$, whenever $|\beta| \geqslant 1$. This will be the approach in the present report although only some of the numerical solutions were obtained after the author became aware of the advantages of this approach.

For two-dimensional, laminar flow with uniform properties, the conservation of the momentum of the fluid in the boundary layer is expressed by the equation:

$$u \frac{\partial u}{\partial x} + v \frac{\partial u}{\partial y} = u_G \frac{du_G}{dx} + \nu \frac{\partial^2 u}{\partial y^2} \qquad \dots (1)$$

and the continuity equation is:

$$\frac{\partial u}{\partial x} + \frac{\partial v}{\partial y} = 0. \qquad \dots (2)$$

In these equations:

x = distance measured parallel to the wall on which the boundary layer occurs

y = distance measured perpendicular to the wall towards the free stream

u = local component of fluid velocity in the x-direction

u_G = value of u in the free stream

v = velocity component in the y-direction, and

ν = kinematic viscosity of the fluid, the ratio of the dynamic viscosity μ to the density ρ.

When mass flows through the wall with a velocity v_0, which may be positive, negative or zero, the boundary conditions to be satisfied are:

$y/$

$$y = 0, \quad u = 0, \quad v = v_0 \left.\vphantom{\begin{matrix}a\\b\end{matrix}}\right\} \qquad \ldots (3)$$
$$y \to \infty, \quad u \to u_G,$$

where v_0 is positive when directed outwards from the wall.

The stream function ψ is now defined by:

$$u = \frac{\partial \psi}{\partial y}, \quad v = -\frac{\partial \psi}{\partial x} \qquad \ldots (4)$$

thus automatically satisfying equation (2), so that equation (1) becomes:

$$\frac{\partial \psi}{\partial y} \cdot \frac{\partial^2 \psi}{\partial x \partial y} - \frac{\partial \psi}{\partial x} \cdot \frac{\partial^2 \psi}{\partial y^2} = u_G \frac{du_G}{dx} + \nu \frac{\partial^3 \psi}{\partial y^3} . \qquad \ldots (5)$$

Spalding[5] has shown that this equation possesses similar solutions when u_G, the fluid velocity in the free stream, satisfies the relationship:

$$\frac{du_G}{dx} = C\, u_G^{2(\beta-1)/\beta} \qquad \ldots (6)$$

where C and β are constants.

When the pressure gradient in the free stream is zero, both du_G/dx and β are zero. In the transformation to be given below, equation (6) is not then used directly but is replaced by the following equivalent form:

$$\frac{1}{\beta} \frac{du_G}{dx} = \frac{1}{(2-\beta)} \cdot \frac{u_G}{x} . \qquad \ldots (7)$$

Another relationship required in the transformation, which is also deducible from equation (6) is:

$$\frac{d^2 u_G}{dx^2} \left/ \frac{du_G}{dx} \right. = 2\left(1 - \frac{1}{\beta}\right)\frac{1}{u_G} \cdot \frac{du_G}{dx} \qquad \ldots (8)$$

which is seen to contain the constant β but not the constant C.

2.2 The equation for similar boundary layers when β is small

When the dimensionless length co-ordinate is taken to be:

$$\eta = y\left(\frac{1}{\beta \nu} \frac{du_G}{dx}\right)^{\frac{1}{2}} \qquad \ldots (9)$$

and the dimensionless stream function is defined as:

$$f = \frac{\psi}{u_G}\left(\frac{1}{\beta \nu} \frac{du_G}{dx}\right)^{\frac{1}{2}} \qquad \ldots (10)$$

substitution into equation (5) gives, after some calculation:

$$\left(- \frac{u_G}{\beta} \frac{du_G}{dx} \right) \left\{ f''' + ff'' + \beta(1 - f'^2) \right\} = 0 \qquad \ldots \ (11)$$

where the primes signify differentiation with respect to the independent variable η.

The velocity equation for similar boundary layers to be used when β is small is then:

$$\boxed{f''' + ff'' + \beta(1 - f'^2) = 0} \qquad \ldots \ (12)$$

and the boundary conditions associated with it are:

$$\left. \begin{array}{l} \eta = 0, \quad f = f_0, \quad f' = 0 \\[2mm] \eta \to \infty, \quad f' \to 1, \end{array} \right\} \qquad \ldots \ (13)$$

where f_0 is a constant related to the velocity v_0 with which mass flows through the wall by

$$f_0 = - \frac{v_0}{\left(\dfrac{\nu}{\beta} \dfrac{du_G}{dx} \right)^{\frac{1}{2}}} . \qquad \ldots \ (14)$$

The group in the first bracket in equation (11) is not zero when the velocity gradient du_G/dx is zero because β is also zero then and, by equation (7), the quantity $- \dfrac{1}{\beta} \dfrac{du_G}{dx}$ does not vanish. That group would, however, be zero if β were infinite and, instead of equation (12), we then have equation (19) of the next section.

When β and du_G/dx in equations (9) and (10) are of opposite sign, η and f are pure imaginary. If we let $i = \sqrt{-1}$ we may then define real quantities $\bar{\eta}$ and $\bar{f}$ by:

$$\eta = i\bar{\eta} , \quad f = i\bar{f} \qquad \ldots \ (15)$$

and obtain the form of equation (12) valid for the imaginary domain. This differs from equation (12) in having a negative sign preceding the first term and the equation which connects the parameter $\bar{f}_0$ with the velocity v_0, corresponding to equation (14), does not have a negative sign.

Although equation (12) has been used for obtaining numerical solutions in the real domain even for large β, see for example Evans[7], it became increasingly more difficult to satisfy the main-stream boundary condition as β increased. It is now realised that the form of the equation to be given in the next section would have been more appropriate for $|\beta| > 1 \cdot 0$.

2.3 The velocity equation when β is large

The real and imaginary domains relating to equation (12) are separated by the line along which $|\beta|$ is infinite. To obtain an equation which can be used for any large value of $|\beta|$, in particular for infinite $|\beta|$, we choose a transformation whose effect is to remove β from equations (9) and (10) and from the mass transfer parameter f_0 as defined by equation (14). Our choice of dependent variable also, incidentally, moves the mass transfer parameter from the boundary conditions into the differential equation but, apart from making the boundary conditions independent of the mass transfer rate, this has little effect on the problem.

The co-ordinates to be used were discussed more fully in an earlier paper, Evans[7], and differ only slightly from those already proposed by Spalding[5]. The independent variable, which is a measure of the distance from the wall, is defined as:

$$\xi = y \left(\frac{1}{\nu} \frac{du_G}{dx} \right)^{\frac{1}{2}} \qquad \qquad \dots (16)$$

and the dependent variable is:

$$\theta = \frac{\psi}{u_G} \left(\frac{1}{\nu} \frac{du_G}{dx} \right)^{\frac{1}{2}} + \beta \frac{v_0}{\left(\nu \frac{du_G}{dx} \right)^{\frac{1}{2}}} . \qquad \dots (17)$$

The mass transfer parameter k_0, a constant when the boundary layer is similar, is taken to be:

$$k_0 = - \frac{v_0}{\left(\nu \frac{du_G}{dx} \right)^{\frac{1}{2}}} . \qquad \qquad \dots (18)$$

The ordinary differential equation which governs the variation of θ as a function of ξ is then:

$$\boxed{\theta''' + \frac{1}{\beta} \theta\theta'' + k_0\theta'' + 1 - \theta'^2 = 0} \qquad \dots (19)$$

with the boundary conditions:

$$\left. \begin{array}{l} \xi = 0, \quad \theta = \theta' = 0 \\[2mm] \xi \to \infty, \quad \theta' \to 1. \end{array} \right\} \qquad \dots (20)$$

The primes in equations (19) and (20) denote differentiation with respect to ξ.

Equation (19) is the form of the velocity equation for similar boundary layers suitable for use when β is large; instead of β itself, however, it would clearly be more appropriate to treat $1/\beta$ as the parameter in this equation.

Examination of equations (16), (17) and (18) shows that the variables ξ and θ and the parameter k_0 are real for accelerated flows, when du_G/dx is positive, and pure imaginary for decelerated flows. Apart from the fact that it can be used when the parameter β is large, there may be a further advantage in using equation (19) in preference to equation (12), for not only does the line $\beta = 0$ divide accelerated flows from decelerated flows, but in the (ξ, θ) co-ordinates it also separates the real from the imaginary domains.

2.4 A simpler form of the velocity equation for infinite β

When β is infinite the second term in equation (19) is zero, so that the equation does not contain the stream function θ explicitly. A simpler form of the equation can then be obtained by taking the fluid velocity $d\theta/d\xi$ as independent variable and the local dimensionless shear $d^2\theta/d\xi^2$ as dependent variable. If we give these quantities the symbols

$$\phi = \frac{d\theta}{d\xi}, \qquad y = \frac{d^2\theta}{d\xi^2}, \qquad \qquad \ldots (21)$$

note that

$$\frac{d^3\theta}{d\xi^3} = y \frac{dy}{d\phi}, \qquad \qquad \ldots (22)$$

substitute into equation (19) and divide by y, we get

$$\boxed{\frac{dy}{d\phi} + k_0 + \frac{(1 - \phi^2)}{y} = 0.} \qquad \qquad \ldots (23)$$

In this equation the independent variable is confined to the fixed narrow range $0 \leqslant \phi \leqslant 1$ and the main-stream boundary condition is

$$\phi = 1, \qquad y = 0. \qquad \qquad \ldots (24)$$

Solutions to equation (23) satisfying (24) will later be given for a wide range in the mass transfer parameter k_0.

Equation (23) holds for accelerated flows when du_G/dx is positive so that ξ, θ and k_0 are real quantities. For decelerated flows du_G/dx is negative and ξ, θ and k_0 are pure imaginary; again we write $\xi = i\bar{\xi}$, $\theta = i\bar{\theta}$ and $k_0 = i\bar{k}_0$, where barred quantities are real, and define new real variables:

$$\bar{\phi} = \frac{d\bar{\theta}}{d\bar{\xi}}, \qquad \bar{y} = \frac{d^2\bar{\theta}}{d\bar{\xi}^2} \qquad \qquad \ldots (25)$$

we get for equation (23):

$$\boxed{-\frac{d\bar{y}}{d\bar{\phi}} + \bar{k}_0 + \frac{(1 - \bar{\phi}^2)}{\bar{y}} = 0} \qquad \qquad \ldots (26)$$

with/

with the boundary condition:

$$\bar{\phi} = 1, \qquad \bar{\gamma} = 0. \qquad \qquad \ldots (27)$$

The relationship between the mass transfer parameter $\bar{k}_0$ and the velocity v_0 is:

$$\bar{k}_0 = \frac{v_0}{\left(\nu \dfrac{du_G}{dx} \right)^{\frac{1}{2}}} . \qquad \qquad \ldots (28)$$

Solutions to equation (26) satisfying (27) will later be given for a range of negative $\bar{k}_0$ satisfying $|\bar{k}_0| \geqslant 8^{\frac{1}{2}}$.

3. Relationships between Functions of the Velocity Boundary Layer

3.1 General formulae

Relationships between functions of the velocity boundary layer will now be given. These have been used in preparing the accompanying tables of numerical solutions and are to be referred to frequently in later sections of the monograph. Most of the formulae will simply be stated, because they are well known and have been derived and discussed in earlier publications, Spalding[5], Spalding and Evans[4], Evans[7].

Three boundary-layer thicknesses are first defined in terms of the similar co-ordinates (η, f) of Section 2.2:

$$\text{Displacement thickness:} \qquad \delta_1^* = \int_0^\infty \left(1 - \frac{df}{d\eta} \right) d\eta, \qquad \ldots (29)$$

$$\text{Momentum thickness:} \qquad \delta_2^* = \int_0^\infty \frac{df}{d\eta} \left(1 - \frac{df}{d\eta} \right) d\eta, \qquad \ldots (30)$$

$$\text{Shear thickness:} \qquad \delta_4^* = \frac{1}{f_0''} . \qquad \ldots (31)$$

Other boundary-layer thicknesses can also be defined but we shall confine our attention to these three. If a double asterisk is used to denote the same thicknesses in terms of the co-ordinates (ξ, θ) of Section 2.3, since $\eta = \xi/\beta^{\frac{1}{2}}$ it follows that $\delta_n^{**} = \delta_n^* \beta^{\frac{1}{2}}$, where the subscript n may be 1, 2 or 4.

These thicknesses are related to each other by the exact relationship:

$$\frac{1}{\delta_4^*} \equiv f_0'' = f_0 + \beta \delta_1^* + (1 + \beta) \delta_2^* \qquad \ldots (32)$$

which is obtained by integrating equation (12) from $\eta = 0$ to $\eta = \infty$.

We also define the following thickness ratios:

$$H_{21} = \frac{1}{H_{12}} = \frac{\delta_2^*}{\delta_1^*} , \qquad H_{24} = f_0'' \, \delta_2^* , \qquad H_{14} = f_0'' \, \delta_1^* \qquad \ldots (33)$$

and the following mass transfer parameters:

$$\frac{v_0 \delta_1}{\nu} = -f_0 \delta_1^* , \qquad \frac{v_0 \delta_2}{\nu} = -f_0 \delta_2^* , \qquad \frac{\nu}{v_0 \delta_4} = -\frac{f_0''}{f_0} \qquad \ldots (34)$$

where the last is written as the reciprocal of a mass transfer parameter because this is the form usually adopted.

It should be noted that because the ratio H_{12} varies over wide ranges, even becoming infinite for flow over a flat plate with a sufficiently high rate of blowing, in the present work its reciprocal H_{21} is often used instead, because over most of the region of interest this remains within fairly narrow limits. It will still be convenient, however, to use H_{12} in some formulae and H_{21} in others.

In terms of the functions just defined, for similar boundary layers the pressure gradient parameter relating to the momentum thickness is:

$$\lambda_2 \equiv \frac{\delta_2^2}{\nu} \frac{du_G}{dx} \simeq \frac{H_{24} + \dfrac{v_0 \delta_2}{\nu}}{1 + \dfrac{1}{\beta} + H_{12}} \qquad \ldots (35)$$

and F_2, the function which gives the rate of growth of δ_2 in the x-direction, is

$$F_2 \equiv \frac{u_G}{\nu} \frac{d\delta_2^2}{dx} = 2 \left(\frac{1}{\beta} - 1 \right) \frac{H_{24} + \dfrac{v_0 \delta_2}{\nu}}{1 + \dfrac{1}{\beta} + H_{12}} . \qquad \ldots (36)$$

It may be of interest to note that only $1/\beta$, but not β itself, occurs in these equations; it is also possible to write the fundamental equation (6) and the definitions in equations (9) and (10) in terms of $1/\beta$ only.

For any uniform-property, laminar boundary layer, whether or not the conditions for similarity hold, the integral momentum equation also applies. In the present notation this is:

$$\boxed{ \frac{1}{2} \frac{u_G}{\nu} \frac{d\delta_2^2}{dx} + (2 + H_{12}) \frac{\delta_2^2}{\nu} \frac{du_G}{dx} = H_{24} + \frac{v_0 \delta_2}{\nu} } \qquad \ldots (37)$$

3.2 Relationships in terms of an arbitrary thickness δ_n

Equations (35), (36) and (37) contain the pressure gradient parameter and the rate of growth function applicable to the momentum thickness δ_2. We

shall now derive a more general form of these equations which apply to an arbitrary thickness δ_n, where the subscript n may be 1, 2 or 4.

When equation (32) is multiplied throughout by the arbitrary thickness δ_n^* the result can be written in the form:

$$H_{n4} = -\frac{v_0 \delta_n}{\nu} + \beta(\delta_n^*)^2 \left\{ H_{1n} + \left(1 + \frac{1}{\beta}\right) H_{2n} \right\} \qquad \ldots (38)$$

where the definitions of the thickness ratios H_{n4}, H_{1n} and H_{2n} are obvious. Since $\lambda_n = \beta(\delta_n^*)^2$ we have:

$$\lambda_n \equiv \frac{\delta_n^2}{\nu} \frac{du_G}{dx} = \frac{H_{n4} + (v_0 \delta_n / \nu)}{\left(1 + \frac{1}{\beta}\right) H_{2n} + H_{1n}} \qquad \ldots (39)$$

which clearly corresponds to equation (35).

Now, for a similar boundary layer λ_n is a constant so that, using equation (6), we get:

$$\frac{\delta_n^2}{\nu} u_G^{2(\beta-1)\beta} = \text{constant.} \qquad \ldots (40)$$

This equation is now differentiated with respect to the distance x, divided by $u_G^{(\beta-2)/\beta}$ and rearranged to give the result:

$$F_n \equiv \frac{u_G}{\nu} \frac{d\delta_n^2}{dx} = 2\left(\frac{1}{\beta} - 1\right) \frac{\delta_n^2}{\nu} \frac{du_G}{dx} \qquad \ldots (41)$$

which is the more general form of equation (36).

To get the more general form of equation (37) we eliminate the parameter β between equations (39) and (41), the result being

$$\frac{1}{2} \frac{u_G}{\nu} \frac{d\delta_n^2}{dx} + (2 + H_{12}) \frac{\delta_n^2}{\nu} \frac{du_G}{dx} = \frac{1}{H_{2n}} \left\{ H_{n4} + \frac{v_0 \delta_n}{\nu} \right\}. \qquad \ldots (42)$$

While this equation appears to be a more general form of the integral momentum equation which applies to any boundary layer, it is in fact applicable only to similar layers as may be suspected from the way in which it was derived.*

In many branches of study concerned with laminar boundary layers, in aeronautical engineering for example, interest is concentrated on the force which the moving fluid exerts on the wall, or more precisely on the stagnant fluid located very close to the wall but which may be regarded as forming part of the wall. The following equations in terms of the shear thickness may therefore prove useful in such studies:

$$\lambda_4 \equiv \frac{\delta_4^2}{\nu} \frac{du_G}{dx} = \frac{1 + (v_0 \delta_4 / \nu)}{\left(1 + \frac{1}{\beta}\right) H_{24} + H_{14}} \qquad \ldots (43)$$

and/

---

*In general the term $-\frac{1}{2} \frac{u_G}{\nu} \delta_2^2 \frac{d}{dx}\left(\frac{\delta_n^2}{\delta_2^2}\right)$ also occurs on the left but for "similar" flows this term is zero because the ratio (δ_n/δ_2) is a constant in the x-direction.

and

$$\frac{1}{2} \frac{u_G}{\nu} \frac{d\delta_4^2}{dx} + (2 + H_{12}) \frac{\delta_4^2}{\nu} \frac{du_G}{dx} = \frac{1}{H_{24}} \left(1 + \frac{v_0 \delta_4}{\nu} \right). \qquad \text{... (44)}$$

3.3 The special case $\beta = -1$

When $\beta = -1$ and $n = 1$ equation (39) reduces to:

$$\lambda_1 = H_{14} + \frac{v_0 \delta_1}{\nu}. \qquad \text{... (45)}$$

It is also known, Evans[7], that for this value of β the following relationship holds:

$$\delta_1^{*2} - 2f_0 \delta_1^* + 2 = 0 \qquad \text{... (46)}$$

which, with different symbols, is:

$$-\lambda_1 + 2 \frac{v_0 \delta_1}{\nu} + 2 = 0. \qquad \text{... (47)}$$

It then follows from equations (45) and (47) that:

$$H_{14} = \frac{\lambda_1}{2} + 1 \qquad \text{... (48)}$$

$$\frac{v_0 \delta_1}{\nu} = \frac{\lambda_1}{2} - 1. \qquad \text{... (49)}$$

Equation (48) means that when the thickness ratio H_{14} is plotted as a function of the pressure gradient parameter λ_1, points for $\beta = -1$ fall on a straight line of slope $\frac{1}{2}$. This line passes through the separation point, when $H_{14} = 0$ and $\lambda_1 = -2$, as well as the point corresponding to an infinite rate of suction, when $H_{14} = 1$ and $\lambda_1 = 0$. From equation (49) the mass transfer parameter $v_0 \delta_1/\nu$ can also be given exactly along this line; it ranges from -2 at separation to -1 for very intensive suction.

4. Variation of Shear Stress near the Main Stream

4.1 Specification of the beginning of main-stream flow

On examination of accurate numerical solutions to equation (12) with boundary conditions (13), the stream function and its first two derivatives are seen to approach their main-stream values in the following order. The stream function f first becomes a linear function of η, at least to the number of significant digits to which the solutions are quoted, then the velocity f' becomes unity, and lastly f'', which is a measure of the local shear, becomes negligibly small. We shall now consider the behaviour of f'' when f and f' are close to their main-stream values because it is often given incorrectly by computers.

The following are three possible ways of specifying the beginning of main-stream flow: (a) the point where f is linear, say, to six significant

digits, (b) where f' is unity to six digits or (c) where f" is zero in the sixth decimal place. The smallest value of η at which main-stream conditions are satisfied depends not only on which of these criteria is used but also on the number of significant digits to which quantities are specified. The present work was planned so as to obtain numerical tables of the stream function and its first derivative, which gives the dimensionless fluid velocity, correct to at least six digits.

This number of digits may seem excessive for boundary-layer theory, which itself contains a number of approximations. The extra effort required to obtain this accuracy, however, has been amply justified by the advantages gained when the solutions were applied, for example, in obtaining other solutions by interpolation or in evaluating quantities associated with the b-boundary layer.

Of the three conditions listed above, (c) is the most acceptable on physical grounds. Unfortunately, however, computed values of f" are considerably less reliable near the main stream than either f or f' , so that for present purposes we shall use condition (b) instead; this turns out to be a less stringent condition than (c). We shall therefore regard main-stream flow as beginning where the dimensionless velocity f' becomes unity to six significant digits.

4.2 A formula for the decrease of wall shear

When equation (12) is divided throughout by f" it becomes:

$$\frac{f'''}{f''} + f + \beta(1 + f')\frac{(1 - f')}{f''} = 0. \qquad \ldots (50)$$

This operation is allowed because, although f" tends to zero for very large η, it is still finite at the point we have chosen as the beginning of main-stream flow.

Now, as the main stream is approached, f' → 1 and f" → 0, so the factor (1 - f')/f" in the last term is indeterminate. It is quite reasonable to <u>assume</u>, however, that it tends to the same value as the ratio -f"/f"'.

The assumption holds only if f' approaches unity rapidly enough. It does not hold, for example, if $(1 - f') \sim A/\eta$, where A is a constant. When $(1 - f') \sim De^{-p\eta^2}$, where D and p are constants, the assumption is reasonably accurate provided $p\eta^2 \gg 1$. For this second example we get by differentiation $f" \sim 2Dp\eta e^{-p\eta^2}$, which means that f" decreases fairly rapidly as η increases. By inserting the above assumption into equation (50), however, we shall see that f" decreases even more rapidly than this for accurate solutions to equation (12).

The above argument can, of course, be presented in the reverse order, namely that if the assumption we are making is valid, then f' must tend to unity fairly rapidly.

By inserting the assumption into equation (50) we then get as the degenerate form of the equation near the main stream:

$$\frac{f'''}{f''} + f - 2\beta\frac{f''}{f'''} = 0. \qquad \ldots (51)$$

This/

This is a quadratic in the quantity:

$$\frac{f'''}{f''} = \frac{d}{d\eta}\left\{\ell n \ f''\right\} \qquad \qquad \dots (52)$$

with the solution:

$$\frac{d}{d\eta}\left\{\ell n \ f''\right\} = -\frac{f}{2} - \tfrac{1}{2}(f^2 + 8\beta)^{\frac{1}{2}} \qquad \qquad \dots (53)$$

where a negative sign is chosen to precede the radical because f'' must be very small and must diminish as η increases.

Now equation (51), and therefore equation (53) also, applies only where the stream function is virtually a linear function of η having the form:

$$f = \eta + f_0 - \delta_1^* . \qquad \qquad \dots (54)$$

The differential sign outside the brackets on the left of equation (53) may therefore be replaced by differentiation with respect to f giving:

$$\frac{d}{df}\left\{\ell n \ f''\right\} = -\frac{f}{2} - \tfrac{1}{2}(f^2 + 8\beta)^{\frac{1}{2}} . \qquad \qquad \dots (55)$$

When this is integrated between the two points $\eta = a$ and $\eta = b$, straightforward calculation leads to the following expression for the ratio of the shear stresses at these two points:

$$\frac{f''_b}{f''_a} = \left\{\frac{f_a + (f_a^2 + 8\beta)^{\frac{1}{2}}}{f_b + (f_b^2 + 8\beta)^{\frac{1}{2}}}\right\}^{2\beta} \exp. - \left\{f_b^2 + f_b(f_b^2 + 8\beta)^{\frac{1}{2}} - f_a^2 - f_a(f_a^2 + 8\beta)^{\frac{1}{2}}\right\} \quad (56)$$

where the subscripts denote values of the functions at the points "a" and "b".

Since f is a linear function of η, it is possible to express the right-hand side of equation (56) in terms of η, but the expression then becomes rather unwieldy and less convenient to use than the above form in terms of the stream function f.

4.3 The special case of zero pressure gradient

The case when the free stream pressure gradient is zero displays some special features, as may be seen by putting $\beta = 0$ into equation (53). This gives:

$$\frac{d}{d\eta}(\ell n \ f'') + f = 0 \qquad \qquad \dots (57)$$

which is, in fact, an exact form of equation (12) for $\beta = 0$.

From this we may deduce:*

$$\ell n \left(\frac{f_0''}{f''} \right) = \int_0^\eta f \, d\eta \qquad \ldots (58)$$

which means that the ratio of the shear stresses at any two points "a" and "b" is exactly:

$$\frac{f_a''}{f_b''} = \exp. - \left\{ \int_{\eta_b}^{\eta_a} f \, d\eta \right\}_{\beta = 0} . \qquad \ldots (59)$$

When both "a" and "b" are in the region where f satisfies equation (54) this ratio becomes:

$$\frac{f_a''}{f_b''} = \exp. - \frac{1}{2} \left\{ (\eta_a - \eta_b)(\eta_a + \eta_b + 2(f_0 - \delta_1^*)) \right\}$$

$$= \exp. - \frac{1}{2} (f_a^2 - f_b^2). \qquad \ldots (60)$$

4.4 Comparison with computed values

It is found from experience that much of the error in computed values of f'' at large η arises from uncertainty in the starting value f_0''. Even when the latter is known accurately to six digits, it is possible for uncertainty in the seventh digit to give rise to appreciable error in f'' after, say 100 steps in the integration process.

A good test of the validity of equation (56), therefore, is to examine the numerical solution for $\beta = -1$ with $f_0 = 1 \cdot 5$. Since we then have $f_0'' = (f_0^2 - 2)^{\frac{1}{2}} = 0 \cdot 5$ exactly, see Evans[7], there is no error in the starting value. Two lines in this solution at the point where the velocity becomes unity to six digits are:

η	f	f'	f''
5·0	5·50000	0·999999	$0 \cdot 622240 \times 10^{-5}$
5·2	5·70000	1·00000	$0 \cdot 218575 \times 10^{-5}$

To four digits the ratio of the second to the first of these values of f'' is $0 \cdot 1182$; when calculated from equation (56) it is $0 \cdot 1189$. The difference

between/

---

*It follows from equation (58) that when $\beta = 0$ the reciprocal of the wall gradient for the b-boundary layer, Spalding and Evans[8], is:

$$\frac{B}{b_0'} = \int_0^\infty (f''/f_0'')^\sigma \, d\eta$$

which, for $\sigma = 1$, immediately reduces to the well-known result $(b_0'/B) = f_0''$.

between these values occurs in the ninth decimal place where, in fact, the error produced by rounding-off within the computer is having some effect.

Equation (56) was also tested at the beginning of free-stream flow with several other numerical solutions and, as expected, the agreement depended on the accuracy of such solutions.

The final conclusion was that the equation gives an adequate description of the rate of decrease of local shear near the main stream and that its accuracy improves with increasing distance from the wall. It can, to some extent, be used as a test of the accuracy of numerical solutions.

5. Some Analytical Solutions

Most solutions to equation (12) with boundary conditions (13) known to the author were obtained by numerical integration. There are, however, a few analytical solutions which are useful both for checking the accuracy of numerical methods of integration and to serve as exact points of reference when plotting relationships between various boundary-layer functions. The solutions for intensive mass transfer to be discussed in Section 8 are also analytical solutions; they become asymptotically exact as the rate of mass transfer increases.

5.1 Two solutions for infinite β

(a) Solution for $k_0 = 0$

When β is infinite and $k_0 = 0$, equation (19) reduces to three terms and the solution which satisfies equation (20) is:

$$\theta = \xi + 2\sqrt{3} - 3\sqrt{2} \tanh \left\{ \frac{\xi}{\sqrt{2}} + \tanh^{-1} \sqrt{\frac{2}{3}} \right\}. \qquad \ldots (61)$$

By differentiation the dimensionless forward velocity of the fluid is:

$$\frac{d\theta}{d\xi} = 3 \tanh^2 \left\{ \frac{\xi}{\sqrt{2}} + \tanh^{-1} \sqrt{\frac{2}{3}} \right\} - 2. \qquad \ldots (62)$$

This solution was discussed more fully in an earlier paper, Evans[9]. In the co-ordinates of Section 2.4 it is:

$$y = \sqrt{\frac{2}{3}} (2 + \phi)^{\frac{1}{2}} (1 - \phi) \qquad \ldots (63)$$

which will be referred to later.

(b) Solution for $k_0 = -5/\sqrt{3}$

When β is infinite and $k_0 = -5/\sqrt{3}$, equation (19) with boundary conditions (20) has the solution:

$$\theta = \xi - \sqrt{3} \left\{ \ell n \, 2 - \sqrt{2} \right\} + 2\sqrt{3} \left\{ \ell n \, Q - \frac{1}{Q} \right\} \qquad \ldots (64)$$

where:/

where:

$$Q = 1 + (\sqrt{2} - 1)e^{-\xi/\sqrt{3}}. \qquad \ldots (65)$$

In this case the dimensionless velocity of the fluid in the boundary layer is given by:

$$\frac{d\theta}{d\xi} = \left(\frac{2}{Q^2} - 1 \right) \qquad \ldots (66)$$

and the boundary-layer functions have the following exact values:

$$k_0 = -5/\sqrt{3}$$

$$\left(\frac{d^2\theta}{d\xi^2} \right)_{\xi=0} = \sqrt{\frac{2}{3}} (\sqrt{2} - 1)$$

$$\delta_1^{**} = \int_0^\infty \left(1 - \frac{d\theta}{d\xi} \right) d\xi = \sqrt{3}(2 - \sqrt{2} + \ell n\ 2)$$

$$\delta_2^{**} = \int_0^\infty \frac{d\theta}{d\xi} \left(1 - \frac{d\theta}{d\xi} \right) d\xi = \frac{1}{\sqrt{3}} (1 + 2\sqrt{2} - 3\,\ell n\ 2)$$

$$\frac{v_0 \delta_2}{\nu} = \frac{5}{3} (1 + 2\sqrt{2} - 3\,\ell n\ 2).$$

Other functions can readily be evaluated from these.

In the co-ordinates of Section 2.4 this solution is:

$$y = \sqrt{\frac{2}{3}} (\phi + 1) \left\{ \sqrt{2} - (\phi + 1)^{\frac{1}{2}} \right\}. \qquad \ldots (67)$$

5.2 The solution for $\beta = -1$ with decelerated flow by Thwaites

Thwaites[10] has given an analytical solution to equation (12) for $\beta = -1$ with decelerated flow, namely when the variables are real. His co-ordinates, however, differ greatly from those used here and an awkward transformation is needed in order to make use of his solution. It was therefore thought worth while expressing the solution directly in terms· of the present formulation of similar boundary layers.

The value $\beta = -1$ also displays some special features in the imaginary domain but no analytical solution has yet been found for that case.

It was shown in an earlier discussion, Evans[7], that when $\beta = -1$ equation (12) reduces to the following first-order equation:

$$2 \frac{df}{d\eta} + f^2 = f_0^2 + 2f_0''\eta + \eta^2 \qquad \text{...} \quad (68)$$

and the solution must satisfy the boundary condition:

$$\frac{df}{d\eta} \to 1 \qquad \text{exponentially as} \quad \eta \to \infty. \qquad \text{...} \quad (69)$$

It was also shown that, following from the definition of the displacement thickness given in equation (29), the following relationships apply for $\beta = -1$:

$$f_0'' = f_0 - \delta_1^* \qquad \text{...} \quad (70)$$

$$\delta_1^* = f_0 + (f_0^2 - 2)^{\frac{1}{2}} \qquad \text{...} \quad (71)$$

so that

$$f_0'' = (f_0^2 - 2)^{\frac{1}{2}}. \qquad \text{...} \quad (72)$$

These relationships are now used to rewrite equation (68) as:

$$\frac{df}{d\eta} + \left(\frac{f}{\sqrt{2}} \right)^2 - \left(\frac{\eta + f_0''}{\sqrt{2}} \right)^2 - 1 = 0. \qquad \text{...} \quad (73)$$

If a new independent variable:

$$\zeta = (\eta + f_0'')/\sqrt{2} \qquad \text{...} \quad (74)$$

and a new dependent variable:

$$J = \frac{1}{\left(\dfrac{f}{\sqrt{2}} - \zeta \right)} \qquad \text{...} \quad (75)$$

are chosen, equation (73) becomes:

$$\frac{dJ}{d\zeta} - 2\zeta J - 1 = 0. \qquad \text{...} \quad (76)$$

This has the solution:

$$J = \frac{\sqrt{\pi}}{2} e^{\zeta^2} \left\{ \text{erf } \zeta + M \right\} \qquad \text{...} \quad (77)$$

where M is a constant of integration. When transformed back to the (η, f) variables this is:

$$f = \eta + f_0'' + \left(\frac{8}{\pi} \right)^{\frac{1}{2}} \frac{\exp. - \{(\eta + f_0'')/\sqrt{2}\}^2}{\{\text{erf}[(\eta + f_0'')/\sqrt{2}] + M\}} . \qquad \text{...} \quad (78)$$

Since $f = f_0$ at $\eta = 0$ we get for the constant M:

$$M = \left(\frac{8}{\pi}\right)^{\frac{1}{2}} \frac{\exp. - \{f_0''/\sqrt{2}\}^2}{(f_0 - f_0'')} - \text{erf}\left(\frac{f_0''}{\sqrt{2}}\right) \qquad \ldots (79)$$

so that the stream function f finally becomes:

$$f = \eta + f_0'' + \frac{(f_0 - f_0'')\exp.\{(f_0''/\sqrt{2})^2 - (\eta + f_0'')^2/2\}}{1 + (\pi/8)^{\frac{1}{2}}(f_0 - f_0'')\{\text{erf}[(\eta + f_0'')/\sqrt{2}] - \text{erf}(f_0''/\sqrt{2})\}\exp.(f_0''/\sqrt{2})^2} \qquad (80)$$

For the particular case of separation with this value of β the values $f_0 = \sqrt{2}$ and $f_0'' = 0$ are substituted into this to give:

$$f = \eta + \frac{\sqrt{2}\, e^{-\eta^2/2}}{1 + (\sqrt{\pi}/2)\text{erf}(\eta/\sqrt{2})} . \qquad \ldots (81)$$

Equation (80) gives f as a function of η and f_0 only, because, by equation (72), f_0'' is a simple function of f_0. For any specified value of the parameter f_0, therefore, the stream function f can be calculated exactly for any η using numerical tables of the exponential and error functions.

The formula for the fluid velocity, obtained from equation (80) by differentiation with respect to η, is rather complicated. To obtain numerical values for the velocity it is easier to evaluate f from equation (80) and then substitute this into equation (68).

The local dimensionless shear may then be evaluated from the formula:

$$f'' = f_0'' + \eta - ff' \qquad \ldots (82)$$

which is obtained from equation (68) by differentiation.

6. Numerical Solutions

6.1 A few general remarks

The numerical tables reproduced in the present report contain only boundary-layer thicknesses, thickness ratios, pressure gradient parameters and rate of growth functions, all for specific values of the parameter β and the appropriate mass transfer parameter. Tables giving the stream function f and its derivatives f' and f'', and for many solutions the function

$$\int_0^\eta f \, d\eta,$$

at regular intervals in the independent variable η, were also obtained and prepared for publication; the relevant tables for β infinite gave values of the local shear y at intervals in the dimensionless velocity ϕ. However, it was decided to omit such tables from this report because they would have occupied an excessive amount of space.

In spite of their absence it will be necessary to refer to these tables when we later discuss the behaviour of solutions, and readers who find that they require copies should send a request to the author.

The/

The solutions are divided into four main groups, each of which was computed at a different time; a fifth group contains some miscellaneous results. Each of these groups will be discussed separately.

The method used for integrating equation (12) was described in an earlier paper, Evans[7]; the method of integrating equation (23) will be discussed in Section 6.5. A programme was prepared for integrating equation (12) numerically on a computer using a Runge-Kutta process. Only approximate values of the wall shear f_0'' were known but these were improved by iteration; the criterion to be satisfied was that, as η increased, the velocity f' should tend to unity from below and remain there for a number of intervals in η.

When f_0'' was known accurately enough for specified values of β and f_0, the data were fed into the computer which then supplied values of f'', f' and f, and for the more recent solutions $\int_0^\eta f\, d\eta$, at regular intervals in the independent variable η starting at $\eta = 0$. This integral is required in solutions of the b-equation.

The displacement thickness δ_1^* was evaluated from the value of the stream function f in the main stream making use of equation (54), and the momentum thickness was obtained by using equation (32).

For $\beta = -1$, however, equation (32) could not be used, so that δ_2^* had to be calculated from the values of f' given by the computer. Instead of evaluating $\int_0^\infty f'(1-f')\,d\eta$ directly, however, the following method was found to be more accurate. The momentum thickness was written as:

$$\delta_2^* = f(\infty) - f_0 - \int_0^\infty f'^2\, d\eta \qquad \text{... (83)}$$

where $f(\infty)$ denotes the value of the stream function given by the computer at some suitable point in the main stream, and the last term on the right was evaluated by the application of Simpson's rule. This method is more accurate because the region near the wall, where f' changes most rapidly, makes only a small contribution to the third term in equation (83).

When the values of f_0'', δ_1^* and δ_2^* were known for specified values of the parameters β and f_0, other functions could be evaluated from the formulae given in Section 3.

6.2 Group I - Solutions for accelerated flows; β positive

The solutions in this group were the first to be computed and are generally less accurate than others which were obtained after gaining some experience with the computer. The solutions are given in sets, each set covering a range of f_0 for a fixed value of β.

Even for these less accurate solutions, most of the boundary-layer functions quoted are known to five significant digits, in many cases six. In the tables of the stream function and its derivatives, both f and f' were accurate

to/

to six digits but the local dimensionless shear f'', although accurate near the wall, gradually became less accurate as the main stream was approached. Instead of diminishing in an exponential manner as given by equation (56), as η increased values of f'' decreased to between 1×10^{-5} and 1×10^{-7}, depending on the solution in question, and changed very little thereafter.

When equation (56) was used as a test of the accuracy of the solutions, it was found that this decreased slightly as both β and f_0 increased in magnitude, remembering that both these parameters are positive for all but a few of these solutions. This decrease in accuracy occurred because as β and f_0 increased the boundary layer became thinner and the size of the interval of integration, which varied little from one solution to the next, introduced some error; for $\beta = 0.5$ and 1.0, however, the interval was smaller and these solutions are consequently more accurate.

6.3 Group II - Solutions for decelerated flows: β negative

For this second group of solutions the free-stream flow is decelerated, the parameter β being in the range $-1 \leqslant \beta \leqslant 0$. For each value of β the mass transfer parameter ranges from the largest value $f_0 = 3.0$ to a lower limit which is that required to give separation, and which therefore depends on the value of β. The separation solutions will be discussed in the next section.

Very few accurate solutions were previously known in this region, although some of low accuracy were cited by Spalding and Evans[4]. The solutions previously found for $\beta = 0$ by Emmons and Leigh[11] were in different similar co-ordinates from those used here and therefore did not include the present numerical values of the parameter f_0; a new set of solutions was therefore obtained for this case.

The solutions in this group are more accurate than most of those in the first group but even with these the function f'' still does not vanish in the main stream but, as with less accurate solutions, decreases to a small value and remains there.

6.4 Group III - Solutions with separation

For the purposes of the present discussion a separation solution to equation (12) with boundary conditions (13) is defined as one for which the dimensionless wall shear f_0'' is zero. We do not consider whether, or under what conditions, such solutions can be associated with fluid flows which involve separation. The present report is restricted to solutions with values of f_0'' which are positive or zero, that is to solutions up to and including separation. Solutions with negative values of f_0'' correspond to back-flow of fluid near the wall, as occurs after separation has taken place; these are not considered here.

Before discussing the present set of separation solutions, however, we consider the particular case of zero main-stream pressure gradient $(\beta = 0)$ which displays some unusual features and is of some importance in boundary-layer theory; the separation solution for this value of β was obtained by Emmons and Leigh[11].

6.4.1 The separation solution for $\beta = 0$

As fluid flows outwards through the wall, the value of the dimensionless wall shear f_0'' diminishes. Emmons and Leigh[11] found that when the pressure gradient in the free stream was zero, the wall shear f_0'' vanished when the

blowing rate had only reached the relatively low value $f_0 = -0 \cdot 875745$. Because of a misinterpretation by the present author, however, the thickness ratio H_{12} for this solution was given incorrectly in the paper by Spalding and Evans[4]. Quantities appearing in the following discussion contain a numerical factor because the present similar co-ordinates differ from those used by Emmons and Leigh.

Their solution was obtained by giving the wall shear $\sqrt{8} f_0''$ the value 1×10^{-7} and adjusting the mass transfer parameter $\sqrt{2} f_0$ so as to satisfy the boundary condition in the main stream, the origin of the independent co-ordinate $\eta/\sqrt{2}$ being at the wall. This operation gave a value of $\eta/\sqrt{2}$ at which the stream function $\sqrt{2} f$ vanished. The origin of the independent variable $\eta/\sqrt{2}$ was then shifted to this point and the published tables were given in terms of this modified co-ordinate.

The tables gave values of the stream function and its first three derivatives for the range -10 to +4 in this modified independent co-ordinate, which was negative towards the wall and positive towards the main stream. The value of H_{12} given by Spalding and Evans[4] was incorrect because the point at which this co-ordinate was -10 was thought to be at the wall, and this was not the case.

Some remarks by Emmons and Leigh are relevant here. They say that (a) the differential equation gives $f' = 0$ for all finite η, (b) for this blowing rate the boundary layer is "blown away" and (c) the modified independent co-ordinate is measured from a point in the boundary region and extends to infinity in both directions. While it is not clear how their displacement of co-ordinates could have been infinite in practice, it must nevertheless have been very much larger than the value 10 assumed when preparing the tables given by Spalding and Evans.

If the magnitude of the shift be denoted by A, which in the absence of more precise information we shall have to assume to be infinite, in terms of quantities given by Emmons and Leigh the displacement thickness is:

$$\delta_1^* = A\sqrt{2} + 4\sqrt{2} - 1 \cdot 23849\sqrt{2} - 7 \cdot 47114\sqrt{2}$$

$$= A\sqrt{2} - 0 \cdot 501785. \qquad \qquad \dots (84)$$

When $\beta = 0$ equation (32) gives the momentum thickness exactly in terms of f_0 and f_0'', and when the latter is zero we have:

$$\delta_2^* = -f_0 = 1 \cdot 23849/\sqrt{2} = 0 \cdot 875745. \qquad \dots (85)$$

Therefore if A is infinite, δ_1^* is also infinite and H_{21} is zero.

The fact that the displacement thickness is infinite also explains why the Nusselt number is always zero for this solution whatever the value of the Prandtl/Schmidt number of the fluid, see Evans[12].

The solutions found by Emmons and Leigh in the neighbourhood of separation are plotted in Figs. 1 and 2. In Fig. 1 the reciprocal of the mass transfer parameter $(v_0 \delta_1/\nu)$ is plotted along the abscissa and the ratio H_{21} along the ordinate so that the separation solution is at the origin. The part of the curve shown as a broken line represents interpolation between the last two solutions given by Emmons and Leigh. The ratio of the ordinate to the

abscissa in this figure is clearly $(v_0\delta_2/\nu)$ and this has the value 0.766929 for the separation solution. Because the curvature of the line in this figure is quite small and because its slope must approach the value 0.766929 at the origin, the error introduced by graphical interpolation is believed to be very small.

Fig. 2 is a better version of part of Fig. 3 of the paper by Spalding and Evans[4] where the mass transfer parameter is now $(v_0\delta_2/\nu)$. The shape of the interpolated portion of this figure was obtained by transferring points from Fig. 1, the value of $(v_0\delta_2/\nu)$ being simply the ratio of the ordinate to the abscissa in that figure.

The lengths of the interpolated portions of Figs. 1 and 2 show the need for further exact solutions between the last two given by Emmons and Leigh although, as stated by those authors, there would appear to be no more solutions beyond the separation point.

This last remark raises an important question, namely, what meaning, if any, should be attached to points beyond the separation point along the line $\lambda_2 = 0$ in the $F_2 - \lambda_2$ plane. In the papers by Spalding and Evans[4] and Evans[7] lines of constant $(v_0\delta_2/\nu)$, when this mass transfer parameter was large, were drawn so as to cut the F_2 axis where:

$$F_2 = 2\frac{v_0\delta_2}{\nu}. \qquad \ldots (86)$$

This relationship comes from the integral momentum equation which, when equation (37) is multiplied throughout by H_{21}, may be written

$$\frac{H_{21}}{2}.F_2 + (2H_{21} + 1)\lambda_2 = H_{21}.H_{24} + H_{21}.\frac{v_0\delta_2}{\nu}. \qquad \ldots (87)$$

When β is sufficiently small, but necessarily positive, the second term on the left is small because λ_2 is small, and when the blowing rate is sufficiently high the first term on the right also becomes very small as both H_{21} and H_{24} are small. For the limiting case of very small β and very intensive blowing, therefore, equation (87) reduces to equation (86).

It should be noted, however, that to apply equation (86) to the case $\beta = 0$, while being useful for plotting lines in the $F_2 - \lambda_2$ plane, contradicts a fundamental tenet of boundary-layer theory, for an infinite displacement thickness is contrary to the assumption that viscous effects are confined to a thin region near the wall boundary.

6.4.2 The present separation solutions

Most of the present separation solutions are new, the various boundary-layer functions for which are given in Table III where three solutions taken from the literature are also included; the first of these three is that for zero main stream pressure gradient discussed in Section 6.4.1. The author also possesses tables, copies of which can be obtained on request, which give the distribution with η of the stream function, its first two derivatives and the function $\int_0^\eta f\,d\eta$. A slightly more accurate solution than was previously available

was also computed for the well-known case of separation with no mass transfer. For this solution f_0 and f_0'' were zero and β was varied so as to satisfy the main-stream boundary condition; for the other solutions, however, the value of β was fixed and the parameter f_0 was varied. The first estimates of the accurate values of f_0 were taken from the paper by Terrill[14], although only a few of the smaller values of β were considered in that paper.

For large negative β the solutions were not very sensitive to changes in f_0; for $\beta = -10$ and -18, for example, four figure accuracy in f_0 was sufficient to satisfy the main-stream boundary condition. The computer, of course, integrated equation (12) although, as has already been pointed out, equation (19) with imaginary variables would have been more suitable for large negative β. Since f_0 was not known very accurately for such values of β, equation (32) was not used to evaluate δ_2^* from δ_1^* but each thickness was calculated separately by applying Simpson's rule to the numerical values of f'. This is why many functions in Table III are specified more accurately than f_0.

The variation of F_2 with λ_2 is shown in Fig. 3 and of F_1 with λ_1 in Fig. 4. As the pressure gradient increases in the negative direction each of the growth functions F_2 and F_1 decreases to a minimum and then increases again when the pressure gradient becomes large and negative. We may see how this is brought about in the case of F_2 by considering the integral momentum equation; a similar argument applies to F_1.

When the wall shear is zero we get from equation (37):

$$\tfrac{1}{2} F_2 = \frac{v_0 \delta_2}{\nu} - (2 + H_{12})\lambda_2. \qquad \ldots (88)$$

A glance at Table III shows that, except very close to the case $\beta = 0$, the ratio H_{12} varies very little along the separation line, being of the order of 3 or 4. We may therefore regard the first term on the right of equation (88) as giving the effect of mass transfer on F_2 and the second term the effect of pressure gradient. Clearly, blowing increases F_2 and suction decreases it and an increasing negative λ_2 (we are not here concerned with positive λ_2) also increases F_2.

F_2 therefore has a minimum value at the point where a balance is achieved between the effects of mass transfer and pressure gradient. For low rates of suction the mass transfer rate is the dominating influence but for intensive suction, although $(v_0 \delta_2/\nu)$ is itself becoming large, the pressure gradient increases more rapidly and soon becomes the controlling influence on F_2.

6.5 Group IV - Solutions for infinite β

It is often useful to relate similar solutions to the velocity equation for β in the range $0 \leqslant \beta \leqslant 2 \cdot 0$ to boundary layers which occur when fluid flows over a wedge of angle $\beta\pi$. The solutions for infinite β may also be better understood and appreciated if they can be related to suitable free-stream flows.

When β is infinite, equation (6) becomes:

$$\frac{du_G}{dx} = C u_G^2 \qquad \ldots (89)$$

and,/

and, since u_G^2 is necessarily positive, the two cases of infinite β are distinguished by the sign of the constant C.

When C is positive the free stream is accelerated. A suitable accelerated flow for which u_G satisfies equation (89) is illustrated in Fig. 5 where fluid flows into a point sink at A_1. If two stream-lines are regarded as porous walls, this first case of infinite β may be associated with the boundary layers occurring along such walls. On physical grounds a boundary layer would be expected in this case at whatever rate mass is transferred inwards or outwards through the porous wall.

When C is negative, the free stream is decelerated and a suitable flow is illustrated in Fig. 6, where fluid flows out of a point source at A_2 and the boundary layer again occurs along porous walls which follow two stream-lines. A boundary layer would be expected in this case only for a sufficiently high rate of suction.

6.5.1 Solutions given in the literature

Throughout the present section we shall use the simpler co-ordinates applicable to infinite β given in Section 2.4.

Two exact analytical solutions for infinite β when the variables are real were given above in Section 5.1; these are expressed in the co-ordinates of Section 2.4, in equation (63) for $k_0 = 0$ and equation (67) for $k_0 = 5/\sqrt{3}$.

Hartree[15] gave numerical tables of solutions to a different problem and included what is, in effect, the solution to equation (23) for $k_0 = -3 \cdot 0$. The various functions were tabulated to four digits and agree in the fourth place with the same solution given in the present paper.

Thwaites[16] also obtained solutions to what is virtually equation (26) with boundary condition (27) for several values of the mass transfer parameter $\bar{k}_0$, although his formulation differs considerably from that used here. He also discussed the unusual behaviour of the solutions, particularly when approaching the limiting case $\bar{k}_0 = -8^{\frac{1}{2}}$.

The most extensive set of solutions taking into account mass transfer were given by Holstein[17]. Other solutions obtained by interpolation between Holstein's results were given by Spalding and Evans[4] and the accuracy of the interpolations was improved and their range extended by Evans[7]. The last reference also contained asymptotic values of thickness ratios for intensive suction and intensive blowing, agreeing largely with those given earlier by Pretsch[18].

Before going on to discuss the numerical solutions for infinite β, we shall first of all see that for this case the equation is such that considerable progress can be made analytically by assuming a series solution.

6.5.2 Series expansions for the dependent variable

(a) When the variables are real

It will be convenient in this section to let primes denote differentiation with respect to ϕ, or in (b) with respect to $\bar{\phi}$.

The aim is to express y as a series in increasing powers of $(\phi - 1)$. Such a series, to be referred to in later sections, can give values of y to

high accuracy by including sufficient terms but was not used to obtain the tabulated solutions, although a similar type of expansion to be given in Section 6.5.2(c) was used to start numerical integrations on a computer for intensive blowing. Thwaites[10] suggested essentially the same approach for solving equation (26) with boundary condition (27).

Since $y = 0$ at $\phi = 1$ the required series takes the form:

$$y = \sum_{m=1}^{\infty} \frac{y_1^{(m)}}{m!} (\phi - 1)^m \qquad \ldots (90)$$

in which $y_1^{(m)}$ is the mth derivative of y with respect to ϕ evaluated at $\phi = 1$. These derivatives may be obtained from equation (23) by differentiation as follows:

Writing the equation as:

$$yy' + k_0 y + (1 - \phi^2) = 0 \qquad \ldots (91)$$

we get by differentiation:

$$yy'' + (y' + k_0)y' - 2\phi = 0. \qquad \ldots (92)$$

By inserting the boundary condition $y = 0$ at $\phi = 1$ into this we get a quadratic in y_1' with the solution:

$$y_1' = -\tfrac{1}{2}\{k_0 + (k_0^2 + 8)^{\frac{1}{2}}\}. \qquad \ldots (93)$$

A positive sign is chosen to precede the radical because solutions must be such that y diminishes with increasing ϕ very close to $\phi = 1$ whatever the value of k_0; in other words y_1' must always be negative.

By differentiation we also get from equation (92):

$$yy''' + (3y' + k_0)y'' - 2 = 0 \qquad \ldots (94)$$

which, when evaluated at $\phi = 1$, gives for the second derivative:

$$y_1'' = \frac{2}{(3y_1' + k_0)}. \qquad \ldots (95)$$

The higher derivatives are obtained by repeated differentiation of equation (94) and evaluating the resulting expressions at $\phi = 1$. This gives the following general formula for the mth derivative at $\phi = 1$:

$$\{(m + 1)y_1' + k_0\}y_1^{(m)} + \binom{m}{2}y_1'' y_1^{(m-1)} + \binom{m}{3}y_1''' y_1^{(m-2)} + \ldots + \binom{m}{m-1}y_1^{(m-1)}y_1'' = 0$$

$$\ldots (96)$$

where $m \geqslant 3$ and the symbol $\binom{m}{n}$ signifies $\dfrac{m!}{(m - n)!\, n!}$.

By its nature the series is most accurate near $\phi = 1$ and least accurate at $\phi = 0$. When sufficient terms are taken it gives high accuracy;

for $k_0 = 0$, for example, even at $\phi = 0$, ten terms give $y_0 = 1 \cdot 15470085$, the exact value being $1 \cdot 15470054$. Since the accuracy improves as k_0 increases in the positive direction, this agreement is highly satisfactory. The accuracy diminishes, however, as k_0 increases in the negative direction, becoming very poor for large negative k_0; it is then necessary to use the series expansion to be given in Section 6.5.2(c).

(b) When the variables are pure imaginary

By applying the same procedure to equation (26) we get:

$$\overline{y_1}' = \tfrac{1}{2} \{\overline{k_0} - (\overline{k_0^2} - 8)^{\frac{1}{2}}\} \qquad \ldots (97)$$

where primes now signify differentiation with respect to $\overline{\phi}$ and a negative sign is chosen to precede the radical because $\overline{y_1}'$ must always be negative and must increase as $\overline{k_0}$, which is negative, increases in magnitude. Clearly, $\overline{y_1}'$ will be real only when $|\overline{k_0}| \geqslant 8^{\frac{1}{2}}$, so setting a limit to the useful solutions to equation (26).

The second derivative of $\overline{y}$ at $\overline{\phi} = 1$ is:

$$\overline{y_1} = - \frac{2}{(3\overline{y_1}' - \overline{k_0})} \qquad \ldots (98)$$

the sign being negative whereas y_1'' was positive. The derivatives of higher order are the same as the corresponding derivatives for y, except that all quantities are written with "bars" and the parameter k_0 is replaced by $-\overline{k_0}$.

(c) A series for intensive blowing when the variables are real

Only equation (23), but not equation (26), need be considered for intensive blowing.

As the rate of blowing increases the local shear y decreases and for intensive blowing y is small throughout the boundary layer. We therefore introduce a scaling factor into equation (23) by taking $R = -k_0 y$ as the dependent variable, the negative sign serving to keep the new variable positive because k_0 is large and negative. When divided by $-k_0$ the equation then becomes:

$$\frac{1}{k_0^2} \frac{dR}{d\phi} - 1 + \frac{(1 - \phi^2)}{R} = 0. \qquad \ldots (99)$$

When k_0^2 is very large the first term is negligible and R becomes approximately:

$$R = (1 - \phi^2) \qquad \ldots (100)$$

so that y has the asymptotic form:

$$y = - \frac{1}{k_0} (1 - \phi^2). \qquad \ldots (101)$$

Fig. 9/

Fig. 9 shows the way in which accurate numerical solutions approach this asymptote as k_0 becomes large and negative.

It is readily shown that if y is given by equation (101) the displacement thickness is:

$$\delta_1^{**} = \int_0^1 \frac{(1 - \phi)}{y} \, d\phi = -k_0 \ell n \, 2 \qquad \qquad \ldots (102)$$

and the momentum thickness is:

$$\delta_2^{**} = \int_0^1 \frac{\phi(1 - \phi)}{y} \, d\phi = -k_0 (1 - \ell n \, 2). \qquad \ldots (103)$$

Since equation (101) also gives $y_0 = -1/k_0$, the thickness ratios tend to the following values for intensive blowing:

$$H_{21} = (1 - \ell n \, 2)/\ell n \, 2 \qquad \qquad \ldots (104)$$

$$H_{24} = (1 - \ell n \, 2) \qquad \qquad \ldots (105)$$

$$H_{14} = \ell n \, 2. \qquad \qquad \ldots (106)$$

These were discussed more fully in an earlier paper, Evans[7].

The series expansion in equation (90) becomes more accurate as the rate of suction increases. We now derive a series of the same kind whose accuracy improves as the rate of blowing increases.

Consider the variable:

$$q = - \frac{k_0}{(1 - \phi^2)} \, y. \qquad \qquad \ldots (107)$$

Since y approximates to equation (101) for large negative k_0, q is then close to unity throughout the boundary layer. When we substitute equation (107) into equation (23) and rearrange, the differential equation for q becomes:

$$(\phi^2 - 1)qq' + 2\phi q^2 + k_0^2(q - 1) = 0 \qquad \qquad \ldots (108)$$

the prime signifying differentiation with respect to ϕ.

We now seek a series for q with the form:

$$q = q_1 + \sum_{m=1}^{\infty} \frac{q_1^{(m)}}{m!} (\phi - 1)^m \qquad \qquad \ldots (109)$$

where $q_1^{(m)}$ is the mth derivative of q at $\phi = 1$.

When equation (108) is evaluated at $\phi = 1$ we get a quadratic for q_1 with the solution:

$$q_1 = -\frac{k_0}{4}\left\{k_0 + (k_0^2 + 8)^{\frac{1}{2}}\right\}. \qquad \dots (110)$$

The derivatives $q_1^{(m)}$ are then obtained by repeated differentiation of equation (108) and putting $\phi = 1$. The first two are:

$$q_1' = -2q_1^2/(6q_1 + k_0^2) \qquad \dots (111)$$

and

$$q_1'' = -2 . \frac{(5q_1 q_1' + 4q_1'^2)}{8q_1 + k_0^2} . \qquad \dots (112)$$

When k_0 is large and negative the series for q converges much more rapidly than the corresponding series for y.

6.5.3 Obtaining solutions by numerical methods

Although the effect of mass transfer on equations (23) and (26) is simply to add a constant to the equations, it was still not possible to obtain analytical solutions as simple as those given in Section 5.1. It was therefore necessary to use numerical methods to obtain solutions. The first such solutions were obtained with a desk calculator but, while these were quite accurate, it soon became clear that a computer would be more economical to obtain the large number of solutions needed to cover the full ranges of the parameter k_0 and $\bar{k}_0$ adequately.

By starting the integration at $\phi = 1$ and proceeding towards $\phi = 0$ the problem is to solve a single, first-order differential equation with known starting values. This is a straightforward problem for solution by a step-by-step Runge-Kutta process on a computer. This process is too well known to warrant discussion here, but some information about it may be obtained from an earlier paper, Evans[7].

When the computing programme was ready, it was necessary to choose an interval of integration which was small enough to give the required accuracy. This was done by trial and error, the interval being decreased successively until the process gave a value of y_0 which agreed in the last digit with the value obtained using the previous interval. The exact solution for $k_0 = 0$ was referred to frequently at this stage. For computing the final solutions the intervals, expressed as powers of 2 because the computer worked in binary numbers, were:

	Range of $\bar{k}_0$ and k_0	Integration interval $\Delta\phi$
Equation (26)	$-8^{\frac{1}{2}}$ to -4	2^{-12}
	$-4\cdot5$ to -10	2^{-11}
	-12 to -20	2^{-9}
Equation (23)	20 to 0	2^{-7}
	$-0\cdot1$ to $-1\cdot0$	2^{-8}
	$-1\cdot2$ to $-4\cdot0$	2^{-11}

For intensive blowing with equation (23), namely when k_0 was beyond $-4\cdot0$, a different approach was used. For these solutions it was found that high accuracy was required at the beginning of the range of integration. As the

computer would have taken a long time to obtain such accuracy, values of y were first found at $\phi = 0 \cdot 96875$ using the series expansion for intensive blowing given above in Section 6.5.1(c). These values were then fed into the computer which continued the integration process using an interval $\Delta\phi = 2^{-11}$.

6.5.4 Calculating boundary-layer functions from numerical tables of y

The computer gave numerical values of y at regular intervals in ϕ. For the displacement thickness δ_1^{**} the integrand is $(1-\phi)/y$, whose value at $\phi = 1$ is readily shown to be $-1/y_1'$, and is known exactly in terms of k_0 from equation (93). Simpson's rule was therefore used in a straightforward manner to evaluate δ_1^{**}. The method was very accurate as the integrand varied only slightly over the range of integration, and even this small variation decreased with increasing suction; for intensive suction the integrand was, in fact, almost a constant.

The momentum thickness δ_2^{**} was then obtained from the relationship:

$$\delta_2^{**} = y_0 - k_0 - \delta_1^{**} \qquad \qquad \dots (113)$$

which is obtained by integrating equation (23) over the range $0 \leqslant \phi \leqslant 1$, the quantity y_0, the value of y at $\phi = 0$, being given by the computer.

The formulae for calculating the other boundary-layer functions listed in Section 3.1 from the quantities k_0, y_0, δ_1^{**} and δ_2^{**} are quite straightforward and need not be listed here. Some care should, however, be taken with the signs of some functions when the variables are pure imaginary.

6.5.5 Tables of solutions

Values of most of the boundary-layer functions defined in Section 3.1 are given in Tables IV-1, IV-2 and IV-3, which are arranged so that functions including and to the right of H_{21} are in order of magnitude running from one table to the next. The rate of growth functions F_2 and F_1 are not given as they are simply $2\lambda_2$ and $2\lambda_1$, respectively, although in some cases care should be taken with the signs.

Tables giving values of y (or $\bar{y}$) as functions ϕ (or $\bar{\phi}$) have also been drawn up but are not included in the present report. The author can make copies available on request.

The intervals in the parameters k_0 and $\bar{k}_0$ are small near zero and $-8^{\frac{1}{2}}$ respectively, because boundary-layer functions then vary rapidly as these parameters change. The values of k_0 and $\bar{k}_0$ were chosen so that the tables could be checked by differencing, as well as to facilitate interpolation between these accurate solutions at some future date.

The number of significant digits retained is at least seven, often more; some reasons for retaining so many digits were given in Section 1.2.

6.5.6 Accuracy of the solutions

The values of y given by the computer at an interval of $\Delta\phi = 2^{-5}$ are believed to be accurate to within a few units in the eighth decimal place. The main source of error in the data of Tables IV-1, IV-2 and IV-3, therefore, is the use of Simpson's rule in evaluating δ_1^{**}. The error due to this is approximately:

$$\text{Error} \sim \frac{\Delta\phi}{90} \times \text{fourth difference of } (1-\phi)/\gamma.$$

The solutions for which $(1-\phi)/\gamma$ had its greatest curvature were tested by this formula and it was concluded that, at worst, the error should not be large in the sixth digit, although most of the functions should be considerably more accurate than this, probably being correct to within three units in the seventh digit.

Tables IV-1, IV-2 and IV-3 were checked by differencing the values of H_{21}, H_{24}, H_{14} and $(v_0 \delta_2/\nu)$ and in this way a number of mistakes were detected. These were corrected but it is not possible to be certain that all such mistakes were found because of the behaviour of some of the functions, particularly those for blowing in Table IV-3.

The interpolated solutions given in an earlier paper, Evans[7], were tested by plotting H_{21} against $(v_0 \delta_2/\nu)$ and comparing with the present values. The over-all agreement was good since the two curves intersected at four places. There were, however, two regions, namely near the limiting case $\bar{k}_0 = -8^{\frac{1}{2}}$ and when the blowing rate was in the range $0 \cdot 5 < \dfrac{v_0 \delta_2}{\nu} < 1 \cdot 0$

where the interpolated solutions were up to 1% in error, although elsewhere the error was less than this. The error near $\bar{k}_0 = -8^{\frac{1}{2}}$ appears to be due to an error in Holstein's[17] solution for this limiting case. His value of γ_0, for example, was $1 \cdot 9257$ compared with the present value $1 \cdot 92058109$. An independent solution obtained on a desk calculator gave $1 \cdot 92058086$.

6.5.7 Curves of some boundary-layer functions

Figures 7, 8 and 9 show the variation of the local shear in the boundary layer for a few selected values of the mass transfer parameter.

Figure 7 shows solutions to equation (26) where the lines are concave upwards, although to this scale the curvature is only apparent for solutions near the limit $\bar{k}_0 = -8^{\frac{1}{2}}$. As the suction rate increases this curvature diminishes and values of $\bar{\gamma}_0$ tend to $-\bar{k}_0$ from below. Corresponding solutions to equation (23) shown in Fig. 8 are concave downwards, the curvature again diminishing as the suction rate increases, but values of γ_0 now approach k_0 from above.

Some solutions to equation (23) for blowing are shown in Fig. 9. Also drawn on this figure are curves of $(1-\phi^2)/(-k_0)$, the asymptote for intensive blowing, Evans[7], thus showing how the accurate solutions approach the asymptote as the blowing rate increases. To this scale the accurate solution for $k_0 = -10$ is identical with the asymptote, although an examination of the accurate value of γ_0 in Table IV-3 (it would be $-1/k_0$ for the asymptote) shows that this solution is still some way from the asymptote.

Figures 10 and 11 show the variation of thickness ratios with the mass transfer parameter $(v_0 \delta_2/\nu)$. Figure 10 applies to suction and moderate blowing and Figure 11 to intensive blowing, where in the latter figure the reciprocal of the mass transfer parameter is plotted along the abscissa.

The variations of the pressure gradient parameters are shown in Figs. 12, 13 and 14. Care should be taken with these figures as the curves

for the displacement thickness and the momentum thickness are drawn to different scales, so that the former is uppermost to the right of Fig. 12 and the latter is uppermost in Fig. 13.

The small amount of curvature in Figs. 12 and 13 means that the pressure gradient parameter can be expressed as a simple function, say a cubic, of the related mass transfer parameter without appreciable loss in accuracy.

6.5.8 A cubic approximation for intensive suction

The curvature of y decreases with increasing suction and when the suction rate is very high y is virtually a linear function of ϕ, represented by the first term in the series expansion of Section 6.5.2. This linear approximation is not, however, very useful except for very intensive suction because, like asymptotes in other branches of mathematics, it must be regarded as only the first stage in a step-by-step approach to the accurate solution. On the other hand a cubic approximation is very satisfactory as long as k_0, or $\bar{k}_0$, is not small.

The use of a polynomial expansion about the point $\phi = 1$ means neglecting terms in high powers of $(\phi-1)$ in the infinite series of Section 6.5.2. Such an expansion gives high accuracy near $\phi = 1$ but lower accuracy near $\phi = 0$. This less accurate region contributes only a part of the displacement thickness δ_1^{**} and contributes even less to the momentum thickness δ_2^{**}.

For this reason a very accurate procedure for applying a cubic approximation is first to evaluate the thicknesses δ_1^{**} and δ_2^{**} and then to substitute these into the equation:

$$y_0 = k_0 + \delta_1^{**} + \delta_2^{**} \qquad \ldots (114)$$

which is equation (32) expressed in the present co-ordinates.

A cubic expansion for y gives for the displacement thickness:

$$\delta_1^{**} = -\int_0^1 \left\{ y_1' + \frac{y_1''}{2!}(\phi - 1) + \frac{y_1'''}{3!}(\phi - 1)^2 \right\}^{-1} d\phi \qquad \ldots (115)$$

which is readily integrated to give:

$$\delta_1^{**} = \frac{1}{S} \ell n \left\{ \frac{(y_1'' + 2S)(3y_1'' - 6S - 2y_1''')}{(y_1'' - 2S)(3y_1'' + 6S - 2y_1''')} \right\}, \qquad \ldots (116)$$

where S is an abbreviation for:

$$S = \left\{ \frac{(y_1'')^2}{4} - \frac{2}{3} y_1' \, y_1''' \right\}^{\frac{1}{2}}. \qquad \ldots (117)$$

The derivatives of y at $\phi = 1$ occurring in equations (116) and (117) are, of course, known functions of k_0 as given in Section 6.5.2(a).

For the momentum thickness we have:

$$\delta_2^{**} = -\int_0^1 \phi \left\{ y_1' + \frac{y_1''}{2!}(\phi - 1) + \frac{y_1'''}{3!}(\phi - 1)^2 \right\}^{-1} d\phi \qquad \ldots (118)$$

which also integrates to give:

$$\delta_2^{**} = \frac{3}{y_1'''}\left\{ \ell n \left(1 - \frac{3y_1'' - y_1'''}{6y_1'} \right) - \left(\frac{y_1''}{2} - \frac{y_1'''}{3} \right) \delta_1^{**} \right\} \qquad \ldots (119)$$

where δ_1^{**} is given by equation (116).

The accuracy of the cubic approximation may be judged from Table A.

TABLE A

Comparison of (a) Accurate Solutions and (b) Cubic Approximation

(i) **Variables real**

k_0		δ_1^{**}	δ_2^{**}	y_0
2	(a)	0·377584	0·186800	2·564384
	(b)	0·377568	0·186797	2·564365
3	(a)	0·286121	0·1421512	3·428272
	(b)	0·286118	0·1421506	3·428269

(ii) **Variables imaginary**

$\bar{k}_0$		$\bar{\delta}_1^{**}$	$\bar{\delta}_2^{**}$	$\bar{y}_0$
$-8^{\frac{1}{2}}$	(a)	0·59531	0·31254	1·92058
	(b)	0·60869	0·31557	1·90416
-3	(a)	0·46499	0·23785	2·29717
	(b)	0·46542	0·23794	2·29664
-4	(a)	0·286366	0·144243	3·569391
	(b)	0·286372	0·144245	3·569384

The cubic approximation clearly becomes very accurate when k_0 (or $\bar{k}_0$) becomes large and gives far better values for real than for pure imaginary variables.

6.6 Group V - Some miscellaneous solutions

We now consider briefly some tables of solutions which, for various reasons, could not be grouped with those given earlier.

6.6.1 Solutions for $\beta = 0$ by Emmons and Leigh

Emmons and Leigh[11] computed an almost complete set of solutions to equation (12) for $\beta = 0$ with both inward and outward mass transfer. The

boundary-layer functions for those solutions were later tabulated by Spalding and Evans[4]. Unfortunately, however, that table not only omitted about one third of the solutions actually computed, but most quantities were rounded off to about four digits, although the original solutions were more accurate than that.

In order to make full use of the accuracy achieved by Emmons and Leigh, therefore, Table V-1 was prepared. Here the accuracy is as high as the original data allowed.

It has already been remarked in Section 6.4.1 that, as is evident also from the values of H_{21} in this table, a few more solutions between the first two would be useful. There also appears to be a small error in the solution for $\sqrt{2}f_0 = 10$, although this is only evident from large-scale graphs of, say, H_{24} against $(v_0\delta_2/v)$. The gap between that solution and the case of infinite f_0 can be filled in quite accurately by use of the asymptotic series to be given in Section 8.

6.6.2 Solutions for $f_0 = 0$ and $1 \cdot 3 \geqslant \dfrac{1}{\beta} \geqslant -1 \cdot 0$

Solutions with zero mass transfer when the parameter β is large are given in Table V-2. These occur on either side of the line which divides the real and imaginary domains relating to equation (12). They were computed by the following method.

Equation (23), which applies to infinite β, takes the following form when β is finite:

$$\frac{dy}{d\phi} + \frac{1}{\beta} \int_0^{\phi} \frac{\phi}{y}\, d\phi + k_0 + \frac{(1 - \phi^2)}{y} = 0 \qquad \qquad \text{... (120)}$$

where we are now interested in solutions for $k_0 = 0$.

When this equation is integrated numerically starting from the wall, the accuracy is high near the wall but decreases as the main stream is approached. This inaccurate region contributes roughly the same amount to the displacement thickness δ_1^{**} as to the momentum thickness δ_2^{**}. It was therefore possible to achieve high accuracy by arranging that the computer evaluate the function:

$$p(\phi) = \int_0^{\phi} \frac{(1 - \phi)^2}{y}\, d\phi$$

since it is clear that at $\phi = 1$ the value of p is $(\delta_1^{**} - \delta_2^{**})$.

The values of the wall shear $y_0 (= \theta_0'')$ required to start these integrations were obtained from the polynomial expansion to be given in Section 8.13, although some were further improved by trial and error.

For the solutions above the broken line in Table V-2, the error is believed to be confined to the last two digits, but those below the line are probably less accurate.

The quantity E_2, which is the correction to a straight-line relationship between F_2 and λ_2, is defined by the equation:

$$F_2 = 0 \cdot 44105 - 5 \cdot 1604\lambda_2 - E_2 \qquad \ldots (121)$$

and from its values in Table V-2 appears to have a stationary value near $\lambda_2 = 0 \cdot 25$.

When the reciprocals of δ_1^{**} and δ_2^{**} are plotted against $1/\beta$ they are found to tend to zero as $1/\beta$ approaches -2, so that the thicknesses themselves become infinite. This value of β, namely $\beta = -0 \cdot 5$, is the limit to meaningful solutions in the imaginary domain relating to equation (12), for not only are the displacement and momentum thicknesses infinite, but so are λ_1, λ_2, F_1 and F_2. The ratio H_{21} tends to unity, however, as may be shown by writing down the form of equation (32) valid for the imaginary domain and dividing by the displacement thickness. When f_0 is zero this gives:

$$- \frac{\overline{f_0''}}{\overline{\delta_1^*}} = \beta + (1 + \beta) H_{21} . \qquad \ldots (122)$$

Because $\overline{f_0''}$ would still be finite for $1/\beta = -2$, this equation gives $H_{21} = 1$ when the displacement thickness is infinite.

6.6.3 Solutions for $f_0 = -0 \cdot 5$ and $0 \leqslant \beta \leqslant 1 \cdot 0$

Only a start has been made on obtaining solutions with blowing when the parameter β is small. The results obtained so far are summarized in Table V-3.

While the accuracy of these solutions is high, it should be emphasized that it becomes progressively more difficult to obtain high accuracy as the parameter f_0, which is negative, increases in magnitude.

7. A General Method of Boundary-Layer Analysis based on the Displacement Thickness

7.1 General methods of boundary-layer analysis

The boundary-layer equations are extremely difficult to integrate when the main-stream pressure gradient and the rate of mass transfer are distributed arbitrarily over the wall surface. For solving general problems of this kind, other methods of boundary-layer analysis have been developed which do not entail the integration of the equations themselves. These general methods are approximate by nature but should, nevertheless, give the order of accuracy required for most practical applications. In some of these methods other differential equations are set up which may be solved in a reasonably short time using methods and equipment which are readily available to engineers. The variables in these new differential equations are given either as numerical tables or in the form of charts, often obtained from accurate similar solutions to the boundary-layer equations.

One such method, with a number of applications, was given in detail by Spalding[5], who also discussed the assumptions underlying the general methods. It was shown that, if δ is any boundary-layer thickness associated with the velocity layer, its rate of growth with distance x may be expressed as a function of the pressure gradient and the mass transfer rate by the differential equation:

$$\frac{u_G}{\nu} \Bigg/$$

$$\frac{u_G}{\nu} \frac{d\delta^2}{dx} = F \left\{ \frac{\delta^2}{\nu} \frac{du_G}{dx}, \frac{v_0\delta}{\nu} \right\} \qquad \ldots (123)$$

where F on the right represents some function of the two groups inside the brackets.

For the thickness δ, Spalding chose the momentum thickness δ_2, the function F then being denoted by F_2. This choice has several advantages, for not only is equation (123) then the integral momentum equation, already given in equation (37), but, for a fixed value of the mass transfer parameter $(v_0\delta_2/\nu)$, the rate of growth function F_2 is then almost a linear function of the pressure gradient parameter λ_2, at least when conditions are not near separation. This linearity greatly simplifies the task of integrating the differential equation.

We now consider a method in which δ in equation (123) is the displacement thickness δ_1. As this is a straightforward modification of that based on δ_2, we shall not give any applications but shall merely discuss the variation of functions required in the method. By plotting these functions we gain a considerable amount of new information about the effects of pressure gradient and mass transfer on laminar boundary layers, especially for decelerated flows where this method may possess some advantages over others.

7.2 Variation of thickness ratios and growth functions

When the values of two thickness ratios are known as functions of the free-stream pressure gradient and the rate of mass transfer, it is possible to evaluate the other boundary-layer functions which are of interest in the present work and to construct tables and charts for use in general methods of boundary-layer analysis. In the method based on the momentum thickness, Spalding[5], Spalding and Evans[4], the ratios H_{24} and H_{12} were a suitable pair. We see from equation (39) with $n = 1$, however, that H_{14} and H_{21} are better for the present method.

There are advantages in using H_{21} instead of H_{12} in boundary-layer calculations for, while the latter varies over wide ranges, becoming particularly large near separation, the former remains within fairly narrow limits, at least in most regions where the velocity equation has so far been explored. In the real domain, except for some large negative values of β, it lies in the range $0 \leqslant H_{21} \leqslant 0\cdot5$. For asymptotic blowing, including both the real and the imaginary domains where solutions exist, Evans[7], the values are in the range $0 \leqslant H_{21} \leqslant 1\cdot0$. The ratio H_{21} is, therefore, not only more suitable for plotting than H_{12} but is also more convenient for interpolation between exact solutions; it was, in fact, used for some earlier interpolations, as may be seen from Figure 3 of the paper by Spalding and Evans[4].

We shall now discuss the variation of the ratios H_{14} and H_{21} with pressure gradient as given by λ_1 and the rate of mass transfer as given by $(v_0\delta_1/\nu)$.

7.2.1 Variation of H_{14}

Fig. 15 shows the variation of H_{14} for decelerated and slightly accelerated free streams with suction and some blowing, and Fig. 16 shows its variation for intensive blowing.

Fig. 15 was constructed by interpolation using data given elsewhere in the present monograph. It has already been shown in Section 3.3 that points

along the line $\beta = -1$ are known exactly. The figure is believed to be fairly accurate, although the region near the negative arm of the abscissa, which is the separation line, did present some difficulty. This figure should be compared with Fig. 4(b) of the paper by Spalding and Evans[4] which showed how the corresponding ratio H_{24} varied in the same region.

The very small amount of curvature of the lines of constant $(v_0 \delta_1/\nu)$ in Fig. 15 is quite striking; it is extremely small for accelerated flows and does not become large even near the separation line.

Fig. 16 was also drawn by interpolation using methods and data given in an earlier paper, Evans[7]. It was shown there that for intensive blowing the dimensionless wall shear f_0'' tends to the asymptotic value:

$$f_0'' = -\frac{\beta}{f_0}.$$

... (124)

When both sides of this equation are multiplied by δ_1^* it becomes:

$$H_{14} = \frac{\nu}{v_0 \delta_1} \cdot \lambda_1.$$

... (125)

This means that, for sufficiently intensive blowing, lines of constant $(v_0 \delta_1/\nu)$ on Fig. 16 become linear with a slope $(\nu/v_0 \delta_1)$. Using this fact together with solutions for $\beta = 1 \cdot 0$, see Evans[7], and for β infinite, lines of constant $(v_0 \delta_1/\nu)$ could be drawn with reasonable accuracy. The short lines on the right of this figure show the asymptotic values of H_{14} for the values of β indicated when the blowing rate is very high; these too were taken from the paper just referred to.

7.2.2 Variation of H_{21}

Figures 17 and 18 are the corresponding figures for H_{21}. Fig. 17 was constructed in the same way as Fig. 15, except that interpolation was necessary along the line $\beta = -1$ since points were not known exactly. The curvature of lines of constant $(v_0 \delta_1/\nu)$, although larger than that of H_{14} in Figs. 15 and 16, is still not great.

There is no reason to expect lines of constant $(v_0 \delta_1/\nu)$ to become linear for intensive blowing when H_{21} is plotted as a function of λ_1. Fig. 18 gives some interpolated curves but, because the lines are not straight and as there are virtually no exact solutions in this region, the accuracy is not expected to be high. In spite of this, however, it was thought worthwhile giving this figure as so little is known about the behaviour of boundary layers under these conditions. The error in the figure is thought to be least near the lines marked $\beta = 1$, $\beta = \pm\infty$ and near the ordinate marked $\beta = 0$, and greatest near the middle of the figure.

7.2.3 Variation of the rate of growth function F_1

When H_{14} and H_{21} are known as functions of the variables λ_1, and $(v_0 \delta_1/\nu)$, by substitution into equation (42) with $n = 1$, we get the rate of growth function F_1 as a function of the same two variables. The resulting values are plotted in Figs. 19, 20 and 21.

The/

The line $\beta = -1$ was again very useful when drawing these figures because points on it were known exactly; by equation (41) the slope of the line is -4 and by equation (49) the value of λ_1 is known for any specified value of the mass transfer parameter $(v_0\delta_1/\nu)$. The separation point on this line has the co-ordinates $\lambda_1 = -2$, $F_1 = 8$ and the mass transfer parameter is $(v_0\delta_1/\nu) = -2$. Because solutions for $\beta = -1$ behave in this special way, some of the lines in Figs. 19 and 20 could be continued as far as $\beta = -1$ in the imaginary domain. This could not be done for all the lines, however, because as $(v_0\delta_1/\nu)$ diminished the curvature increased, eventually becoming too large for such extrapolation to be accurate.

Fig. 19 covers decelerated and accelerated flows with suction and a moderate rate of blowing, and Fig. 20 shows on a larger scale the region of Fig. 19 which is likely to be of greatest use in practical applications. Fig. 21 shows how F_1 varies for intensive blowing but the accuracy is considerably lower than in Figs. 19 and 20 because it was drawn from values of H_{21} taken from Fig. 18.

In Fig. 19 the portions of the lines of constant $(v_0\delta_1/\nu)$ lying in the decelerated region are much longer than the portions in the accelerated region, at least if attention be confined to the real domain. This effect, which arises because the displacement thickness becomes large as separation is approached, is well illustrated by the line of no mass transfer for which the part of the line in the range $-0{\cdot}198838 \leqslant \beta \leqslant 0$ is more than twice as long as that for the range $0 \leqslant \beta \leqslant \infty$. This means that the general method based on the displacement thickness could give high accuracy when applied in the decelerated region.

On the other hand, the method has two serious disadvantages. Firstly, the lines of constant $(v_0\delta_1/\nu)$ are not very straight, so that the first steps in the method of integration given by Spalding[5] would be less accurate than is the case with the method based on the momentum thickness. It should, however, be possible to devise a method of step-by-step integration which depends less on a linear approximation to the curves. For example, when the interval of integration is small enough, equation (123) may be written:

$$\frac{u_G}{\nu}\frac{d\delta^2}{dx} = j_1 + j_2\frac{\delta^2}{\nu}\frac{du_G}{dx} \qquad \dots (126)$$

where j_1 and j_2 are quantities whose values depend on the local values of $\dfrac{\delta^2}{\nu}\dfrac{du_G}{dx}$ and $\dfrac{v_0\delta}{\nu}$; these can be obtained from the similar solutions. Now, not only is equation (126) virtually exact but it is also exactly integrable, see Spalding[5]. By carefully selecting j_1 and j_2 at each step in the integration procedure, therefore, the curvature of the lines in Fig. 19 should present no barrier to being able to integrate equation (123) accurately.

The second disadvantage of the method based on δ_1 is that the $F_1 - \lambda_1$ relationship cannot be used near the separation point for $\beta = 0$ because, while F_2 remains finite, F_1 becomes infinite; however, practical problems which require the use of this region of the $F_1 - \lambda_1$ plane should be rare.

7.2.4/

7.2.4 Variation of F_2 and H_{24} for decelerated flows

The functions F_2 and H_{24} are required in the general method based on the momentum thickness, but when the paper by Spalding and Evans[4] was published little information was available for decelerated flows. By making use of solutions given elsewhere in this monograph, however, Figs. 22 and 23 could be drawn to show the variation of these functions in this region.

These figures are largely self-explanatory and should be used in conjunction with the discussions by Spalding[5] and Spalding and Evans[4]. In Fig. 22 there is some uncertainty about the accuracy of the curves of constant $(v_0 \delta_2 / \nu)$ for negative values of this parameter beyond $-0 \cdot 55$, and such curves are shown as broken lines. Corresponding curves could not be drawn with much confidence in Fig. 23 and have therefore been omitted.

8. Some Asymptotic Series for Intensive Mass Transfer
(By H. L. Evans and Joan D. Hayhurst)

8.1 Outline of section

Watson[6] has given solutions to equation (12) with boundary conditions (13) for suction in the form of asymptotic series in inverse powers of the mass transfer parameter f_0. These solutions become asymptotically exact as f_0 becomes large. Series were given for the dimensionless wall shear, the displacement and momentum thicknesses and the thickness ratio H_{12}; other boundary-layer functions are readily calculated from these quantities.

The first term in the series corresponds to the asymptotic suction profile and Watson obtained the next three terms, and for the wall shear the next four terms. That work has been recalculated and the coefficients given by Watson were confirmed, except for a small misprint in the published series for the wall shear. The next term in each series was also calculated, although the ratio H_{21} was obtained in preference to H_{12} obtained by Watson.

Unfortunately, however, to obtain this next term required such a long calculation that a plan for obtaining further terms was abandoned. Apart from a brief statement of the method, details of the calculations will not be given as they may be found in Watson's paper.

When the values of functions calculated from the asymptotic series are compared with accurate solutions obtained by numerical integration, for most values of the parameter β the series are found to be reasonably accurate when the mass transfer parameter is larger than $3 \cdot 0$, although this depends to some extent on the magnitude of β.

As the mass transfer parameter decreases below $3 \cdot 0$, the accuracy diminishes because not enough terms are known and the remainder is no longer negligible. Provided the mass transfer parameter is not too small, however, a simple correction can be added which improves the accuracy and slightly extends the lower limit of mass transfer to which the series may be applied.

Only a trivial change is required to use the series for small β in the imaginary domain, but when β is large in either domain the series must be changed by a transformation of co-ordinates.

When the same approach is applied to blowing, a series in inverse powers of the mass transfer parameter is obtained for the wall shear; this series also becomes asymptotically exact as the blowing rate increases. However, the present authors were unable to obtain asymptotic series for the other boundary-layer functions. When the remainder is not negligible in the series for the wall shear, the accuracy is improved by applying the Euler transformation. Again, by making straightforward changes for the imaginary domain and for large β in either domain, the series can be used for all values of β. The accuracy is acceptable for a wide range of β when the mass transfer parameter is larger than 2·0.

Finally, when there is no mass transfer and β is large, the dimensionless wall shear is expressed as a polynomial in inverse powers of β by fitting to known numerical values. This applies to the real and imaginary domains and the accuracy is high in the range $2 \cdot 0 \leqslant 1/\beta \leqslant -1 \cdot 0$ but diminishes fairly rapidly outside this range.

8.2 Evaluation of the series for suction

Because the velocity layer becomes thinner as the suction rate increases, in order to study its behaviour for intensive suction we extend the co-ordinates by an amount which is proportional to the rate of mass transfer. We therefore introduce the co-ordinates:

$$\alpha = f_0 \eta \qquad \qquad \ldots (127)$$

$$g = f_0 (f - f_0) \qquad \qquad \ldots (128)$$

into equation (12) and divide by f_0^2 to get:

$$\frac{d^3 g}{d\alpha^3} + \frac{d^2 g}{d\alpha^2} + \frac{1}{f_0^2} \left\{ g \frac{d^2 g}{d\alpha^2} + \beta \left[1 - \left(\frac{dg}{d\alpha} \right)^2 \right] \right\} = 0. \qquad \qquad \ldots (129)$$

The boundary conditions from equation (13) are then:

$$\left. \begin{array}{l} \alpha = 0, \qquad g = \dfrac{dg}{d\alpha} = 0 \\[3ex] \alpha \to \infty, \qquad \dfrac{dg}{d\alpha} \to 1. \end{array} \right\} \qquad \qquad \ldots (130)$$

A solution to equation (129) is now assumed to have the form

$$g = g_1 + \frac{g_2}{f_0^2} + \frac{g_3}{f_0^4} + \frac{g_4}{f_0^6} + \ldots \qquad \qquad \ldots (131)$$

and to satisfy the boundary conditions:

$$\left. \begin{array}{ll} g_1(0) = g_1'(0) = 0, & g_1'(\infty) = 1, \\[2ex] g_r(0) = g_r'(0) = g_r'(\infty) = 0, & \text{for } r \geqslant 2 \end{array} \right\} \qquad \qquad \ldots (132)$$

where the primes now denote differentiation with respect to α.

The/

The assumed solution will clearly become asymptotically more accurate as f_0^2 increases.

When we substitute equation (131) into equation (129) and equate coefficients in power of f_0^{-2}, we get differential equations for the functions g_r which are solved in turn. As r increases the solutions become progressively more complex, containing polynomials of increasing orders in α and β with powers of $e^{-\alpha}$ as factors. These solutions were then used to evaluate boundary-layer thicknesses, and the results are expressed in the form of suitable dimensionless groups in the next section.

8.3 The asymptotic series for suction

(1) The displacement thickness

If δ_1^* is the displacement thickness in terms of the co-ordinates (η, f), as a function of the quantities g_r it is:

$$- \frac{v_0 \delta_1}{\nu} \equiv f_0 \delta_1^* = \alpha(\infty) - g_1(\infty) - \frac{g_2(\infty)}{f_0^2} - \frac{g_3(\infty)}{f_0^4} - \ldots \qquad \ldots (133)$$

When expressed in terms of the parameter β this series is:

$$- \frac{v_0 \delta_1}{\nu} = 1 + \frac{a_1}{f_0^2} + \frac{a_2}{f_0^4} + \frac{a_3}{f_0^6} + \frac{a_4}{f_0^8} + \ldots \qquad \ldots (134)$$

where the first four coefficients are:

$a_1 = -(5 + 7\beta)/4$

$a_2 = (359 + 783\beta + 460\beta^2)/72$

$a_3 = -(56,670 + 156,611\beta + 150,450\beta^2 + 51,589\beta^3)/1728$

$$a_4 = \left\{ \begin{array}{l} 152,018,034 + 493,420,561\beta + 615,401,188\beta^2 \\ + 355,775,339\beta^3 + 82,230,278\beta^4 \end{array} \right\} \Big/ 518,400.$$

A useful check of these coefficients is afforded by the case $\beta = -1$, see Evans[7], since the series must reduce to the first terms in the expansion of:

$$- \frac{v_0 \delta_1}{\nu} = f_0^2 \left\{ 1 - \left(1 - \frac{2}{f_0^2} \right)^{\frac{1}{2}} \right\}, \qquad \beta = -1. \qquad \ldots (135)$$

(2) The momentum thickness

This required a much longer calculation from the functions g_r than did the displacement thickness. The result was:

$$- \frac{v_0 \delta_2}{\nu} \equiv f_0 \delta_2^* = \frac{1}{2} + \frac{b_1}{f_0^2} + \frac{b_2}{f_0^4} + \frac{b_3}{f_0^6} + \frac{b_4}{f_0^8} + \ldots \qquad \ldots (136)$$

where/

where the coefficients are:

$$b_1 = -(10 + 11\beta)/12$$

$$b_2 = (550 + 1{,}035\beta + 497\beta^2)/144$$

$$b_3 = -(234{,}192 + 586{,}816\beta + 494{,}763\beta^2 + 142{,}469\beta^3)/8{,}640$$

$$b_4 = \left\{ \begin{array}{l} 131{,}557{,}872 + 398{,}264{,}275\beta + 453{,}852{,}685\beta^2 \\ + 233{,}270{,}315\beta^3 + 46{,}184{,}438\beta^4 \end{array} \right\} \Big/ 518{,}400.$$

(3) The thickness ratio H_{21}

The ratio H_{21} was obtained by dividing equation (136) by equation (134), and the result was:

$$H_{21} \equiv \frac{\delta_2^*}{\delta_1^*} = \frac{1}{2} + \frac{c_1}{f_0^2} + \frac{c_2}{f_0^4} + \frac{c_3}{f_0^6} + \frac{c_4}{f_0^8} + \dots \qquad \dots (137)$$

with the coefficients:

$$c_1 = -(5 + \beta)/24$$

$$c_2 = (307 + 384\beta + 53\beta^2)/288$$

$$c_3 = -(144{,}059 + 286{,}802\beta + 162{,}151\beta^2 + 16{,}828\beta^3)/17{,}280$$

$$c_4 = \left\{ \begin{array}{l} 87{,}698{,}885 + 226{,}566{,}669\beta + 204{,}261{,}172\beta^2 \\ + 71{,}360{,}511\beta^3 + 5{,}862{,}933\beta^4 \end{array} \right\} \Big/ 1{,}036{,}800.$$

(4) The wall shear

The wall shear could have been evaluated directly from the known quantities $g_r''(0)$, but we get one more term in the expansion by substituting equations (134) and (136) into the exact relationship:

$$-\frac{\nu}{v_0 \delta_4} \equiv \frac{f_0''}{f_0} = 1 - \frac{\beta}{f_0^2} \cdot \frac{v_0 \delta_1}{\nu} - \frac{(1+\beta)}{f_0^2} \cdot \frac{v_0 \delta_2}{\nu} \cdot \qquad \dots (138)$$

This gives the series:

$$-\frac{\nu}{v_0 \delta_4} = 1 + \frac{d_1}{f_0^2} + \frac{d_2}{f_0^4} + \frac{d_3}{f_0^6} + \frac{d_4}{f_0^8} + \frac{d_5}{f_0^{10}} + \dots \qquad \dots (139)$$

where the coefficients are:

$d_1 /$

$$d_1 = (1 + 3\beta)/2$$

$$d_2 = -(5 + 18\beta + 16\beta^2)/6$$

$$d_3 = (550 + 2303\beta + 3098\beta^2 + 1417\beta^3)/144$$

$$d_4 = -\left\{ \begin{array}{l} 117,096 + 552,179\beta + 932,317\beta^2 \\ + 694,741\beta^3 + 200,207\beta^4 \end{array} \right\} \bigg/ 4,320$$

$$d_5 = \left\{ \begin{array}{l} 131,557,872 + 681,840,181\beta + 1,345,537,521\beta^2 \\ + 1,302,524,188\beta^3 + 635,230,092\beta^4 \\ + 128,414,716\beta^5 \end{array} \right\} \bigg/ 518,400.$$

The case $\beta = -1$, Evans[7], may also be used to check the coefficients in equation (139) as the series then reduces to the binomial expansion of:

$$-\frac{\nu}{v_0 \delta_4} = \left(1 - \frac{2}{f_0^2}\right)^{\frac{1}{2}}, \qquad \beta = -1. \qquad \ldots (140)$$

8.4 Application of the series in the imaginary domain

In the imaginary domain we write $\eta = i\bar{\eta}$, $f = i\bar{f}$ and $f_0 = i\bar{f}_0$, where the barred quantities are real. The above series can be used in the imaginary domain simply by replacing f_0 by $i\bar{f}_0$, or f_0^2 by $-\bar{f}_0^2$. Care should, however, be taken with the signs of both β and $\bar{f}_0$ for, while f_0 is positive for suction, $\bar{f}_0$ is negative. Further, when $|\beta|$ is large in either domain the method in the next section must be used.

8.5 The series when $|\beta|$ is large

When $|\beta|$ is large in either the real or imaginary domains, successive coefficients in each of the above series increase in magnitude and, depending on the relative values of β and f_0, the series may either converge very slowly or even diverge.

This difficulty is readily overcome, however, by expressing the series in the co-ordinates of Section 2.3. If we consider only the wall shear, for example, equation (139) then becomes:

$$-\frac{\nu}{v_0 \delta_4} = 1 + \frac{e_1}{k_0^2} + \frac{e_2}{k_0^4} + \frac{e_3}{k_0^6} + \frac{e_4}{k_0^8} + \frac{e_5}{k_0^{10}} + \ldots \qquad \ldots (141)$$

where the coefficients are simply:

$$e_r = \frac{d_r}{\beta^r}. \qquad \ldots (142)$$

For sufficiently large k_0 the series then converges very rapidly for large β. The series for the boundary-layer thicknesses and the thickness ratio H_{21} for large β are obtained in the same way.

8.6 Comparison with accurate numerical solutions

The asymptotic series give high accuracy for sufficiently large values of the mass transfer parameter, which may be f_0, $\bar{f}_0$, k_0 or $\bar{k}_0$, the last of which applies to equation (19) when ξ and θ are pure imaginary. The series generally give boundary-layer functions correct to six digits when the mass transfer parameter, ignoring its sign, is greater than 10, although the accuracy depends to some extent on the value of β. When the mass transfer parameter is as small as 2, however, the terms omitted from the infinite series are not negligible so that the accuracy is poor.

In Table B* the series are compared with known accurate solutions for values of the mass transfer parameter at which the series are just becoming inaccurate. We only consider solutions either in the real domain relating to equation (12) or along the line which divides the real and imaginary domains, because no solutions with suction are known in the imaginary domain. The series also apply there, of course, but the accuracy is probably lower than in the real domain because the fluid velocity then approaches its main-stream value more slowly.

The accurate solutions for $\beta = 0$ where f_0 contains the factor $\sqrt{2}$ were obtained by Emmons and Leigh[11] and the wall shear for $\beta = 0 \cdot 5$, $f_0 = 5 \cdot 0$ was given by Stewart and Prober[19]; the other solutions were computed by the present authors.

When we examine Table B, as well as values given by Watson[6], we see that the asymptotic series are most accurate near $\beta = -1$. The accuracy for $\beta = -1$ when $f_0 = 2 \cdot 0$ is better, for example, than for $\beta = 1$ when f_0 is as high as $4 \cdot 0$.

From equations (14) and (18) we have $f_0 = \sqrt{\beta}\, k_0$ so that, for $\beta = 1$ the series expansions are the same in the (ξ, θ) as in the (η, f) co-ordinates. If we consider only positive β, a glance at the coefficients in the asymptotic expansions shows that when $\beta < 1$ the (η, f) co-ordinates would give better convergence, but when $\beta > 1$ the (ξ, θ) co-ordinates should be better; close to $\beta = 1$ either can be used. Such poor accuracy was obtained for $\beta = 2 \cdot 0$ and $f_0 = 3 \cdot 0$ that the values could not be included in Table B. The reason, of course, is that while f_0 appears to be quite large, the relevant parameter is then k_0 and as this is only $2 \cdot 121$ the low accuracy is not so surprising. This is what first made it necessary to use the (ξ, θ) co-ordinates for $|\beta| > 1$ in preference to the more usual (η, f) co-ordinates.

8.7 Adding a correction for the remainder

The Euler transformation, which will be discussed in Section 8.11, often improves the convergence of a series but did not appear to work well for suction, probably because too few terms in the series were known. On the other hand a simple method of allowing for the remainder was used which, it was realised later, is equivalent to summing the series as far as the penultimate term and applying the Euler transformation to the rest of the series.

In this method the magnitude of the remainder was assumed to be half that of the last known term and its sign to be that of the first neglected term; this sign was readily determined by inspection. The values marked "c" in Table B show that this gave a worthwhile improvement in accuracy.

When/

---

*See pp.53 and 54.

When the mass transfer parameter was large enough for the series to give functions accurately to five or six digits, however, this correction introduced a small error instead of eliminating one, although the difference between values with and without the correction was fortunately very small.

Table B

Comparison of the Asymptotic Series for Suction with Accurate Solutions

a. Accurate values

b. Values from series

c. Values from series with a correction for the remainder (see text)

β	Mass transfer parameter		$-\dfrac{\nu}{v_0\,\delta_4}$	H_{21}	$-\dfrac{v_0\,\delta_2}{\nu}$	$-\dfrac{v_0\,\delta_1}{\nu}$
$\pm\infty$	$-\bar{k}_0 = 3{\cdot}0$	a	0·765723	0·511510	0·713536	1·394961
		b	0·7757	0·5091	0·681	1·338
		c	0·7736	0·5095	0·687	1·351
	4·0	a	0·892348	0·503703	0·576973	1·145463
		b	0·89249	0·503647	0·57616	1·1440
		c	0·892369	0·503690	0·57684	1·14525
	5·0	a	0·934952	0·502043	0·543543	1·082663
		b	0·934960	0·502038	0·543472	1·08254
	6·0	a	0·956032	0·501324	0·528543	1·054293
		b	0·956033	0·501324	0·528533	1·054275
$-1{\cdot}0$	$f_0 = 2{\cdot}0$	a	0·707107	0·449981	0·527186	1·171573
		b	0·70764	0·45040	0·527094	1·1694
		c	0·70721	0·45020	0·52732	1·17114
	2·5	a	0·824621	0·470465	0·515685	1·096118
		b	0·824651	0·470523	0·515699	1·09593
		c	0·824605	0·470490	0·515738	1·09622
	3·0	a	0·881917	0·480167	0·510296	1·062746
		b	0·881920	0·480233	0·510358	1·062719
$-0{\cdot}5$	$f_0 = 2{\cdot}0$	a	0·937175	0·466871	0·440136	0·942736
		b	0·937076	0·509	0·538	1·04
	2·5	a	0·959906	0·476755	0·456647	0·957823
		b	0·959899	0·4828	0·470	0·972
		c	0·959909	0·47748	0·4581	0·9593
	3·0	a	0·972188	0·482841	0·467390	0·968000
		b	0·972188	0·4840	0·4701	0·9707
		c	0·972190	0·482805	0·46725	0·96783

Table B (Continued)

β	Mass transfer parameter			$-\dfrac{\nu}{v_0 \delta_4}$	H_{21}	$-\dfrac{v_0 \delta_2}{\nu}$	$-\dfrac{v_0 \delta_1}{\nu}$
0·0	$f_0 = 4\sqrt{2}$	{	a	1·0537	0·4831	0·4296	0·889399
			b	1·0581	0·495	0·465	0·929
	3·0	⌠	a	1·048367	0·484327	0·435303	0·898778
		⎨	b	1·0507	0·4915	0·456	0·922
		⌡	c	1·04852	0·48502	0·4367	0·9000
	$5\sqrt{2}$	⌠	a	1·03596	0·48768	0·44951	0·921724
		⎨	b	1·03634	0·4894	0·4543	0·9271
		⌡	c	1·03593	0·48762	0·44910	0·92113
	$6\sqrt{2}$	{	a	1·02569	0·49087	0·46245	0·942091
			b	1·02574	0·49109	0·46326	0·9431
0·5	$f_0 = 3·0$	{	a	1·115278	0·48532	0·41004	0·84489
			b	1·135	0·509	0·492	0·95
	5·0	{	a	1·046080	-	-	-
			b	1·046150			
1·0	$f_0 = 3·0$	{	a	1·175547	0·48585	0·38931	0·80130
			b	1·262	0·543	0·62	1·11
	4·0	⌠	a	1·107237	0·490043	0·424633	0·866521
		⎨	b	1·1111	0·4946	0·443	0·891
		⌡	c	1·107170	0·49023	0·42449	0·86574
	5·0	⌠	a	1·071908	0·492736	0·446136	0·905426
		⎨	b	1·07223	0·49335	0·4486	0·9086
		⌡	c	1·071813	0·49261	0·44545	0·9044
	10·0	{	a	1·019396	0·497729	0·483799	0·972013
			b	1·019396	0·497729	0·483801	0·972017
$+\infty$	$k_0 = 3·0$	⌠	a	1·142757	0·496822	0·426454	0·858363
		⎨	b	1·1444	0·49717	0·4317	0·8677
		⌡	c	1·14228	0·496737	0·4249	0·8556
	3·5	⌠	a	1·108587	0·497463	0·441896	0·888299
		⎨	b	1·10889	0·497546	0·4432	0·8905
		⌡	c	1·10842	0·497421	0·44118	0·8870
	4·0	{	a	1·085203	0·497940	0·453165	0·910081
			b	1·085265	0·497963	0·45352	0·91071
	4·5	{	a	1·068537	0·498300	0·461576	0·926302
			b	1·068553	0·498308	0·46169	0·92651
	5·0	{	a	1·056265	0·498577	0·467986	0·938642
			b	1·056270	0·498580	0·468028	0·938718

8.8 An asymptotic series for the wall shear with intensive blowing

Outward mass transfer has an opposite effect to suction because it increases the thickness of the velocity boundary layer. To analyse the case of blowing, therefore, we transform the differential equation by contracting the co-ordinates, the amount of contraction again being proportional to the rate of mass transfer. As with most transformations of the velocity equation, it is useful to ensure also that the forward velocity of the fluid is still given by the gradient of the dependent variable in the new co-ordinates. A transformation which does this is:

$$\chi = \frac{\eta}{f_0}, \qquad h = \frac{f}{f_0} \qquad \qquad \dots (143)$$

which gives on substitution into equation (12):

$$\frac{1}{f_0^2} \frac{d^3 h}{d\chi^3} + h \frac{d^2 h}{d\chi^2} + \beta \left\{ 1 - \left(\frac{dh}{d\chi} \right)^2 \right\} = 0 \qquad \qquad \dots (144)$$

with boundary conditions:

$$\left. \begin{array}{l} \chi = 0, \qquad h = 1, \qquad \dfrac{dh}{d\chi} = 0 \\[3mm] \chi \rightarrow \infty, \qquad \dfrac{dh}{d\chi} \rightarrow 1. \end{array} \right\} \qquad \dots (145)$$

We again assume a series solution having the form:

$$h = h_1 + \frac{h_2}{f_0^2} + \frac{h_3}{f_0^4} + \frac{h_4}{f_0^6} + \frac{h_5}{f_0^8} + \dots \qquad \qquad \dots (146)$$

and satisfying the boundary conditions:

$$\left. \begin{array}{llll} h_1(0) = 1, & h_1'(0) = 0, & h_1'(\infty) = 1 \\[2mm] h_r(0) = h_r'(0) = h_r'(\infty) = 0, & \text{for } r \geqslant 2 \end{array} \right\} \qquad \dots (147)$$

where primes signify differentiation with respect to χ.

When we substitute equation (146) into equation (144) and equate coefficients in powers of f_0^{-2} we get a set of differential equations for the functions h_r. Apart from that for h_1, however, these are not easy to solve. On the other hand, when the equations are evaluated at the wall where $\chi = 0$, the wall shear for any particular value of r, namely $h_r''(0)$, may be expressed as a function of the wall shear for lower values of r. Since the first of these is simply $h_1''(0) = -\beta$, each $h_r''(0)$ can be expressed as a function of β.

By differentiating equation (146) twice and inserting these values of $h_r''(0)$ we get finally:

$$\frac{\nu}{v_0 \delta_4} \equiv -\frac{f_0''}{f_0} = \frac{q_1}{f_0^2} + \frac{q_2}{f_0^6} + \frac{q_3}{f_0^{10}} + \frac{q_4}{f_0^{14}} + \dots \qquad \qquad \dots (148)$$

where the coefficients are:

$$q_1 = \beta$$

$$q_2 = (1 - 2\beta)\beta^2$$

$$q_3 = (13 - 18\beta)(1 - 2\beta)\beta^3$$

$$q_4 = (448 - 1098\beta + 684\beta^2)(1 - 2\beta)\beta^4$$

$$q_5 = (29,075 - 96,262\beta + 107,948\beta^2 - 41,048\beta^3)(1 - 2\beta)\beta^5$$

$$q_6 = \left\{ \begin{array}{l} 3,052,533 - 12,307,766\beta + 18,883,332\beta^2 \\ -13,082,408\beta^3 + 3,456,288\beta^4 \end{array} \right\} (1 - 2\beta)\beta^6$$

$$q_7 = \left\{ \begin{array}{l} 473,813,584 - 2,207,664,996\beta + 4,168,446,244\beta^2 \\ - 3,991,748,504\beta^3 + 1,940,450,160\beta^4 \\ - 383,354,208\beta^5 \end{array} \right\} (1 - 2\beta)\beta^7 .$$

8.9 Application of the series in the imaginary domain

Except that $-(f_0''/f_0)$ changes sign to become $(\overline{f_0''}/\overline{f_0})$, the series in equation (148) can be used in the imaginary domain simply by writing $\overline{f_0}$ for f_0, although it must be remembered that β is then negative and $\overline{f_0}$ positive.

8.10 The series for intensive blowing when $|\beta|$ is large

The form of the series in the co-ordinates of Section 2.3, applicable when $|\beta|$ is large, can again be written down with very little calculation. It is:

$$\frac{v}{v_0 \delta_4} \equiv -\frac{\theta_0''}{k_0} = \frac{s_1}{k_0^2} + \frac{s_2}{k_0^6} + \frac{s_3}{k_0^{10}} \frac{s_4}{k_0^{14}} + \ldots \qquad \ldots (149)$$

where the coefficients are simply:

$$s_r = \frac{q_r}{\beta^{2r-1}} . \qquad \ldots (150)$$

8.11 Comparison with values in the literature

Few accurate solutions to equation (12) with intensive blowing could be found in the literature. In Table C* values of the wall shear given by equations (148) and (149) are compared with accurate values known to the authors. Those for $\beta = 0.5$ were given by Stewart and Prober[19] and most of the others were obtained by the present authors.

Each coefficient after the first in equation (148) contains the factor $(1 - 2\beta)$ and is therefore identically zero for $\beta = 0.5$. The series then reduces to the first term and was not expected to be particularly useful for this value of β. According to the numerical solutions obtained by Stewart and Prober[19], however, even this is a good approximation when $|f_0| \geqslant 2.5$.

Table C/

*See p.57.

Table C

Comparison of the Series for Intensive Blowing with Values given in the Literature

a. Values in the literature

b. From asymptotic series

c. From series after applying the Euler transformation

β	Mass transfer parameter		$-\dfrac{\nu}{v_0 \delta_4}$
$\pm \infty$	$k_0 = -3 \cdot 0$	a	0·10880273
		b	0·10898
		c	0·1088043
	$-3 \cdot 5$	a	0·08065090
		b	0·0806534
		c	0·08065066
	$-4 \cdot 0$	a	0·06204187
		b	0·06204192
		c	0·06204182
	$-5 \cdot 0$	a	0·039875482
		b	0·039875481
		c	0·039875478
$1 \cdot 0$	$f_0 = -2 \cdot 0$	a	0·23790490
		b	0·23867
		c	0·23790494
	$-2 \cdot 5$	a	0·15635564
		b	0·15635586
		c	0·15635536
	$-3 \cdot 0$	a	0·10981770
		b	0·10981764
	$-3 \cdot 5$	a	0·08111
		b	0·081106011
	$-4 \cdot 0$	a	0·06225
		b	0·062260505
	$-4 \cdot 5$	a	0 04927
		b	0 049263733
	$-5 \cdot 0$	a	0 03994
		b	0 039936506
$0 \cdot 5$	$f_0 = -2 \cdot 0$	a	0·12489365
		b	0·125
	$-2 \cdot 5$	a	0 05555551
		b	0 05555556

For $\beta = 1.0$ and $|f_0| \geq 3.5$ only four-figure accuracy was previously available, but the values obtained from the series are given in Table C to as many digits as are likely to be accurate.

With some lower values of the mass transfer parameter, it was clear from the last terms in the series that the remainder could not be neglected. Where this occurred, therefore, the convergence was improved by applying the Euler transformation, and the values obtained in this way are marked "c" in the table. For an arbitrary convergent series, not necessarily an alternating one because the terms t_k may have any sign, the transformation is represented briefly by the relationship:

$$\sum_{k=0}^{\infty} (-1)^k t_k = \sum_{\ell=0}^{} \frac{\Delta^\ell t_0}{2^{\ell+1}} \qquad \dots (151)$$

where Δ is the forward difference operator with respect to k defined by $\Delta t_k = (t_k - t_{k+1})$. The transform is discussed in many textbooks, for example Hartree[20].

It often gives the best results when applied, not to the whole series, but to the series after a number of terms. In Table C, for example, when $\beta = \infty$ it was applied after four terms; when $\beta = 1$ it was applied after two terms for $f_0 = -2 \cdot 0$, and after three terms for $f_0 = -2 \cdot 5$ but was not worth applying for $f_0 = -3 \cdot 0$ and larger, because the last term was already very small in the eighth decimal place.

Care should be exercised, however, if values of f_0'' obtained from the series are to be used in starting numerical integrations of equation (12). While the series gives f_0'' accurately when referring to the <u>differential</u> equation (12), for reasons which are not clear to the authors, this is not necessarily the most suitable value to apply to the corresponding <u>difference</u> equation solved by a computer. The point is illustrated by the following values which are quoted to as many digits as were given in the original publications; in the first reference a more accurate value than that quoted appears to have been used for $f_0 = -2 \cdot 0$ but was not given in the paper.

<u>Table D</u>

<u>Table D</u>

<u>Values of the Wall Shear</u> $-(\nu/v_0\delta_4)$ for $\beta = 1$

Source	$f_0 = -2 \cdot 0$	$f_0 = -3 \cdot 0$
Eckert, Donoughe and Moore[21]	$0 \cdot 2379$	$0 \cdot 1098177094$
Evans[7]	$0 \cdot 2379049$	$0 \cdot 1098176962$
Stewart and Prober[19]	$0 \cdot 2379052_{75}$	$0 \cdot 10981771$
Asymptotic series	$0 \cdot 2379049_{4}$	$0 \cdot 10981764$

8.12 <u>An expansion for the wall shear when $f_0 = 0$ and $|\beta|$ is large</u>

The asymptotic series given in earlier parts of Section 8 were obtained analytically from the differential equation for similar boundary layers. We shall now obtain an expression for the wall shear when $|\beta|$ is large and f_0 zero using the simpler procedure of fitting a polynomial to known numerical values.

It has already been shown that when $|\beta|$ is large it is better to use the co-ordinates of Section 2.3 and to regard $1/\beta$ as the parameter. The advantages of these co-ordinates are further demonstrated in Table E* by the small variation in θ_0'' over a wide range of β.

A polynomial of the form:

$$\theta_0'' = \frac{2}{\sqrt{3}} + \frac{t_1}{\beta} + \frac{t_2}{\beta^2} + \frac{t_3}{\beta^3} + \dots + \frac{t_9}{\beta^9} , \qquad \dots (152)$$

was fitted to the nine values taken from the literature and marked by an asterisk in Table E. After several attempts with other combinations these were considered to be the most reliable. Most of the values from the literature quoted in Table E have already been quoted in earlier papers, see for example Evans[7]. The only two values for negative $1/\beta$ were obtained by R. M. Terrill in some unpublished work with E. J. Watson at Manchester University.

The first term on the right of equation (152) is the exact value of θ_0'' for $1/\beta = 0$ and by solving nine simultaneous equations the other coefficients were found to be:

$$t_1 = 0 \cdot 0746156909 \qquad\qquad t_6 = -0 \cdot 0000475768$$
$$t_2 = 0 \cdot 0050885071 \qquad\qquad t_7 = -0 \cdot 0000910583$$
$$t_3 = -0 \cdot 0018430607 \qquad\quad t_8 = 0 \cdot 0000458438$$
$$t_4 = -0 \cdot 0003055921 \qquad\quad t_9 = -0 \cdot 0000069397$$
$$t_5 = 0 \cdot 0004313478$$

Equation (152) is very accurate in the range $2 \cdot 0 \geqslant 1/\beta \geqslant -1 \cdot 0$. Comparison with published values for positive $1/\beta$, other than those used for obtaining the coefficients, shows that the formula gives values of θ_0'' at

least/

least as accurately as they are known. Near $1/\beta = 0$ the formula is probably more accurate than published values but it is not possible to judge its accuracy for negative $1/\beta$.

The table also contains values of θ_0'' obtained from the polynomial when $1/\beta$ is given the values $1\cdot3(0\cdot1)-1\cdot0$. These required only small adjustments for use in computing the numerical solutions to equation (19) discussed in Section 6.62.

Equation (152) should only be used with caution for extrapolation outside the range $2\cdot0 \geqslant 1/\beta \geqslant -1\cdot0$, as may be seen from the error in the first two lines of Table E. The reason for this is that equation (152) is a closed polynomial and not simply the first ten terms in an exact infinite series for θ_0''. This also means that the Euler transformation cannot be applied to improve its accuracy.

Table E/

Table E

The Wall Shear when $f_0 = 0$ and $|\beta|$ is Large

*Values used to obtain coefficients in the polynomial

$\dfrac{1}{\beta}$	θ_0''	
	From the literature	From the polynomial
10/3	1·414503	1·3960128
2·5	1·350958	1·3507180
2·0	1·311938*	1·3119376
5/3	1·2856195*	1·2856195
1·3	–	1·2564794
1·25	1·2524974*	1·2524974
1·2	–	1·2485146
1·1	–	1·2405492
1·0	1·2325877*	1·2325877
0·9	–	1·2246352
5/6	1·2193413*	1·2193413
0·8	–	1·2166975
0·7	–	1·2087811
0·625	1·20286232*	1·20286232
0·6	–	1·2008936
0·5	1·1930432*	1·1930432
0·4	–	1·1852393
1/3	1·180059	1·1800675
0·3	–	1·1774920
0·25	1·173642	1·1736429
0·2	1·169811	1·1698121
1/7	1·165455	1·1654583
0·1	1·162205	1·1622111
0·05	1·158418	1·1584438
0	1·154700538	1·154700538
-0·1	–	1·1472917
-0·2	–	1·1399951
-0·25	1·136391824*	1·136391824
-0·3	–	1·1328200
-0·4	–	1·1257741
-0·5	–	1·1188628
-0·6	–	1·1120891
-0·7	–	1·1054540
-0·8	–	1·0989570
-0·9	–	1·0925972
-1·0	1·086375740*	1·086375740

8.13/

8.13 The variation of some functions with intensive suction

Figures 24 to 28 show on a large scale the variation of some boundary-layer functions under conditions of intensive suction. Figures 24 and 25 show how F_2 and H_{24}, respectively, vary with the pressure gradient as measured by λ_2, the mass transfer parameter being $(v_0 \delta_2/\nu)$. In Figs. 26, 27 and 28 which show the variation of F_1, H_{21} and H_{14}, the pressure gradient is given by λ_1 and the rate of mass transfer by $(v_0 \delta_1/\nu)$. The data for drawing these figures were obtained from the asymptotic series given in Section 8.3.

Such narrow ranges of pressure gradient and mass transfer are covered in these figures that the lines along which the relevant mass transfer parameter is a constant are virtually linear. The real and imaginary domains indicated in these figures refer, of course, to equation (12), not to equation (19).

The figures are to a large extent self-explanatory but the following points are worth noting.

In Fig. 24 the slope of the lines of constant $(v_0 \delta_2/\nu)$ is roughly $-4 \cdot 2$; the value -8 given in the Appendix to the paper by Spalding and Evans[4] is much too large because the argument presented there was not correct.

But a more important point to note is that, since these figures were drawn it has been realised that there are some, but probably small, regions included in the figures where meaningful solutions to equation (12) satisfying boundary conditions (13) do not exist; this will be discussed more fully in Section 9. As we do not yet possess enough reliable information to be able to mark off such regions for exclusion, however, the figures are given without modification.

9. Concluding Discussion

9.1 Our present knowledge of accurate similar solutions

It was seen in Section 1.3 that few solutions accurate to six digits were known before the start of the present investigations. While our knowledge of similar solutions has been appreciably extended by the data contained in the present monograph, there still remain extensive regions where few, if any, even approximate solutions exist. As a result of the investigations, several important questions have also arisen about the behaviour of solutions and further work is required in order to answer them.

Most of the solutions of high accuracy now known are indicated diagrammatically in the $F_2-\lambda_2$ plane in Fig. 29. The shaded region in that figure contains large numbers of solutions and is fairly adequately covered. Solutions are also known along the full lines, in some cases extending as far as the indicated values of λ_2 which lie beyond the range of the figure.

The unmarked regions signify one of three things. They may contain solutions of low accuracy, such as those obtained by interpolation; or there may be only incomplete solutions available, as is the case when accurate values of f_0'' are known but no estimates of either δ_1^* or δ_2^*; or, finally, there may be no solutions of any kind.

There is, of course, more information of the required accuracy available than could be accommodated on Fig. 29; we know, for example, the asymptotic behaviour of solutions with intensive blowing. The main conclusion

to be drawn from that figure, however, is that a great deal more work is needed before it can be claimed that enough solutions are known to equation (12) satisfying boundary conditions (13).

9.2 Solutions required in the near future

Accurate data in <u>any</u> of the unmarked regions of Fig. 29 where solutions are known to exist would be useful in supplementing our present knowledge. The need for obtaining solutions with accelerated flows for low and moderate rates of blowing is urgent, however, if for no other reason than that practical problems involving mass transfer occur more frequently under such conditions than any other.

Since the wall shear for blowing, whether it be f_0'' or θ_0'', can now be evaluated accurately when the appropriate mass transfer parameter is beyond -2, one major obstacle to the computation of solutions has been removed. Another troublesome one still remains, however, for when integration is carried out in the direction from the wall towards the main stream, as the rate of blowing increases it becomes progressively more difficult to satisfy the main-stream boundary condition. This difficulty is also alleviated, but probably not entirely overcome, by the method of integration described in Section 6.6.2 which of course can be used whether β is large or small. The method is described more fully in a recent publication, Evans[22].

There is less urgency about the decelerated region with β beyond -1. The interest in solutions in the imaginary domain relating to equation (12) may be more academic than practical. Information in that region, while being difficult to compute, would help clear up a number of uncertainties about the behaviour of solutions. In particular it is necessary to establish where boundary-layer solutions exist for, as we shall see, some areas must be excluded for various reasons.

9.3 Mangler's treatment of the asymptotic behaviour of solutions near the main stream

For some values of the parameter β, solutions to equation (12) satisfying boundary conditions (13) do not behave like boundary layers, either because the displacement thickness is not finite or because the dimensionless fluid velocity is not confined to the range $0 \leqslant u/u_G \leqslant 1 \cdot 0$. When the limits to boundary-layer solutions are considered in Section 9.4 it will be necessary to refer to Mangler's treatment of the asymptotic behaviour of solutions near the main stream. His approach, which is outlined briefly below, is more informative than the analysis of the same problem given in Section 4.

There are advantages in considering equation (19) instead of equation (12) and, as solutions for infinite β are now known, we shall in general assume that both k_0 and β are finite.

The following variables are introduced into equation (19):

$$z = \xi - \delta_1^{**} + k_0\beta \qquad \qquad \dots (153)$$

$$w = 1 - \theta' \qquad \qquad \dots (154)$$

so that the displacement thickness δ_1^{**} may be written:

$$\delta_1^{**}/$$

$$\delta_1^{**} = \int_0^\infty (1-\theta') d\xi = \int_{-\delta_1^{**}+k_0\beta}^\infty w \, dz. \qquad \ldots (155)$$

Since the stream function θ is then:

$$\theta = z - k_0\beta + \int_z^\infty w \, dz \qquad \ldots (156)$$

equation (19) becomes:

$$w'' + \frac{z}{\beta} w' - 2w = -w^2 - \frac{w'}{\beta} \int_z^\infty w \, dz \qquad \ldots (157)$$

where primes signify differentiation with respect to z.

The function w is small near the main-stream and terms on the right of equation (157) become much smaller than those on the left. Mangler's asymptotic form of the velocity equation near the main stream is therefore:

$$w'' + \frac{z}{\beta} w' - 2w = 0 \qquad \ldots (158)$$

and solutions are required such that $w \to 0$ as $z \to \infty$.

When a solution of the form:

$$w = z^r e^{mz^2} \sum_{n=0}^\infty \frac{Pn}{z^n} \qquad \ldots (159)$$

is assumed, it is found by standard methods that m has the two values $m = 0$ and $m = -1/2\beta$ and the solutions for these two cases are:

__m = 0__

$$w_1 = p_0 z^{2\beta} \left\{ 1 + (2\beta-1) \frac{\beta^2}{z^2} + \ldots \right\}$$

$$+ p_1 z^{2\beta-1} \left\{ 1 + (2\beta-1)(2\beta-2) \frac{\beta}{3z^2} + \ldots \right\} \qquad \ldots (160)$$

__m = -1/2\beta__

$$w_2 = p_0 z^{2\beta-1} e^{-z^2/2\beta} \left\{ 1 - (2\beta-1)(2\beta-2) \frac{\beta}{2z^2} + \ldots \right\}$$

$$+ p_1 z^{2\beta-2} e^{-z^2/2\beta} \left\{ 1 - (2\beta-2)(2\beta-3) \frac{\beta}{3z^2} + \ldots \right\} \qquad \ldots (161)$$

where p_0 and p_1 are arbitrary constants in each case.

For/

For decelerated flows the variable z is pure imaginary. If we then write $z = i\bar{z}$, where $\bar{z}$ is real, and change w to $\bar{w}$, close to the main stream the function $\bar{w}$ obeys an equation which differs from equation (158) only in having a negative in place of a positive sign preceding the first term. The solutions to this are:

m = 0

$$\bar{w}_1 = p_0 \bar{z}^{-2\beta} \left\{ 1 - (2\beta-1) \frac{\beta^2}{\bar{z}^2} + \ldots \right\}$$

$$+ p_1 \bar{z}^{-2\beta-1} \left\{ 1 - (2\beta-1)(2\beta-2) \frac{\beta}{3\bar{z}^2} + \ldots \right\} \qquad \ldots (162)$$

m = 1/2β

$$\bar{w}_2 = p_0 \bar{z}^{-(2\beta+1)} e^{\bar{z}^2/2\beta} \left\{ 1 + (2\beta+1)(2\beta+2) \frac{\beta}{2\bar{z}^2} + \ldots \right\}$$

$$+ p_1 \bar{z}^{-(2\beta+2)} e^{\bar{z}^2/2\beta} \left\{ 1 + (2\beta+2)(2\beta+3) \frac{\beta}{3\bar{z}^2} + \ldots \right\}$$

$$\ldots (163)$$

p_0 and p_1 again being arbitrary constants.

When the parameter β is infinite it is necessary to change the independent co-ordinate from z to $z_1 = (z - k_0 \beta)$. The asymptotic equation (158) then has the form:

$$w'' + k_0 w' - 2w = 0 \qquad \ldots (164)$$

the primes now signifying differentiation with respect to z_1. For pure imaginary variables this equation becomes:

$$\bar{w}'' - \bar{k}_0 \bar{w}' + 2\bar{w} = 0 \qquad \ldots (165)$$

where the primes mean differentiation with respect to $\bar{z}_1$.

9.4 Limits to boundary-layer solutions

We now discuss the limiting values of the parameters β and f_0 (or k_0) beyond which solutions to equation (12) do not behave like boundary layers. Two of the known limits are marked on Fig. 29; they are:

1. The separation solution for flow over a flat plate when the displacement thickness becomes infinite, and

2. The case of infinite β with imaginary variables when $\bar{k}_0$ reaches the limiting value $\bar{k}_0 = -8\bar{z}$; for smaller values of $\bar{k}_0$ the gradient $(d\bar{y}/d\bar{\phi})$ (see Section 6.5.2(b)) at the main-stream edge of the boundary layer becomes imaginary. This limit is also deducible by an examination of solutions to equation (165).

It/

It is readily shown that no boundary-layer solutions exist for $\beta = 0$ with imaginary variables, for the equation is then:

$$-\bar{f}''' + \bar{f}\bar{f}'' = 0 \qquad \qquad \ldots \text{(166)}$$

where the primes mean differentiation with respect to the dimensionless distance $\bar{\eta}$. Reference to Section 4.3 shows that the dimensionless shear is then:

$$\bar{f}'' = \bar{f}_0'' \exp.\left\{ \int_0^{\bar{\eta}} \bar{f} \, d\bar{\eta} \right\} \qquad \qquad \ldots \text{(167)}$$

where $\bar{f}_0''$ is its value at the wall. Now, near the main stream the exponent $\int_0^{\bar{\eta}} \bar{f} \, d\bar{\eta}$ is large and increasing in magnitude. Solutions to equation (166), therefore, do not approach the state of inviscid flow at large distances from the wall and consequently cannot be associated with any real boundary layers.

By examination of the asymptotic solutions in equations (160) to (163), however, we can exclude a wide range of β values extending on either side of $\beta = 0$ in the imaginary domain indicated in Fig. 29.

From equation (155) the contribution to the displacement thickness from points near the main stream is:

$$\text{Contribution to} \quad \delta_1^{**} = \int_z^{\infty} w \, dz \qquad \qquad \ldots \text{(168)}$$

where z is large.

We therefore have:

(a) <u>For accelerated flows</u>

This is the case of real variables in equation (19).

When β is positive the solution w_2 in equation (161) must be used for large z. When z is large enough this reduces to the first term and so it is:

$$w_2 \simeq p_0 \, z^{2\beta-1} \, e^{-z^2/2\beta} \qquad \qquad \ldots \text{(169)}$$

which rapidly decreases to zero as z increases. When this is inserted for w in equation (168) we see that δ_1^{**} remains finite for all positive β.

When β is negative the solution w_1 in equation (160) must be chosen and for large z this is:

$$w_1 \simeq p_0 \, z^{2\beta} \qquad \qquad \ldots \text{(170)}$$

which gives a finite contribution to δ_1^{**} only when $|\beta| > 0.5$.

With/

With accelerated flows, therefore, there are no solutions with a finite displacement thickness beyond the value $\beta = -0\cdot5$; this limiting line is shown in Fig. 29.

Because the momentum thickness will also be infinite for $\beta = -0\cdot5$, the line for no mass transfer marked in Fig. 29 will meet the line $\beta = -0\cdot5$ at infinity. The slope of the zero mass transfer line has the following approximate values near the values of β indicated:

$\beta =$	$-0\cdot198838$	0	$1\cdot0$	$\pm\infty$	$-1\cdot0$
Slope of line $(v_0\delta_2/\nu) = 0$	$-6\cdot24$	$-5\cdot31$	$-5\cdot07$	$-5\cdot05$	$-5\cdot28$

and for very highly accelerated flows this slope must clearly approach that of the line $\beta = -0\cdot5$ in Fig. 29, namely $-6\cdot0$.

It is interesting to note that the no-mass transfer line seems to possess a stationary value.

(b) **For decelerated flows**

This is the case of imaginary variables in equation (19).

When β is negative the asymptotic solution $\overline{w}_2$ in equation (163) must be chosen for large $\overline{z}$. When z is large enough this is

$$\overline{w}_2 \simeq p_0\overline{z}^{-(2\beta+1)} e^{\overline{z}^2/2\beta}$$

and clearly $\overline{\delta}_1^{**}$ is finite whatever negative value β may have.

When β is positive on the other hand, neither $\overline{w}_1$ nor $\overline{w}_2$ gives a finite displacement thickness. Therefore there appear to be no boundary-layer solutions for decelerated flows below the line for infinite β shown in Fig. 29.

9.5 **Some unresolved questions concerning the behaviour of solutions**

In the next stage of the work, not only is there need for further accurate solutions but answers should also be provided to a number of questions about the behaviour of solutions, prompted to some extent by the conclusions arrived at in Section 9.4.

One such question, possibly a minor one, concerns the behaviour of solutions close to that which gives separation for $\beta = 0$. When β is small and positive there is a slight but favourable pressure gradient which prevents the wall shear from decreasing to zero however large the blowing rate may be. According to equation (148), when β is very small and f_0 large and negative, the dimensionless wall shear is approximately:

$$f_0'' = -\frac{\beta}{f_0} \qquad \qquad \dots (172)$$

so that it may become very small but not zero, unless β is itself zero. What, however, happens to the displacement thickness? Does it become large very rapidly as occurs with $\beta = 0$?

The behaviour of solutions for accelerated flows as β approaches the limiting value -0.5 is quite reasonable because the displacement thickness increases gradually as β approaches this limit; at the limit, of course, the displacement thickness is infinite.

The explanation of the behaviour of solutions near the limits with decelerated flows is not so acceptable, however. The following argument will be given in terms of the form of equation (19) with imaginary variables, so that the parameter is $1/\beta$ instead of β itself. On examination of the results given elsewhere in the monograph one is prompted to ask the following questions:

1. How is it possible to reconcile the following two solutions?

	$1/\beta$	$\bar{k}_0$	λ_2	$(v_0\delta_2/\nu)$
(a)	0·0	$8^{\frac{1}{2}}$ = 2·828	-0·0977	-0·8840
(b)	-0·0555	2·520	-0·4219	-1·637

Solution (a) is the limiting case for infinite β and (b) is the separation solution for $\beta = -18$. Although $\bar{k}_0$ is larger in (a) than in (b), yet how is it possible to obtain a boundary-layer solution, namely (b), whose value of $1/\beta$ is not very different from zero, but with values of λ_2 and $(v_0\delta_2/\nu)$ which are well beyond those for the limiting case for $1/\beta = 0$?

2. With decelerated flows what happens to solutions as $1/\beta$ passes through zero?

It appears from the earlier conclusions that as long as $|\bar{k}_0| \geqslant 8^{\frac{1}{2}}$ and $1/\beta$ is negative or zero, the displacement thickness remains finite. As soon as $1/\beta$ becomes positive, however, the displacement thickness suddenly becomes infinite. Although it has not yet been possible to find a flaw in the mathematical arguments leading to these conclusions, such unexpected behaviour by the solutions does prompt one to ask whether those arguments are indeed correct.

Acknowledgements

---

*Now Professor of Mathematics, University of Tasmania, Hobart, Tasmania, Australia.

References

No.	Author(s)	Title, etc.
1	L. Howarth	On the solution of the laminar boundary layer equations. Proc. Roy. Soc. A, <u>164</u>, 547-579 (1938).
2	H. Görtler	A new series for the calculation of steady laminar boundary-layer flows. J. Math & Mechs., <u>6</u>, 1 (1957).
3	H. W. Hahnemann	Zur exakten Lösung der vollständigen Bewegungsgleichung und der Energiegleichung für die laminare Strömung um ebene Keilkörper. Int. J. Heat Mass Transfer, <u>5</u>, 189-209 (1962).
4	D. B. Spalding and H. L. Evans	Mass transfer through laminar boundary layers - 2. Auxiliary functions for the velocity boundary layer. Int. J. Heat Mass Transfer, <u>2</u>, 199-221 (1961).
5	D. B. Spalding	Mass transfer through laminar boundary layers - 1. The velocity boundary layer. Int. J. Heat Mass Transfer, <u>2</u>, 15-32 (1961).
6	E. J. Watson	The asymptotic theory of boundary-layer flow with suction. Parts I, II and III. R.& M.2619 (September, 1947).
7	H. L. Evans	Mass transfer through laminar boundary layers - 8. Further solutions to the velocity equation. Int. J. Heat Mass Transfer, <u>5</u>, 373-407 (1962).
8	D. B. Spalding and H. L. Evans	Mass transfer through laminar boundary layers - 3. Similar solutions of the b-equation. Int. J. Heat Mass Transfer, <u>2</u>, 314-341 (1961).
9	H. L. Evans	Mass transfer through laminar boundary layers - 7. Further similar solutions to the b-equation for the case $B = 0$. Int. J. Heat Mass Transfer, <u>5</u>, 35-57 (1962).
10	B. Thwaites	The development of the laminar boundary layer under conditions of continuous suction - Part I. A.R.C.11 830 - F.M.1296 (1948).
11	H. W. Emmons and D. Leigh	Tabulation of the Blasius function with blowing and suction. Harvard Univ. Combustion Aero. Lab., Interim Technical Report No.9 (1953).
12	H. L. Evans	Mass transfer through laminar boundary layers - 6. Methods of evaluating the wall gradient (b_0'/B) for similar solutions; some new values for zero main-stream pressure gradient. Int. J. Heat Mass Transfer, <u>3</u>, 321-339 (1961).

References (Continued)

No.	Author(s)	Title, etc.

13 W. B. Brown
    and
    P. L. Donoughe

Tables of exact laminar boundary-layer solutions when the wall is porous and fluid properties are variable.
N.A.C.A. T.N.2479 (1951).

14 R. M. Terrill

Laminar boundary-layer flow near separation with and without suction.
Phil. Trans. Roy. Soc. A, 253, No.1022, 55 (1960).

15 D. R. Hartree

Note on a set of solutions to the equation
$y'' + (2/x)y' - y^2 = 0$.
Mem. & Proc. Manchester Lit. Phil. Soc., 81, 19-28 (1937).

16 B. Thwaites

On two solutions of the boundary-layer equations, in 50 Jahre Grenzschichtforschung, (ed. H. Görtler and W. Tollmien), 210 (1955).

17 H. Holstein

Ähnliche laminare Reibungsschichten an durch-lässigen Wänden, Deutsche Luftfahrtforschung, U.M. 3050 (1943).

18 J. Pretsch

Die laminare Grenzschicht bei starkem Absaugen und Ausblasen, Deutsche Luftfahrtforschung, U.M.3091 (1944).

19 W. E. Stewart
    and
    R. Prober

Heat transfer and diffusion in wedge flows with rapid mass transfer.
Int. J. Heat Mass Transfer, 5, 1149-1163 (1962).

20 D. R. Hartree

Numerical Analysis. Clarendon Press, Oxford, (1952).

21 E. R. G. Eckert,
    P. L. Donoughe
    and
    B. J. Moore

Velocity and friction characteristics of laminar viscous boundary-layer and channel flow over surfaces with ejection or suction.
N.A.C.A. T.N. 4102 (1957).

22 H. L. Evans

Integration of the velocity equation of the laminar boundary layer including the effects of mass transfer.
A.I.A.A. Journal 1, 1677 (1963).

23 W. Mangler

Die "ähnlichen" Lösungen der Prandtlschen Grenzschichtgleichungen, Z. angew. Math. Mech. 23, 241-251 (1943).

SOLUTIONS FOR ACCELERATED FLOWS: β POSITIVE

Numerical solutions are tabulated for the following eleven values of the parameter β:

$$\beta = 0 \cdot 1(0 \cdot 1)0 \cdot 6, \ 0 \cdot 8, \ 1 \cdot 0, \ 1 \cdot 2, \ 1 \cdot 6, \ 2 \cdot 0,$$

for each of which the mass transfer parameter f_0 is given the seven values:

$$f_0 = 3 \cdot 0(0 \cdot 5)0 \cdot 0.$$

For $\beta = 1 \cdot 0$ the following additional solutions are given:

Intensive suction: $f_0 = 10, \ 5, \ 4;$

Blowing: $f_0 = -0 \cdot 5, \ -1 \cdot 0, \ -1 \cdot 5.$

TABLE I-1.

SOLUTIONS TO THE VELOCITY EQUATION FOR $\beta=0.1$, $\quad 3.0 \geqslant f_0 \geqslant 0$

f_o	f_o''	δ_1^*	δ_2^*	$\dfrac{\nu_o \delta_2}{\nu}$	H_{12}	H_{24}	$\lambda_2 \equiv \dfrac{\delta_2^2}{\nu}\dfrac{d u_G}{d x}$	$F_2 \equiv \dfrac{u_G}{\nu}\dfrac{d \delta_2^2}{d x}$
3.0	3.18716	0.29566	0.14327	−0.42980	2.0637	0.45662	0.20526(−2)	0.036946
2.5	2.714434	0.34123	0.16392	−0.40980	2.0817	0.44495	0.26869(−2)	0.048365
2.0	2.24974	0.40161	0.19053	−0.38105	2.1079	0.42863	0.36300(−2)	0.065341
1.5	1.79668	0.48448	0.22567	−0.33850	2.1469	0.40545	0.50925(−2)	0.091665
1.0	1.36101	0.60338	0.27334	−0.27334	2.2074	0.37202	0.74714(−2)	0.13448
0.5	0.952276	0.78402	0.33989	−0.16994	2.3067	0.32366	0.11552(−1)	0.20794
0.0	0.587035	1.08032	0.43546	0.0	2.4809	0.25563	0.18962(−1)	0.34132

TABLE I-2.

SOLUTIONS TO THE VELOCITY EQUATION FOR $\beta = 0.2,\ 3.0 \geq f_o \geq 0$

f_o	f_o''	δ_1^*	δ_2^*	$\dfrac{v_o\,\delta_2}{\nu}$	H_{12}	H_{24}	$\lambda_2 \equiv \dfrac{\delta_2^2}{\nu}\dfrac{du_q}{dx}$	$F_2 \equiv \dfrac{u_q}{\nu}\dfrac{d\delta_2^2}{dx}$
3.0	3.2282	0.29191	0.14152	-0.42455	2.0628	0.45684	0.40053(-2)	0.032042
2.5	2.76083	0.33572	0.16141	-0.40351	2.0800	0.44561	0.52103(-2)	0.041683
2.0	2.3028	0.39313	0.18681	-0.37362	2.1044	0.43019	0.69797(-2)	0.055838
1.5	1.858094	0.47073	0.21996	-0.32994	2.1401	0.40870	0.96762(-2)	0.077410
1.0	1.43292	0.57953	0.26418	-0.26418	2.1937	0.37855	0.13958(-1)	0.11166
0.5	1.037156	0.73886	0.32449	-0.16224	2.2770	0.33654	0.21058(-1)	0.16847
0.0	0.686708	0.98416	0.40823	0.0	2.4108	0.28033	0.33330(-1)	0.26664

TABLE I-3.

SOLUTIONS TO THE VELOCITY EQUATION FOR $\beta = 0.3$, $3.0 \geq f_0 \geq 0$.

f_0	f_0''	δ_1^*	δ_2^*	$\dfrac{u_0 \delta_2}{\nu}$	H_{12}	H_{24}	$\lambda_2 \equiv \dfrac{\delta_2^2}{\nu}\dfrac{du_G}{dx}$	$F_2 \equiv \dfrac{u_G}{\nu}\dfrac{d\delta_2^2}{dx}$
3.0	3.26828	0.28834	0.13983	-0.41949	2.0621	0.45700	0.58657(-2)	0.027373
2.5	2.80588	0.33053	0.15902	-0.39754	2.0786	0.44618	0.75858(-2)	0.035401
2.0	2.35391	0.38527	0.18333	-0.36666	2.1015	0.43154	0.10083(-1)	0.047054
1.5	1.916588	0.45824	0.21471	-0.32206	2.1343	0.41150	0.13830(-1)	0.064538
1.0	1.50031	0.55856	0.25596	-0.25596	2.1823	0.38401	0.19654(-1)	0.091718
0.5	1.114818	0.70121	0.31112	-0.15556	2.2538	0.34684	0.29039(-1)	0.13551
0.0	0.774755	0.91099	0.38574	0.0	2.3617	0.29885	0.44639(-1)	0.20831

TABLE I-4.

SOLUTIONS TO THE VELOCITY EQUATION FOR $\beta = 0.4$, $3.0 \geqslant f_0 \geqslant 0$.

f_0	f_0''	δ_1^*	δ_2^*	$\dfrac{v_0 \delta_2}{\nu}$	H_{12}	H_{24}	$\lambda_2 = \dfrac{\delta_2^2}{\nu}\dfrac{du_G}{dx}$	$F_2 \equiv \dfrac{u_G}{\nu}\dfrac{d\delta_2^2}{dx}$
3.0	3.30747	0.28493	0.13821	-0.41463	2.0616	0.45713	0.76408(-2)	0.022922
2.5	2.84970	0.32561	0.15675	-0.39188	2.0773	0.44669	0.98282(-2)	0.029485
2.0	2.40326	0.37793	0.18006	-0.36012	2.0989	0.43273	0.12969(-1)	0.038906
1.5	1.97252	0.44682	0.20985	-0.31478	2.1292	0.41393	0.17615(-1)	0.052844
1.0	1.563888	0.53992	0.24851	-0.24851	2.1726	0.38864	0.24703(-1)	0.074109
0.5	1.186757	0.66913	0.29936	-0.14968	2.2352	0.35527	0.35847(-1)	0.10754
0.0	0.854421	0.85264	0.36669	0.0	2.3252	0.31331	0.53785(-1)	0.16135

TABLE I-5.

SOLUTIONS TO THE VELOCITY EQUATION FOR $\beta = 0.5,\ 3.0 \geqslant f_0 \geqslant 0$

f_0	f_0''	δ_1^*	δ_2^*	$\dfrac{v_e\,\delta_2}{\nu}$	H_{21}	H_{24}	λ_2	F_2
3.0	3.3458266	0.2816513	0.1366673	– 0.4100019	0.4852358	0.4572651	0.009338976	0.01867795
2.5	2.8923738	0.3209478	0.1545999	– 0.3864998	0.4816980	0.4471607	0.01195056	0.02390113
2.0	2.4510130	0.3710622	0.1769880	– 0.3539760	0.4769766	0.4337999	0.01566238	0.03132475
1.5	2.0261761	0.4363261	0.2053420	– 0.3080130	0.4706159	0.4160591	0.02108267	0.04216534
1.0	1.62419876	0.5232081	0.2417298	– 0.2417298	0.4620146	0.3926172	0.02921665	0.05843330
0.5	1.254022540	0.6413407	0.2889015	– 0.1444508	0.4504649	0.3622890	0.04173204	0.08346408
0.0	0.92768006	0.8045491	0.3502703	0.0	0.4353622	0.3249388	0.06134464	0.1226893

TABLE I-6.

SOLUTIONS TO THE VELOCITY EQUATION FOR $\beta = 0.6,\ 3.0 \geq f_o \geq 0$.

f_o	f_o''	δ_1^*	δ_2^*	$\dfrac{v_o\,\delta_2}{\nu}$	H_{12}	H_{24}	$\lambda_2 = \dfrac{\delta_2^2}{\nu}\dfrac{du_G}{dx}$	$F_2 = \dfrac{u_G}{\nu}\dfrac{d\,\delta_2^2}{dx}$
3.0	3.3834	0.27850	0.13519	-0.40557	2.0601	0.45740	0.010966	0.014621
2.5	2.933988	0.31650	0.15256	-0.38140	2.0746	0.44761	0.013965	0.018620
2.0	2.497306	0.36461	0.17409	-0.34818	2.0944	0.43476	0.018184	0.024246
1.5	2.077807	0.42661	0.20115	-0.30173	2.1209	0.41795	0.024277	0.032369
1.0	1.681678	0.50808	0.23552	-0.23552	2.1573	0.39607	0.033282	0.044376
0.5	1.317387	0.61693	0.27952	-0.13976	2.2071	0.36824	0.046879	0.062505
0.0	0.9958366	0.76397	0.33591	0.0	2.2743	0.33451	0.067701	0.090268

TABLE I-7

SOLUTIONS TO THE VELOCITY EQUATION FOR $\beta = 0.8$, $3.0 \geq f_o \geq 0$

f_o	f_o''	δ_1^*	δ_2^*	$\dfrac{\mathcal{N}_o \delta_2}{\nu}$	H_{12}	H_{24}	$\lambda_2 = \dfrac{\delta_2^2}{\nu}\dfrac{du_c}{dx}$	$F_2 = \dfrac{u_c}{\nu}\dfrac{d\delta_2^2}{dx}$
3.0	3.456353	0.27258	0.13238	-0.39714	2.0591	0.45755	0.014020	0.0070098
2.5	3.014297	0.30825	0.14872	-0.37180	2.0727	0.44829	0.017694	0.0088471
2.0	2.585974	0.35279	0.16875	-0.33750	2.0906	0.43638	0.022781	0.011391
1.5	2.175753	0.40920	0.19355	-0.29033	2.1142	0.42112	0.029969	0.014985
1.0	1.789455	0.48169	0.22450	-0.22450	2.1456	0.40173	0.040320	0.020160
0.5	1.434611	0.57584	0.26330	-0.13165	2.1870	0.37773	0.055462	0.027731
0.0	1.1202677	0.69868	0.31185	0.0	2.2404	0.34936	0.0778‑0	0.038900

TABLE I-8

SOLUTIONS TO THE VELOCITY EQUATION FOR $\beta = 1.0$, $10 \geq f_0 \geq -1.5$

f_0	f_0''	δ_1^*	δ_2^*	$\dfrac{v_0 \delta_2}{\nu}$	H_{21}	H_{24}	λ_2
10.0	10.193961	0.0972013	0.0483799	-0.483799	0.497729	0.493183	0.00234061
5.0	5.3595396	0.1810852	0.0892272	-0.446136	0.492736	0.478217	0.00796149
4.0	4.4289466	0.2166303	0.1061582	-0.4246328	0.4900432	0.4701690	0.01126956
3.0	3.52664010	0.2671050	0.1297676	-0.3893028	0.4858299	0.4576436	0.01683963
2.5	3.09112450	0.3007199	0.1452023	-0.3630058	0.4828490	0.4488384	0.02108371
2.0	2.67005580	0.3421973	0.1639293	-0.3278586	0.4790491	0.4377004	0.02687282
1.5	2.26764600	0.3939862	0.1868299	-0.2802449	0.4742042	0.4236641	0.03490541
1.0	1.88931375	0.4593224	0.2149957	-0.2149957	0.4680714	0.4061943	0.04622315
0.5	1.54175106	0.5423340	0.2497085	-0.1248543	0.4604331	0.3849883	0.06235433
0.0	1.23258760	0.6479004	0.2923436	0.0	0.4512168	0.3603391	0.08546477
-0.5	0.969229535	0.7809627	0.3441334	0.1720667	0.4406528	0.3335443	0.1184278
-1.0	0.756574938	0.9449815	0.4057967	0.4057967	0.4294229	0.3070156	0.1646710
-1.5	0.594281857	1.13998	0.47715	0.71573	0.41856	0.28356	0.22767

TABLE I-9

SOLUTIONS TO THE VELOCITY EQUATION FOR $\beta = 1.2$, $3.0 \geqslant f_0 \geqslant 0$

f_0	f_0''	δ_1^*	δ_2^*	$\dfrac{v_0\,\delta_2}{\nu}$	H_{12}	H_{24}	$\lambda_2 = \dfrac{\delta_2^2}{\nu}\dfrac{du_q}{dx}$	$F_2 = \dfrac{u_q}{\nu}\dfrac{d\delta_2^2}{dx}$
3.0	3.594534	0.26200	0.12733	-0.38199	2.0577	0.45769	0.019456	-0.0064852
2.5	3.1648758	0.29379	0.14197	-0.35493	2.0694	0.44932	0.024187	-0.0080622
2.0	2.750172	0.33263	0.15955	-0.31910	2.0848	0.43879	0.030547	-0.010182
1.5	2.354448	0.38052	0.18083	-0.27125	2.1043	0.42575	0.039239	-0.013080
1.0	1.982722	0.44002	0.20668	-0.20668	2.1290	0.40979	0.051260	-0.017087
0.5	1.6409684	0.51430	0.23809	-0.11905	2.1601	0.39070	0.068024	-0.022675
0.0	1.3357215	0.60689	0.27612	0.0	2.1979	0.36882	0.091491	-0.030497

TABLE I-10.

SOLUTIONS TO THE VELOCITY EQUATION FOR $\beta = 1.6$, $3.0 \geq f_0 \geq 0$.

f_0	f_0''	δ_1^*	δ_2^*	$\dfrac{v_0 \delta_2}{\nu}$	H_{12}	H_{24}	$\lambda_2 \equiv \dfrac{\delta_2^2}{\nu}\dfrac{du_c}{dx}$	$F_2 \equiv \dfrac{u_4}{\nu}\dfrac{d\delta_2^2}{dx}$
3.0	3.723984	0.25275	0.12292	−0.36876	2.0562	0.45775	0.024175	−0.018131
2.5	3.304409	0.28148	0.13617	−0.34043	2.0671	0.44996	0.029668	−0.022251
2.0	2.900391	0.31596	0.15187	−0.30374	2.0805	0.44048	0.036903	−0.027677
1.5	2.515558	0.35763	0.17052	−0.25578	2.0973	0.42895	0.046523	−0.034892
1.0	2.154214	0.40819	0.19273	−0.19273	2.1179	0.41518	0.059432	−0.044574
0.5	1.8212023	0.46962	0.21916	−0.10958	2.1428	0.39913	0.076850	−0.057637
0.0	1.52151386	0.54402	0.25042	0.0	2.1724	0.38102	0.10034	−0.075252

TABLE I-II.

SOLUTIONS TO THE VELOCITY EQUATION FOR $\beta = 2.0, \quad 3.0 \geq f_0 \geq 0$

f_0	f_0''	δ_1^*	δ_2^*	$\dfrac{v_0\,\delta_2}{\nu}$	H_{12}	H_{24}	$\lambda_2 \equiv \dfrac{\delta_2^2}{\nu}\dfrac{du_G}{dx}$	$F_2 \equiv \dfrac{u_G}{\nu}\dfrac{d\,\delta_2^2}{dx}$
3.0	3.8461402	0.24458	0.11899	-0.35697	2.0555	0.45765	0.028317	-0.028317
2.5	3.4349672	0.27080	0.13112	-0.32780	2.0653	0.45039	0.034385	-0.034385
2.0	3.0396070	0.30185	0.14530	-0.29060	2.0774	0.44165	0.042224	-0.042224
1.5	2.6633174	0.33877	0.16193	-0.24290	2.0921	0.43127	0.052443	-0.052443
1.0	2.30981668	0.38278	0.18142	-0.18142	2.1099	0.41905	0.065826	-0.065826
0.5	1.9831240	0.43521	0.20423	-0.10212	2.1310	0.40502	0.083420	-0.083420
0.0	1.6872179	0.49743	0.23079	0.0	2.1553	0.38939	0.10653	-0.10653

SOLUTIONS FOR DECELERATED FLOWS; β NEGATIVE

Numerical solutions are tabulated for the following values of the parameters β and corresponding values of f_0:

β	f_0
0·0	3·0(0·5)0·0
−0·1	3·0(0·5)0·0
−0·2	3·0(0·5)0·5, 0·0031
−0·3	3·0(0·5)0·5, 0·2461
−0·4	3·0(0·5)0·5, 0·4567
−0·5	3·0(0·5)1·0, 0·6460
−0·6	3·0(0·5)1·0, 0·8196
−0·8	3·0(0·5)1·5, 1·1332
−1·0	3·0(0·5)1·5, $\sqrt{2}$

Except for the first two values of β, the values of f_0 on the right of this table, quoted only as far as the fourth decimal place, give the separation solutions. More accurate values of f_0 and detailed tabulations of these and other separation solutions are given in Group III.

TABLE II-1.

SOLUTIONS TO THE VELOCITY EQUATION FOR $\beta = 0.0$, $3.0 \geq f_o \geq 0$

f_o	f_o''	δ_1^*	δ_2^*	$\frac{v_o \delta_2}{y}$	H_{21}	H_{24}	F_2
3.0	3.1451010	0.2995928	0.1451010	-0.4353030	0.4843274	0.4563573	0.04210860
2.5	2.6665666	0.3470936	0.1665666	-0.4164165	0.4798896	0.4441609	0.05548886
2.0	2.1945090	0.4107680	0.1945090	-0.3890080	0.4735252	0.4268408	0.07566362
1.5	1.7319130	0.4997125	0.2319130	-0.3478695	0.4640929	0.4016531	0.1075673
1.0	1.2836345	0.6308872	0.2836345	-0.2836345	0.4495804	0.3640830	0.1608971
0.5	0.8579159	0.8398180	0.3579159	-0.1789580	0.4261827	0.3070617	0.2562076
0.0	0.4696000	1.2167681	0.4696000	0.0	0.3859404	0.2205242	0.4410483

TABLE II-2.

SOLUTIONS TO THE VELOCITY EQUATION FOR $\beta = -0.1, 3.0 \geq f_0 \geq 0$

f_o	f_o''	δ_1^*	δ_2^*	$\dfrac{u_o \delta_2}{\nu}$	H_{21}	H_{24}	λ_2	F_2
3.0	3.1019533	0.3037209	0.1470282	-0.4410846	0.4840898	0.4560746	-0.002161729	0.04755804
2.5	2.6171134	0.3533247	0.1693843	-0.4234608	0.4794012	0.4432979	-0.002869104	0.06312029
2.0	2.1368524	0.4207035	0.1988031	-0.3976062	0.4725492	0.4248129	-0.003952267	0.08694988
1.5	1.6632368	0.5167353	0.2387893	-0.3581840	0.4621115	0.3971632	-0.005702033	0.1254447
1.0	1.1994892	0.6631504	0.2953380	-0.2953380	0.4453560	0.3542547	-0.008722453	0.1918940
0.5	0.7504018	0.9116167	0.3795150	-0.1897575	0.4163098	0.2847887	-0.01440316	0.3168696
0.0	0.3192696	1.4426978	0.5150438	0.0	0.3570005	0.1644378	-0.02652701	0.5835943

TABLE II-3.

SOLUTIONS TO THE VELOCITY EQUATION FOR $\beta = -0.2$, $3.0 \geq f_0 \geq 0.0030926$

f_0	δ_0^*	δ_1^*	δ_2^*	$\dfrac{v_0 \delta_2}{\nu}$	$H_{2,1}$	$H_{2,4}$	λ_2	F_2
3.0	3.0576278	0.3080690	0.1490520	-0.4471560	0.4838267	0.4557455	-0.004443298	0.05331958
2.5	2.5659078	0.3599824	0.1723804	-0.4309510	0.4788579	0.4423122	-0.005943000	0.07131600
2.0	2.0764478	0.4315499	0.2034472	-0.4068944	0.4714338	0.4224475	-0.008278152	0.09933782
1.5	1.5899375	0.5359597	0.2464118	-0.3696177	0.4597581	0.3917794	-0.01214376	0.1457251
1.0	1.1066908	0.7018353	0.3088223	-0.3088223	0.4400210	0.3417708	-0.01907424	0.2288909
0.5	0.6229144	1.0102405	0.4062031	-0.2031016	0.4020855	0.2530298	-0.03300019	0.3960023
0.0030926	0.0	2.3548790	0.5848540	-0.0018087	0.2483584	0.0	-0.06841084	0.8209301

TABLE II-4

SOLUTIONS TO THE VELOCITY EQUATION FOR $\beta = -0.3$, $3.0 \geq f_o \geq 0.2461484$

f_o	f_o'	δ_1^*	δ_2^*	$\dfrac{v_o \delta_2}{\nu}$	H_{21}	H_{24}	λ_2	F_2
3.0	3.0120275	0.3126613	0.1511798	-0.4535394	0.4835258	0.4553577	-0.006856599	0.05942386
2.5	2.5127634	0.3671264	0.1755733	-0.4389333	0.4782367	0.4411742	-0.009247794	0.08014755
2.0	2.0129036	0.4434698	0.2084922	-0.4169844	0.4701384	0.4196747	-0.01304070	0.1130194
1.5	1.5110704	0.5579409	0.2549324	-0.3823986	0.4569165	0.3852208	-0.01949716	0.1689754
1.0	1.0023506	0.7496238	0.3246253	-0.3246253	0.4330510	0.3253884	-0.03161448	0.2739921
0.5	0.4596192	1.1632899	0.4408660	-0.2204330	0.3789821	0.2026305	-0.05830885	0.5053434
0.2461484	0.0	2.0885724	0.5434619	-0.1338109	0.2602074	0.0	-0.08860525	0.7679122

TABLE II-5.

SOLUTIONS TO THE VELOCITY EQUATION FOR $\beta = -0.4$, $3.0 \geq f_o \geq 0.456757$

f_o	f_o''	δ_1^*	δ_2^*	$\dfrac{v_o \, \delta_2}{\nu}$	H_{21}	H_{24}	λ_2	F_2
3.0	2.9650480	0.3175165	0.1534243	-0.4602729	0.4832010	0.4549104	-0.009415608	0.06590926
2.5	2.4574680	0.3748150	0.1789900	-0.4474750	0.4775423	0.4398622	-0.01281497	0.08970478
2.0	1.9457416	0.4566548	0.2140059	-0.4280118	0.4686382	0.4164002	-0.01831941	0.1282359
1.5	1.4253550	0.5834469	0.2645563	-0.3968345	0.4534368	0.3770866	-0.02799602	0.1959721
1.0	0.8816612	0.8112085	0.3435743	-0.3435743	0.4235339	0.3029161	-0.04721732	0.3305212
0.5	0.1901886	1.5112398	0.4911409	-0.2455705	0.3249920	0.09340940	-0.09648775	0.6754143
0.456757	0.0	1.911524	0.513088	-0.234356	0.268418	0.0	-0.105304	0.737126

TABLE II-6.

SOLUTIONS TO THE VELOCITY EQUATION FOR $\beta = -0.5$, $3.0 \geqq f_o \geqq 0.645966$

f_o	f_o''	δ_1^*	δ_2^*	$\dfrac{v_o \delta_2}{\nu}$	H_{21}	H_{24}	λ_2	F_2
3.0	2.9165650	0.3226665	0.1557965	-0.4673895	0.4828406	0.4543906	-0.01213627	0.07281765
2.5	2.3997647	0.3831293	0.1826587	-0.4566468	0.4767547	0.4383379	-0.01668210	0.1000926
2.0	1.8743500	0.4713681	0.2200681	-0.4401362	0.4668710	0.4124846	-0.02421499	0.1452899
1.5	1.3309692	0.6136199	0.2755583	-0.4133375	0.4490700	0.3667596	-0.03796619	0.2277971
1.0	0.7354607	0.8961188	0.3670402	-0.3670402	0.4095888	0.2699436	-0.06735926	0.4041555
0.645966	0.0	1.781075	0.489143	-0.315970	0.274634	0.0	-0.119630	0.717782

TABLE II - 7.

SOLUTIONS TO THE VELOCITY EQUATION FOR $\beta = -0.6$, $3.0 \geq f_0 \geq 0.819612$

f_0	f_0''	δ_1^*	δ_2^*	$\dfrac{v_0 \delta_2}{\nu}$	H_{21}	H_{24}	λ_2	F_2
3.0	2.8664360	0.3281457	0.1583086	-0.4749258	0.4824339	0.4537815	-0.01503697	0.08019715
2.5	2.3393454	0.3921666	0.1866134	-0.4665335	0.4758524	0.4365532	-0.02089474	0.1114386
2.0	1.7979424	0.4879503	0.2267815	-0.4535630	0.4647635	0.4077401	-0.03085791	0.1645755
1.5	1.2251993	0.6502213	0.2883302	-0.4324953	0.4434340	0.3532620	-0.04988058	0.2660298
1.0	0.5414380	1.0293784	0.3976626	-0.3976626	0.3863133	0.2153096	-0.09488132	0.5060337
0.819612	0.0	1.678970	0.469425	-0.384746	0.279591	0.0	-0.132216	0.705152

TABLE II-8.

SOLUTIONS TO THE VELOCITY EQUATION FOR $\beta = - 0.8, 3.0 \geqslant f_0 \geqslant 1.1331752$

f_0	f_0''	δ_1^*	δ_2^*	$\dfrac{\nu_0 \delta_2}{\nu}$	H_{21}	H_{24}	λ_2	F_2
3.0	2.7605600	0.3402545	0.1638180	-0.4914540	0.4814573	0.4522294	-0.02146907	0.09661082
2.5	2.2087760	0.4129185	0.1955540	-0.4888850	0.4735898	0.4319350	-0.03059310	0.1376689
2.0	1.6255360	0.5287640	0.2427360	-0.4854720	0.4590630	0.3945761	-0.04713662	0.2121148
1.5	0.9587710	0.7569940	0.3218310	-0.4827465	0.4251434	0.3085622	-0.08286015	0.3728707
1.1331752	0.0	1.5260219	0.4382116	-0.4965705	0.2871594	0.0	-0.1536235	0.6913059

TABLE II-9.

SOLUTIONS TO THE VELOCITY EQUATION FOR $\beta = -1.0$, $3.0 \geq f_o \geq (2)^{\frac{1}{2}}$

f_o	f_o''	δ_1^+	δ_2^+	$\dfrac{\nu_o \delta_2}{y}$	H_{21}	H_{24}	λ_2	F_2
3.0	$(7)^{\frac{1}{2}}$	$3.0-(7)^{\frac{1}{2}}$	0.1700985	-0.5102955	0.4801665	0.4500383	-0.02893350	0.1157340
2.5	$(17/4)^{\frac{1}{2}}$	$2.5-(17/4)^{\frac{1}{2}}$	0.2062741	-0.5156853	0.4704649	0.4252449	-0.04254900	0.1701960
2.0	$(2)^{\frac{1}{2}}$	$2.0-(2)^{\frac{1}{2}}$	0.2635928	-0.5271856	0.4499811	0.3727765	-0.06948116	0.2779246
1.5	0.5	1.0	0.3767333	-0.5651000	0.3767333	0.1883667	-0.1419280	0.5677119
$(2)^{\frac{1}{2}}$	0.0	$(2)^{\frac{1}{2}}$	0.4140719	-0.5855861	0.2927930	0.0	-0.1714555	0.6858220

SOLUTIONS WITH SEPARATION

Numerical solutions are tabulated for twenty-six values of the parameter β in the range $0 \leqslant \beta \leqslant -18$; with $f_0'' = 0$ the mass transfer parameter f_0 was adjusted for each β so as to satisfy the main-stream boundary condition.

Three solutions are quoted from the literature, that for $\beta = 0$ and two others for small negative β. The other values of β included are:

$$\beta = 0(0 \cdot 05) - 0 \cdot 2(0 \cdot 1) - 1 \cdot 0(0 \cdot 5) - 5 \cdot 0, -7, -10, -18$$

as well as the case when $f_0 = 0$ for which $\beta = -0 \cdot 19883768$.

TABLE III

SEPARATION SOLUTIONS TO THE VELOCITY EQUATION OF THE LAMINAR BOUNDARY LAYER WITH MASS TRANSFER

' Solution by Emmons and Leigh [11]
* Solutions by Brown and Donoughe [13]

β	f_0	δ_1^*	δ_2^*	H_{21}	$\dfrac{v_0 \delta_1}{\nu}$	$\dfrac{v_0 \delta_2}{\nu}$	λ_1	λ_2	F_1	F_2
0 ' *	− 0.875745	∞	0.875745	0.0	∞	0.766929	0.0	0.0	∞	1.533859
−0.014484 *	− 0.70456	4.5078	0.78117	0.17329	3.176	0.55038	−0.29432	−0.0088385	41.229	1.2381
−0.05 *	− 0.5008333	3.4050893	0.7064082	0.2074566	1.7053821	0.3537927	−0.5797317	−0.0249506	24.34873	1.0479263
−0.087160 *	− 0.34609	2.9570	0.66148	0.22370	1.0234	0.22893	−0.76211	−0.038137	19.012	0.95139
−0.10	− 0.2996851	2.8540745	0.6501028	0.2277806	0.8553236	0.1948261	−0.8145741	−0.0422634	17.92063	0.9297940
−0.15	− 0.1376368	2.5554773	0.6128922	0.2398347	0.3517277	0.0843565	−0.9795696	−0.0563455	15.02007	0.8639648
−0.19883768	0.0	2.3588478	0.5854342	0.2481865	0.0	0.0	−1.1063653	−0.0681483	13.34106	0.8217629
−0.2	0.0030926	2.3548790	0.5848540	0.2483584	−0.0072827	−0.0018087	−1.1090910	−0.0684108	13.30909	0.8209301
−0.3	0.2461484	2.0885724	0.5434619	0.2602073	−0.5140988	−0.1338109	−1.3086404	−0.0886052	11.34155	0.7679122
−0.4	0.456757	1.911524	0.513088	0.268418	−0.873102	−0.234356	−1.461570	−0.105304	10.23099	0.737126
−0.5	0.645966	1.781075	0.489143	0.274634	−1.150514	−0.315970	−1.586114	−0.119630	9.51668	0.717782
−0.6	0.819612	1.678970	0.469425	0.279591	−1.376104	−0.384746	−1.691364	−0.132216	9.02061	0.705152
−0.7	0.981231	1.595774	0.452703	0.283689	−1.565823	−0.444206	−1.782546	−0.143458	8.65808	0.696795
−0.8	1.1331752	1.5260219	0.4382116	0.2871594	−1.7292502	−0.4965705	−1.8629943	−0.1536235	8.383474	0.6913059
−0.9	1.2770976	1.4662691	0.4254459	0.2901554	−1.8725687	−0.5433359	−1.9349506	−0.1629038	8.169791	0.6878160
−1.0	√2	√2	0.4140719	0.2927930	−2.0	−0.5855861	−2.0	−0.1714555	8.0	0.6858220
−1.5	2.0245	1.22606	0.37079	0.30242	−2.48215	−0.75066	−2.25485	−0.20623	7.51616	0.68742
−2.0	2.5489	1.10402	0.34084	0.30873	−2.81402	−0.86876	−2.43772	−0.23235	7.31316	0.69704
−2.5	3.01653	1.01570	0.31818	0.31326	−3.06390	−0.95979	−2.57914	−0.25309	7.22159	0.70866
−3.0	3.4429	0.94754	0.30014	0.31676	−3.26227	−1.03336	−2.69348	−0.27026	7.18260	0.72069
−3.5	3.8378	0.89272	0.28531	0.31959	−3.42608	−1.09496	−2.78933	−0.28490	7.17256	0.73261
−4.0	4.2062	0.84706	0.27265	0.32188	−3.56290	−1.14682	−2.87005	−0.29735	7.17512	0.74338
− 5	4.884	0.77498	0.25227	0.32552	−3.78500	−1.23211	−3.00297	−0.31821	7.20712	0.76371
− 7	6.065	0.67522	0.22308	0.33038	−4.09519	−1.35296	−3.19144	−0.34834	7.29472	0.79621
−10	7.561	0.58100	0.19455	0.33485	−4.39296	−1.47098	−3.37566	−0.37849	7.42645	0.83268
−18	10.69	0.44930	0.15309	0.34073	−4.80299	−1.63655	−3.63366	−0.42187	7.67106	0.89061

SOLUTIONS FOR INFINITE β

With β infinite, solutions are given for the values of the relevant mass transfer parameter given below.

Variables imaginary; suction only

$$-\bar{k}_0 = \sqrt{8},\ 2 \cdot 85(0 \cdot 05)3 \cdot 2(0 \cdot 2)4 \cdot 0(0 \cdot 5)10 \cdot 0(2 \cdot 0)20 \cdot 0$$

Variables real

Suction

$$k_0 = 0 \cdot 0(0 \cdot 1)1 \cdot 0(0 \cdot 2)3 \cdot 0 \quad \text{and} \quad 1 \cdot 0(0 \cdot 5)10 \cdot 0(2 \cdot 0)20 \cdot 0$$

Blowing

$$-k_0 = 0 \cdot 0(0 \cdot 1)1 \cdot 0(0 \cdot 2)3 \cdot 0 \quad \text{and}$$

$$1 \cdot 0(0 \cdot 5)4 \cdot 0(1 \cdot 0)10 \cdot 0(2 \cdot 0)20 \cdot 0.$$

TABLE IV-1

FUNCTIONS OF THE LAMINAR BOUNDARY LAYER WITH SUCTION WHEN β IS INFINITE AND THE VARIABLES ARE IMAGINARY

Some quantities must be multiplied by the powers of ten given in brackets

$-\overline{k_0}$	$\overline{\delta_0}$	$\overline{\delta_1^{**}}$	$\overline{\delta_2^{**}}$	H_{21}	H_{24}	H_{14}	$-\lambda_2$	$-\dfrac{v_0\delta_2}{\nu}$	$-\lambda_1$	$-\dfrac{v_0\delta_1}{\nu}$
$\sqrt{8}$	1.92058109	0.5953089	0.3125371	0.5249998	0.6002528	1.1433391	0.9767944(-1)	0.8839884	0.3543927	1.6837879
2.85	2.01174369	0.5518840	0.2863723	0.5188995	0.5761077	1.1102492	0.8200910(-1)	0.8161611	0.3045760	1.5728694
2.9	2.12314612	0.5127966	0.2640573	0.5149358	0.5606323	1.0887420	0.6972627(-1)	0.7657662	0.2629603	1.4871100
2.95	2.21442220	0.4861812	0.2493966	0.5129704	0.5522693	1.0766105	0.6219865(-1)	0.7357199	0.2363722	1.4342346
3.0	2.29716795	0.4649868	0.2378452	0.5115095	0.5463704	1.0681529	0.5657034(-1)	0.7135356	0.2162128	1.3949605
3.05	2.37476069	0.4470614	0.2281780	0.5103951	0.5418680	1.0616637	0.5206518(-1)	0.6994427	0.1998639	1.3635372
3.1	2.44878155	0.4314130	0.2198054	0.5095011	0.5382554	1.0564363	0.4831442(-1)	0.6813968	0.1861172	1.3373804
3.15	2.52013147	0.4174743	0.2123943	0.5087601	0.5352614	1.0520901	0.4511132(-1)	0.6690419	0.1742848	1.3150440
3.2	2.58938497	0.4048818	0.2057333	0.5081316	0.5327226	1.0483948	0.4232617(-1)	0.6583464	0.1639293	1.2956217
3.4	2.85190135	0.3638656	0.1842330	0.5063216	0.5254144	1.0377088	0.3394181(-1)	0.6263923	0.1323982	1.2371431
3.6	3.09943739	0.3325663	0.1679963	0.5051512	0.5206940	1.0307685	0.2822275(-1)	0.6047866	0.1106004	1.1972388
3.8	3.33763756	0.3073559	0.1550066	0.5043228	0.5173557	1.0258425	0.2402704(-1)	0.5890250	0.9446763(-1)	1.1679523
4	3.56939107	0.2863657	0.1442433	0.5037030	0.5148606	1.0221511	0.2080612(-1)	0.5769730	0.8200530(-1)	1.1454627
4.5	4.13036797	0.2459831	0.1236489	0.5026723	0.5107155	1.0160008	0.1528905(-1)	0.5564201	0.6050770(-1)	1.1069240
5	4.67475882	0.2165326	0.1087086	0.5020427	0.5081865	1.0122376	0.1181756(-1)	0.5435430	0.4688636(-1)	1.0826629
5.5	5.20891837	0.1938448	0.9723685(-1)	0.5016222	0.5064988	1.0097216	0.945005(-2)	0.5348027	0.3757580(-1)	1.0661463
6	5.73613396	0.1757155	0.8809049(-1)	0.5013244	0.5053041	1.0079385	0.7759934(-2)	0.5285429	0.3087595(-1)	1.0542933
6.5	6.25564406	0.1608389	0.8059705(-1)	0.5011042	0.5044218	1.0066205	0.6495885(-2)	0.5238808	0.2586915(-1)	1.0454528
7	6.77729102	0.1483800	0.7432895(-1)	0.5009363	0.5037489	1.0056146	0.5524793(-2)	0.5203026	0.2201663(-1)	1.0386602
7.5	7.29322595	0.1377754	0.6899862(-1)	0.5008050	0.5032025	1.0048273	0.4760810(-2)	0.5174896	0.1898207(-1)	1.0333157
8	7.80696724	0.1286285	0.6440428(-1)	0.5007000	0.5028021	1.0041983	0.4147911(-2)	0.5152342	0.1654529(-1)	1.0290278
8.5	8.31894980	0.1206507	0.6039951(-1)	0.5006147	0.5024605	1.0036870	0.3648101(-2)	0.5133958	0.1455659(-1)	1.0255309
9	8.82949833	0.1136265	0.5687513(-1)	0.5005444	0.5021789	1.0032654	0.3234780(-2)	0.5118762	0.1291099(-1)	1.0226389
9.5	9.33886077	0.1073914	0.5374785(-1)	0.5004857	0.5019437	1.0029131	0.2888831(-2)	0.5106046	0.1153291(-1)	1.0202181
10	9.84723003	0.1018170	0.5095293(-1)	0.5004362	0.5017452	1.0026158	0.2596201(-2)	0.5095293	0.1036671(-1)	1.0181704
12	11.87341590	0.8437261(-1)	0.4221149(-1)	0.5002985	0.5011946	1.0017910	0.1781810(-2)	0.5065379	0.7187371(-2)	1.0124713
14	13.89186658	0.7207850(-1)	0.3605492(-1)	0.5002174	0.5008701	1.0013049	0.1299957(-2)	0.5047689	0.5195310(-2)	1.0090990
16	15.90558940	0.6293345(-1)	0.3147715(-1)	0.5001656	0.5006626	1.0009937	0.9908110(-3)	0.5036344	0.3960620(-2)	1.0069353
18	17.91620413	0.5585906(-1)	0.2793682(-1)	0.5001306	0.5005218	1.0007822	0.7804659(-3)	0.5028628	0.3120234(-2)	1.0054630
20	19.92466355	0.5022077(-1)	0.2511568(-1)	0.5001054	0.5004215	1.0006319	0.6307974(-3)	0.5023136	0.2522126(-2)	1.0044154

TABLE IV-2.

FUNCTIONS OF THE LAMINAR BOUNDARY LAYER WITH SUCTION WHEN β IS INFINITE AND THE VARIABLES ARE REAL

Some quantities must be multiplied by the powers of ten given in brackets

k_0	γ_0	δ_1^{**}	δ_2^{**}	H_{21}	H_{24}	H_{14}	λ_2	$-\frac{v_0\delta_2}{\nu}$	λ_1	$-\frac{v_0\delta_1}{\nu}$
20	20.07466971	0.4978322(-1)	0.2488649(-1)	0.4998972	0.4995881	0.9993817	0.6193374(-3)	0.4977298	0.2478369(-2)	0.9956644
18	18.08288122	0.5525882(-1)	0.2762240(-1)	0.4998731	0.4994926	0.9992387	0.7629970(-3)	0.4972032	0.3053537(-2)	0.9946588
16	16.09310817	0.6207874(-1)	0.3102943(-1)	0.4998399	0.4993600	0.9990399	0.9628255(-3)	0.4964709	0.3853770(-2)	0.9932598
14	14.10618891	0.7080242(-1)	0.3538649(-1)	0.4997921	0.4991685	0.9987523	0.1252204(-2)	0.4954109	0.5012983(-2)	0.9912339
12	12.12349509	0.8234547(-1)	0.4114962(-1)	0.4997193	0.4988772	0.9983149	0.1693291(-2)	0.4937954	0.6780776(-2)	0.9881456
10	10.14742734	0.9831105(-1)	0.4911629(-1)	0.4996009	0.4984040	0.9976042	0.2412410(-2)	0.4911629	0.9665063(-2)	0.9831105
9.5	9.65490537	0.1033006	0.5160480(-1)	0.4995597	0.4982395	0.9973572	0.2663055(-2)	0.4902456	0.1067101(-1)	0.9813554
9	9.16316624	0.1088129	0.5435334(-1)	0.4995119	0.4980487	0.9970707	0.2954286(-2)	0.4891801	0.1184025(-1)	0.9793161
8.5	8.67233668	0.1149328	0.5740389(-1)	0.4994562	0.4978259	0.9967359	0.3295207(-2)	0.4879331	0.1320955(-1)	0.9769287
8	8.18257156	0.1217639	0.6080771(-1)	0.4993905	0.4975634	0.9963414	0.3697578(-2)	0.4864617	0.1482644(-1)	0.9741108
7.5	7.69406196	0.1294340	0.6462800(-1)	0.4993125	0.4972518	0.9958729	0.4176778(-2)	0.4847100	0.1675315(-1)	0.9707547
7	7.20704588	0.1381025	0.6894338(-1)	0.4992189	0.4968781	0.9953111	0.4753190(-2)	0.4826037	0.1907230(-1)	0.9667175
6.5	6.72182310	0.1479703	0.7385280(-1)	0.4991056	0.4964255	0.9946302	0.5454236(-2)	0.4800432	0.2189521(-1)	0.9618070
6	6.23877544	0.1592934	0.7948207(-1)	0.4989666	0.4958708	0.9937956	0.6317400(-2)	0.4768924	0.2537438(-1)	0.9557602
5.5	5.75839523	0.1724021	0.8599315(-1)	0.4987941	0.4951826	0.9927594	0.7394822(-2)	0.4729623	0.2972248(-1)	0.9482116
5	5.28132557	0.1877285	0.9359711(-1)	0.4985771	0.4943168	0.9914551	0.8760419(-2)	0.4679856	0.3524198(-1)	0.9386423
4.5	4.80841733	0.2058449	0.1025725	0.4982997	0.4932112	0.9897881	0.1052111(-1)	0.4615760	0.4237212(-1)	0.9263020
4	4.34081137	0.2275201	0.1132913	0.4979395	0.4917760	0.9876219	0.1283491(-1)	0.4531650	0.5176541(-1)	0.9100305
3.5	3.88005585	0.2537998	0.1262561	0.4974632	0.4898806	0.9847564	0.1594059(-1)	0.4418962	0.6441433(-1)	0.8882993
3.0	3.42827210	0.2861209	0.1421512	0.4968223	0.4873331	0.9809002	0.2020697(-1)	0.4264537	0.8186516(-1)	0.8583626
2.8	3.25069179	0.3011630	0.1495288	0.4965045	0.4860720	0.9789881	0.2235886(-1)	0.4186806	0.9069915(-1)	0.8432564
2.6	3.07523339	0.3176389	0.1575945	0.4961434	0.4846397	0.9768139	0.2483601(-1)	0.4097456	0.1008945	0.8258612
2.5	2.98838052	0.3264697	0.1619108	0.4959444	0.4838511	0.9756157	0.2621511(-1)	0.4047770	0.1065825	0.8161743
2.4	2.90215900	0.3357280	0.1664310	0.4957318	0.4830093	0.9743360	0.2769929(-1)	0.3994345	0.1127133	0.8057471
2.2	2.73176479	0.3556332	0.1761316	0.4952619	0.4811501	0.9715063	0.3102233(-1)	0.3874895	0.1264750	0.7823931
2.0	2.56438396	0.3775839	0.1868000	0.4947246	0.4790270	0.9682702	0.3489426(-1)	0.3736001	0.1425696	0.7551678
1.8	2.40038892	0.4018373	0.1985516	0.4941095	0.4766011	0.9645658	0.3942275(-1)	0.3573929	0.1614732	0.7233071
1.6	2.24019249	0.4286797	0.2115128	0.4934053	0.4738294	0.9603250	0.4473767(-1)	0.3384205	0.1837663	0.6858875
1.5	2.16165869	0.4431692	0.2184895	0.4930160	0.4722997	0.9579806	0.4773766(-1)	0.3277342	0.1963989	0.6647538
1.4	2.08424720	0.4584265	0.2258207	0.4925997	0.4706662	0.9554741	0.5099500(-1)	0.3161490	0.2101548	0.6417971
1.2	1.93304202	0.4914205	0.2416215	0.4916797	0.4670645	0.9499365	0.5838094(-1)	0.2899458	0.2414941	0.5897046
1.0	1.78709566	0.5280280	0.2590676	0.4906323	0.4629786	0.9436366	0.6711604(-1)	0.2590676	0.2788136	0.5260280
0.9	1.71626219	0.5478060	0.2684562	0.4900571	0.4607412	0.9401787	0.7206873(-1)	0.2416106	0.3000914	0.4930254
0.8	1.64694566	0.5686315	0.2783142	0.4894456	0.4583683	0.9365052	0.7745878(-1)	0.2226513	0.3233418	0.4549052
0.7	1.57921363	0.5905532	0.2886604	0.4887966	0.4558565	0.9326097	0.8332484(-1)	0.2020623	0.3487531	0.4133073
0.6	1.51313256	0.6136193	0.2995133	0.4881093	0.4532033	0.9284873	0.8970820(-1)	0.1797080	0.3765286	0.3681716
0.5	1.44876708	0.6378769	0.3108902	0.4873828	0.4504075	0.9241350	0.9665273(-1)	0.1554451	0.4068869	0.3189384
0.4	1.38617917	0.6633717	0.3228075	0.4866164	0.4474691	0.9195520	0.1042047	0.1291230	0.4400620	0.2653487
0.3	1.32542728	0.6901464	0.3352809	0.4858113	0.4443904	0.9147389	0.1124133	0.1005843	0.4763020	0.2070439
0.2	1.26656544	0.7182421	0.3483234	0.4849665	0.4411743	0.9097006	0.1213292	0.6966467(-1)	0.5158717	0.1436484
0.1	1.20964237	0.7476954	0.3619470	0.4840834	0.4378264	0.9044405	0.1310056	0.3619470(-1)	0.5590484	0.7476954(-1)
0.0	1.15470054	0.7785391	0.3761615	0.4831633	0.4343539	0.8989795	0.1414975	0.0000000	0.6061231	0.0000000

TABLE IV-2.contd.

FUNCTIONS OF THE LAMINAR BOUNDARY LAYER WITH BLOWING WHEN β IS INFINITE AND THE VARIABLES ARE REAL

Some quantities must be multiplied by the powers of ten given in brackets

$-k_o$	δ_o	δ_1^{**}	δ_2^{**}	H_{21}	H_{24}	H_{14}	λ_2	$\dfrac{v_o \delta_2}{\nu}$	λ_1	$\dfrac{v_o \delta_1}{\nu}$
0.0	1.15470054	0.7785391	0.3761615	0.4831633	0.4343539	0.8989795	0.1414975	0.0	0.6061231	0.0
0.1	1.10177538	0.8108008	0.3909745	0.4822079	0.4307661	0.8933204	0.1528611	0.3909745(-1)	0.6573980	0.8108008(-1)
0.2	1.05089450	0.8445031	0.4063914	0.4812196	0.4270745	0.8874837	0.1651540	0.8127828(-1)	0.7131855	0.1689006
0.3	1.00207700	0.8796622	0.4224148	0.4802012	0.4232922	0.8814893	0.1784343	0.1267244	0.7738056	0.2638987
0.4	0.95533296	0.9162881	0.4390449	0.4791560	0.4194341	0.8753602	0.1927604	0.1756180	0.8395838	0.3665152
0.5	0.91066307	0.9543838	0.4562792	0.4780878	0.4155167	0.8691221	0.2081907	0.2281396	0.9108485	0.4771919
0.6	0.86805842	0.9939457	0.4741208	0.4770007	0.4115576	0.8628029	0.2247829	0.2844765	0.9872920	0.5963674
0.7	0.82750049	0.1034963(1)	0.4925379	0.4758992	0.4075253	0.8564321	0.2425935	0.3447765	0.1071148(1)	0.7244738
0.8	0.78896135	0.1077417(1)	0.5115445	0.4747879	0.4035889	0.8500402	0.2616778	0.4092356	0.1160827(1)	0.8619335
0.9	0.75240407	0.1121284(1)	0.5311204	0.4736718	0.3996172	0.8436584	0.2820889	0.4780084	0.1257277(1)	0.1009155(1)
1.0	0.71778325	0.1166532(1)	0.5512513	0.4725556	0.3956789	0.8373171	0.3038779	0.5512513	0.1360797(1)	0.1166532(1)
1.2	0.65413183	0.1261020(1)	0.5931114	0.4703424	0.3879730	0.8248736	0.3517811	0.7117336	0.1590173(1)	0.1513225(1)
1.4	0.59750654	0.1360529(1)	0.6369771	0.4681832	0.3805980	0.8129253	0.4057398	0.8917679	0.1851040(1)	0.1904741(1)
1.6	0.57165053	0.1412038(1)	0.6596130	0.4671356	0.3770681	0.8071920	0.4350894	0.9894196	0.1993851(1)	0.2118056(1)
1.8	0.54733081	0.1464643(1)	0.6826878	0.4661121	0.3736561	0.8016442	0.4660627	0.1092301(1)	0.2145129(1)	0.2343429(1)
2.0	0.50298658	0.1572916(1)	0.7300703	0.4641507	0.3672155	0.7911558	0.5330026	0.1314126(1)	0.2474066(1)	0.2831249(1)
2.2	0.46384661	0.1684892(1)	0.7789543	0.4621169	0.3611153	0.7815316	0.6067697	0.1557909(1)	0.2838362(1)	0.3369785(1)
2.4	0.42930139	0.1800126(1)	0.8291749	0.4606204	0.3559659	0.7727968	0.6875310	0.1824185(1)	0.3240455(1)	0.3960278(1)
2.6	0.39877898	0.1918201(1)	0.8805777	0.4590643	0.3511559	0.7649384	0.7754171	0.2113386(1)	0.3679496(1)	0.4603663(1)
2.8	0.38486103	0.1978183(1)	0.9066777	0.4583385	0.3489449	0.7613257	0.8220644	0.2266694(1)	0.3913209(1)	0.4945458(1)
3.0	0.37175731	0.2038736(1)	0.9330212	0.4576469	0.3468575	0.7579150	0.8705286	0.2425855(1)	0.4156445(1)	0.5300714(1)
3.2	0.34777020	0.2161392(1)	0.9863782	0.4563625	0.3430329	0.7516677	0.9729419	0.2761859(1)	0.4671615(1)	0.6051898(1)
3.4	0.32640820	0.2285873(1)	0.1040535(1)	0.4552003	0.3396391	0.7461278	0.1082713(1)	0.3121604(1)	0.5225217(1)	0.6857620(1)
3.5	0.28227814	0.2603465(1)	0.1178814(1)	0.4527865	0.3327533	0.7349011	0.1389602(1)	0.4125848(1)	0.6778028(1)	0.9112126(1)
4	0.24816748	0.2927883(1)	0.1320285(1)	0.4509349	0.3276517	0.7266053	0.1743152(1)	0.5281139(1)	0.8572498(1)	0.1171153(2)
5	0.21937741	0.3589732(1)	0.1904427(1)	0.4484025	0.3209269	0.7157116	0.2626817(1)	0.8048225(1)	0.1288618(2)	0.1794866(2)
6	0.19664129	0.4261993(1)	0.2202477(1)	0.4468380	0.3169202	0.7092507	0.3626957(1)	0.1144262(2)	0.1816458(2)	0.2557196(2)
7	0.14273902	0.4940262(1)	0.2502660(1)	0.4458218	0.3143794	0.7051682	0.4850903(1)	0.1541734(2)	0.2440619(2)	0.3458184(2)
8	0.12493923	0.5622279(1)	0.2804281(1)	0.4451327	0.3126805	0.7024432	0.6263309(1)	0.2002128(2)	0.3161002(2)	0.4497823(2)
9	0.11107733	0.6306796(1)	0.3106928(1)	0.4444443	0.3114920	0.7005421	0.7863992(1)	0.2523853(2)	0.3977568(2)	0.5676117(2)
10	0.09998004	0.6993052(1)	0.3410610(1)	0.4442878	0.3106307	0.6991657	0.9653000(1)	0.3106928(2)	0.4890278(2)	0.6993052(2)
12	0.08332530	0.8369033(1)	0.3714292(1)	0.4438138	0.3094945	0.6973522	0.1379597(2)	0.4457150(2)	0.7004072(2)	0.1004284(3)
14	0.07142485	0.9747977(1)	0.4323448(1)	0.4435226	0.3088016	0.6962478	0.1869220(2)	0.6052827(2)	0.9502305(2)	0.1364717(3)
16	0.06249809	0.1112877(2)	0.4933732(1)	0.4433315	0.3083489	0.6955266	0.2434171(2)	0.7893972(2)	0.1238494(3)	0.1780603(3)
18	0.05555450	0.1251028(2)	0.5544772(1)	0.4431994	0.3080370	0.6950303	0.3074449(2)	0.9980589(2)	0.1565197(3)	0.2251941(3)
20	0.04999938	0.1389366(2)	0.6156342(1)	0.4431045	0.3078133	0.6946742	0.3790055(2)	0.1231268(3)	0.1930337(3)	0.2778731(3)

SOME MISCELLANEOUS SOLUTIONS

The following sets of numerical solutions are tabulated:

.1. Solutions for $\beta = 0$ by Emmons and Leigh

The mass transfer parameter is given the following values:

Suction

$$\sqrt{2}f_0 = 0 \cdot 0(0 \cdot 05)0 \cdot 5(0 \cdot 1)1 \cdot 5(0 \cdot 5)3 \cdot 0(1 \cdot 0)6 \cdot 0, \ 10, \ \infty.$$

Blowing

$$- \sqrt{2}f_0 = 0 \cdot 0(0 \cdot 05)1 \cdot 2, \ 1 \cdot 23849$$

where the last value gives separation.

2. Solutions for no mass transfer and β large

The mass transfer parameter equal to zero, solutions are tabulated for the following values of $1/\beta$:

$$1/\beta = 1 \cdot 3(0 \cdot 1)-1 \cdot 0 \quad \text{and} \quad -0 \cdot 25.$$

3. Solutions for β small and slight blowing

Solutions are tabulated for $f_0 = -0 \cdot 5$ and the following values of β:

$$\beta = 0 \cdot 0(0 \cdot 1)0 \cdot 5, \ 1 \cdot 0.$$

$f_2 f_0$	f_0^*	δ_1^*	δ_2^*	H_{21}	H_{2*}	H_{1*}	$\dfrac{v_0 \delta_1}{\nu}$	$\dfrac{v_0 \delta_2}{\nu}$	F_2
1.23849	0.0	∞	0.875745	0.0	0.0	0.0	∞	0.766929	1.533859
-1.2	0.004748	5.55229	0.853276	0.153680	0.004051	0.02636	4.71127	0.724029	1.456160
-1.15	0.01365	4.52237	0.82882	0.16896	0.01129	0.06037	3.59615	0.67235	1.36726
-1.1	0.02444	3.82022	0.80226	0.21000	0.01961	0.09337	2.97143	0.62401	1.28724
-1.05	0.036709	3.41167	0.779171	0.228384	0.028603	0.12524	2.53304	0.578505	1.214215
-1.00	0.050229	3.10476	0.757336	0.243927	0.038040	0.15595	2.19540	0.535518	1.142116
-0.95	0.064856	2.86049	0.736607	0.257511	0.047680	0.18552	1.92154	0.494816	1.085180
-0.90	0.080462	2.65887	0.716858	0.269610	0.057685	0.21394	1.69209	0.456206	1.027771
-0.85	0.096969	2.48803	0.698010	0.280547	0.067685	0.24126	1.49541	0.419533	0.974436
-0.80	0.11430	2.34044	0.67999	0.29054	0.077723	0.26751	1.32395	0.38466	0.92477
-0.75	0.13239	2.21109	0.66272	0.29973	0.087738	0.29273	1.17261	0.35146	0.87840
-0.70	0.15119	2.09635	0.64617	0.30824	0.097694	0.31695	1.03764	0.31984	0.83507
-0.65	0.17065	1.99358	0.63027	0.31615	0.10756	0.34020	0.91629	0.28968	0.79448
-0.60	0.19073	1.90080	0.61499	0.32354	0.11730	0.36254	0.806441	0.26092	0.75643
-0.55	0.21140	1.81649	0.60031	0.33048	0.12691	0.38401	0.706449	0.23347	0.72074
-0.50	0.23262	1.73941	0.58617	0.33699	0.13636	0.40462	0.614974	0.20724	0.68719
-0.45	0.25437	1.66860	0.57257	0.34314	0.14565	0.42444	0.530945	0.18219	0.65567
-0.40	0.27660	1.60327	0.55944	0.34894	0.15474	0.44346	0.453474	0.15823	0.62595
-0.35	0.29931	1.54274	0.54680	0.35443	0.16366	0.46175	0.381808	0.13533	0.59798
-0.30	0.32246	1.48648	0.53459	0.35963	0.17238	0.47933	0.315530	0.11340	0.57157
-0.25	0.34603	1.43403	0.52281	0.36457	0.18091	0.49623	0.253504	0.092421	0.54666
-0.20	0.37008	1.38498	0.511429	0.369268	0.189233	0.512454	0.195865	0.0723268	0.523119
-0.15	0.394371	1.33901	0.500437	0.373783	0.197358	0.528066	0.142023	0.0530794	0.500874
-0.10	0.419102	1.29581	0.489813	0.377998	0.205282	0.543077	0.0916276	0.0346350	0.479834
-0.05	0.444183	1.25514	0.47538	0.382059	0.21303	0.557513	0.0443759	0.0169542	0.459913
0.05	0.469600	1.21678	0.459984	0.385937	0.220524	0.571399	0.0	0.0	0.441048
0.10	0.495339	1.18052	0.456671	0.389645	0.227848	0.584758	-0.047376	-0.0162629	0.423171
0.15	0.521382	1.14621	0.441655	0.393184	0.234972	0.597613	-0.0810493	-0.0316673	0.406209
0.20	0.547721	1.11368	0.432919	0.396573	0.241907	0.609986	-0.118124	-0.0468446	0.390118
0.25	0.574340	1.08279	0.424455	0.399818	0.248643	0.621890	-0.153129	-0.0612238	0.374838
0.30	0.601232	1.05343	0.416253	0.402927	0.255196	0.633356	-0.186222	-0.0750339	0.360324
0.35	0.628385	1.02548	0.408298	0.405910	0.261567	0.644396	-0.217537	-0.0883006	0.346533
0.40	0.655785	0.998838	0.400579	0.408773	0.267756	0.655023	-0.247199	-0.101048	0.333415
0.45	0.683422	0.973432	0.393095	0.411512	0.273765	0.665265	-0.275328	-0.113301	0.320927
0.50	0.711293	0.949157	0.385830	0.414152	0.279606	0.675129	-0.302020	-0.125082	0.309047
0.55	0.739383	0.925949	0.371931	0.416686	0.285276	0.684631	-0.327372	-0.136411	0.297730
0.6	0.796195	0.882476	0.358821	0.421463	0.296130	0.702623	-0.374403	-0.157797	0.276665
0.7	0.853796	0.842525	0.346440	0.425888	0.306260	0.719344	-0.417029	-0.177607	0.257505
0.8	0.912125	0.805211	0.334737	0.429979	0.315997	0.734911	-0.455780	-0.195976	0.240041
0.9	0.971133	0.771666	0.32366	0.433785	0.325074	0.749190	-0.491085	-0.213025	0.224098
1.0	1.03077	0.740107	0.31318	0.43732	0.33362	0.762880	-0.523335	-0.22886	0.20951
1.1	1.09100	0.710791	0.30325	0.44061	0.34168	0.775473	-0.552865	-0.24360	0.19616
1.2	1.15178	0.683475	0.29382	0.44369	0.34928	0.787213	-0.579948	-0.25732	0.18392
1.3	1.21306	0.658405	0.28487	0.44653	0.35642	0.798200	-0.604864	-0.27009	0.17266
1.4	1.27482	0.634148	0.27637	0.45173	0.36316	0.808405	-0.627775	-0.28201	0.16230
1.5	1.33703	0.611810	0.23961	0.46207	0.36951	0.818008	-0.648922	-0.29313	0.15276
2.0	1.65382	0.518557	0.2104	0.4695	0.39627	0.857600	-0.733351	-0.33886	0.11483
2.5	1.9782	0.448164	0.1870	0.4753	0.4162	0.88656	-0.792250	-0.3719	0.08854
3.0	2.3083	0.393434	0.1519	0.4831	0.4317	0.90816	-0.834599	-0.3967	0.06994
4	2.9803	0.314450	0.12714	0.48768	0.4527	0.93716	-0.869399	-0.4296	0.04615
5	3.66267	0.260703	0.10900	0.49087	0.46567	0.954869	-0.921724	-0.4495	0.03233
6	4.35164	0.222053	0.06662	0.49689	0.47433	0.966295	-0.942091	-0.46245	0.023762
10	7.13969	0.138098			0.4899	0.985997	-0.976500	-0.4852	0.009417
∞	∞	0.0	0.0	0.5	0.5	1.0	-1.0	-0.5	0.0

TABLE V-2.

SOLUTIONS TO THE VELOCITY EQUATION FOR NO MASS TRANSFER WITH $1.3 \geq \frac{1}{\beta} \geq -1.0$

Solutions below the broken line are less accurate than those above

$\frac{1}{\beta}$	θ_o''	$\delta_1^{**} - \delta_2^{**}$	δ_1^{**}	δ_2^{**}	H_{21}	H_{24}	λ_2	F_2	E_2
1.3	1.25647933	0.3441687	0.6206265	0.2764578	0.4454496	0.3473635	0.07642890	0.04585734	0.00079
1.2	1.24851453	0.3478487	0.6293068	0.2814581	0.4472510	0.3514045	0.07921865	0.03168746	0.00056
1.1	1.24054914	0.3516431	0.6383870	0.2867439	0.4491694	0.3557199	0.08222206	0.01644441	0.00031
1.0	1.23258760	0.3555568	0.6479004	0.2923436	0.4512168	0.3603391	0.08546477	0.0	0.00002
0.9	1.22463510	0.3595952	0.6578848	0.2982896	0.4534070	0.3652959	0.08897669	- 0.01779534	- 0.00031
0.8	1.21669745	0.3637634	0.6683827	0.3046193	0.4557558	0.3706295	0.09279291	- 0.03711717	- 0.00068
0.7	1.20878116	0.3680669	0.6794425	0.3113757	0.4582811	0.3763850	0.09695480	- 0.05817288	- 0.00110
0.6	1.20089372	0.3725107	0.6911196	0.3186089	0.4610040	0.3826154	0.1015116	- 0.08120928	- 0.00158
0.5	1.19304340	0.3771000	0.7034774	0.3263773	0.4639486	0.3893823	0.1065222	- 0.1065222	- 0.00212
0.4	1.18523949	0.3818396	0.7165896	0.3347500	0.4671432	0.3967589	0.1120575	- 0.1344690	- 0.00274
0.3	1.17749210	0.3867337	0.7305417	0.3438080	0.4706206	0.4048312	0.1182039	- 0.1654855	- 0.00344
0.2	1.16981218	0.3917861	0.7454343	0.3536482	0.4744191	0.4137020	0.1250671	- 0.2001073	- 0.00424
0.1	1.16221114	0.3969998	0.7613862	0.3643864	0.4785829	0.4234939	0.1327774	- 0.2389993	- 0.00514
0.0	1.15470054	0.4023776	0.7785391	0.3761615	0.4831633	0.4343539	0.1414975	- 0.2829949	- 0.00614
- 0.1	1.1472917	0.4079216	0.7970638	0.3891421	0.4882196	0.4464596	0.1514316	- 0.3331495	- 0.00725
- 0.2	1.1399951	0.4136339	0.8171679	0.4035340	0.4938202	0.4600268	0.1628397	- 0.3908153	- 0.00845
- 0.25	1.13639183	0.4165528	0.8278894	0.4113366	0.4968497	0.4674396	0.1691978	- 0.4229945	- 0.00908
- 0.3	1.1328200	0.4195098	0.8391040	0.4195943	0.5000503	0.4753248	0.1760593	- 0.4577543	- 0.00973
- 0.4	1.1257741	0.4255222	0.8631797	0.4376574	0.5070293	0.4927034	0.1915440	- 0.5363232	- 0.01107
- 0.5	1.1188628	0.4316699	0.8897985	0.4581286	0.5148678	0.5125830	0.2098818	- 0.6296454	- 0.01238
- 0.6	1.1120891	0.4379406	0.9194752	0.4815347	0.5237060	0.5355095	0.2318756	- 0.7420020	- 0.01352
- 0.7	1.1054540	0.4443411	0.9528895	0.5085484	0.5336909	0.5621769	0.2586215	- 0.8793130	- 0.01423
- 0.8	1.0989570	0.4509036	0.9909481	0.5400445	0.5449776	0.5934857	0.2916481	- 1.0499331	- 0.01404
- 0.9	1.0925972	0.4577198	1.0348811	0.5771613	0.5577079	0.6306048	0.3331152	- 1.2658377	- 0.01212
- 1.0	1.0863757	0.4656966	1.0863757	0.6206792	0.5713301	0.6742908	0.3852426	- 1.5409705	- 0.00599

Solutions to the Velocity Equation for $f_0 = -0.5$, $0 \leq \beta \leq 1.0$

β	$f_0^{"}$	δ_1^{*}	δ_2^{*}	$\dfrac{v_0 \, \delta_2}{\nu}$	H_{21}	H_{24}	λ_2	F_2
0.0	0.14847634	2.1118674	0.6484763	0.3242382	0.3070630	0.09628339	0.0	0.3410431
0.1	0.295166500	1.6178749	0.5757991	0.2878996	0.3559041	0.1699566	0.03315446	0.5967803
0.2	0.406219118	1.3796359	0.5252433	0.2626216	0.3807115	0.2133639	0.05517610	0.4414088
0.3	0.500323400	1.2262543	0.4864978	0.2432489	0.3967348	0.2434062	0.07100403	0.3313521
0.4	0.583678009	1.1155525	0.4553264	0.2276632	0.4081623	0.2657640	0.08292887	0.2487866
0.5	0.659363833	1.0303663	0.4294538	0.2147269	0.4167972	0.2831663	0.09221528	0.1844306
1.0	0.969229552	0.78096245	0.3441336	0.1720668	0.4406531	0.3335444	0.1184279	0.0
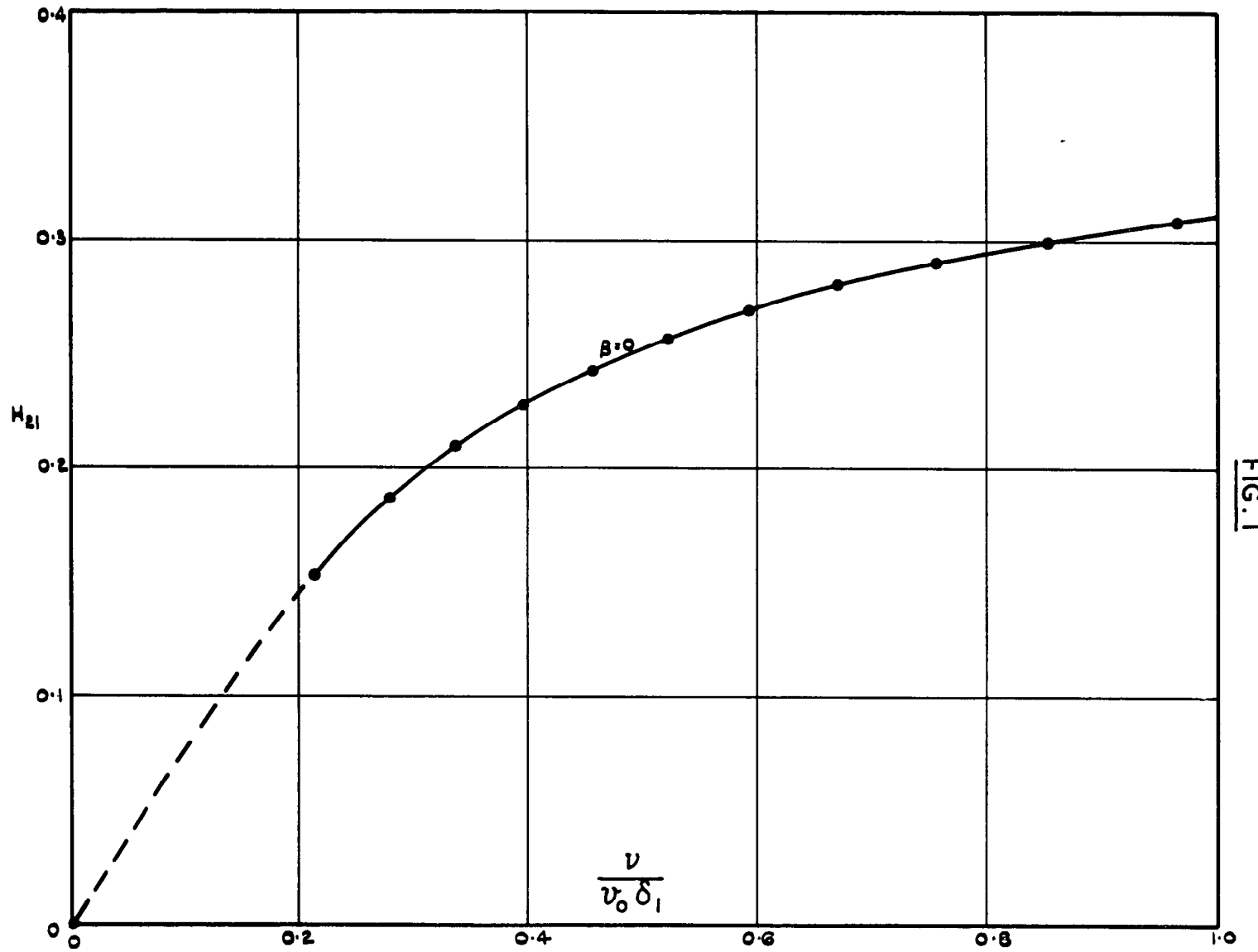
H_{21} as a function of $\left(v / v_o \delta_1\right)$ for the solutions near separation when $\beta = 0$ obtained
by Emmons and Leigh (11); the broken part of the curve represents interpolation

FIG. 2
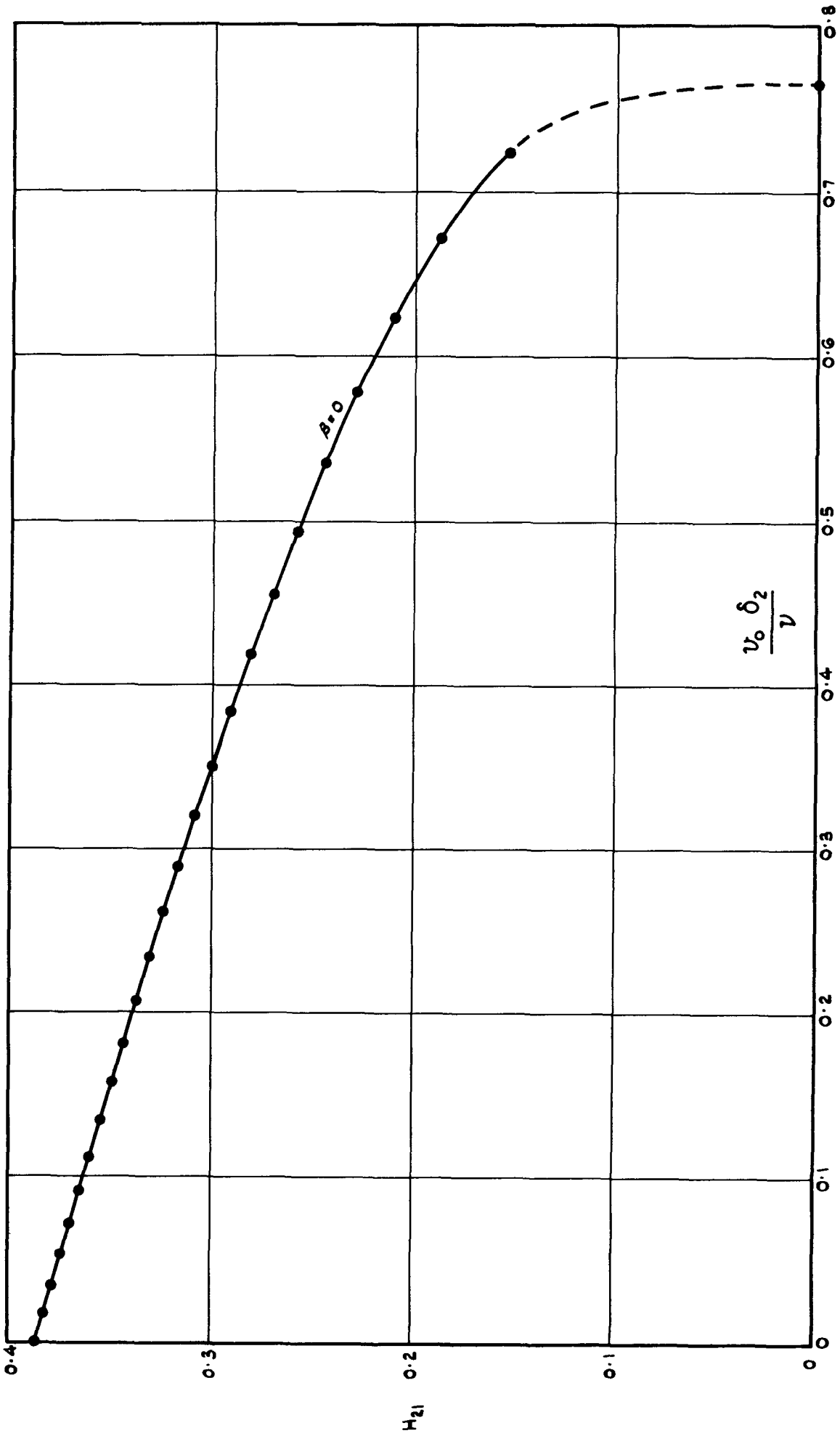
H_{21} as a function of $\left(\dfrac{v_0\,\delta_2}{v}\right)$ for the solutions near separation when $\beta = 0$; broken part of the curve

— denotes interpolation

FIG. 3
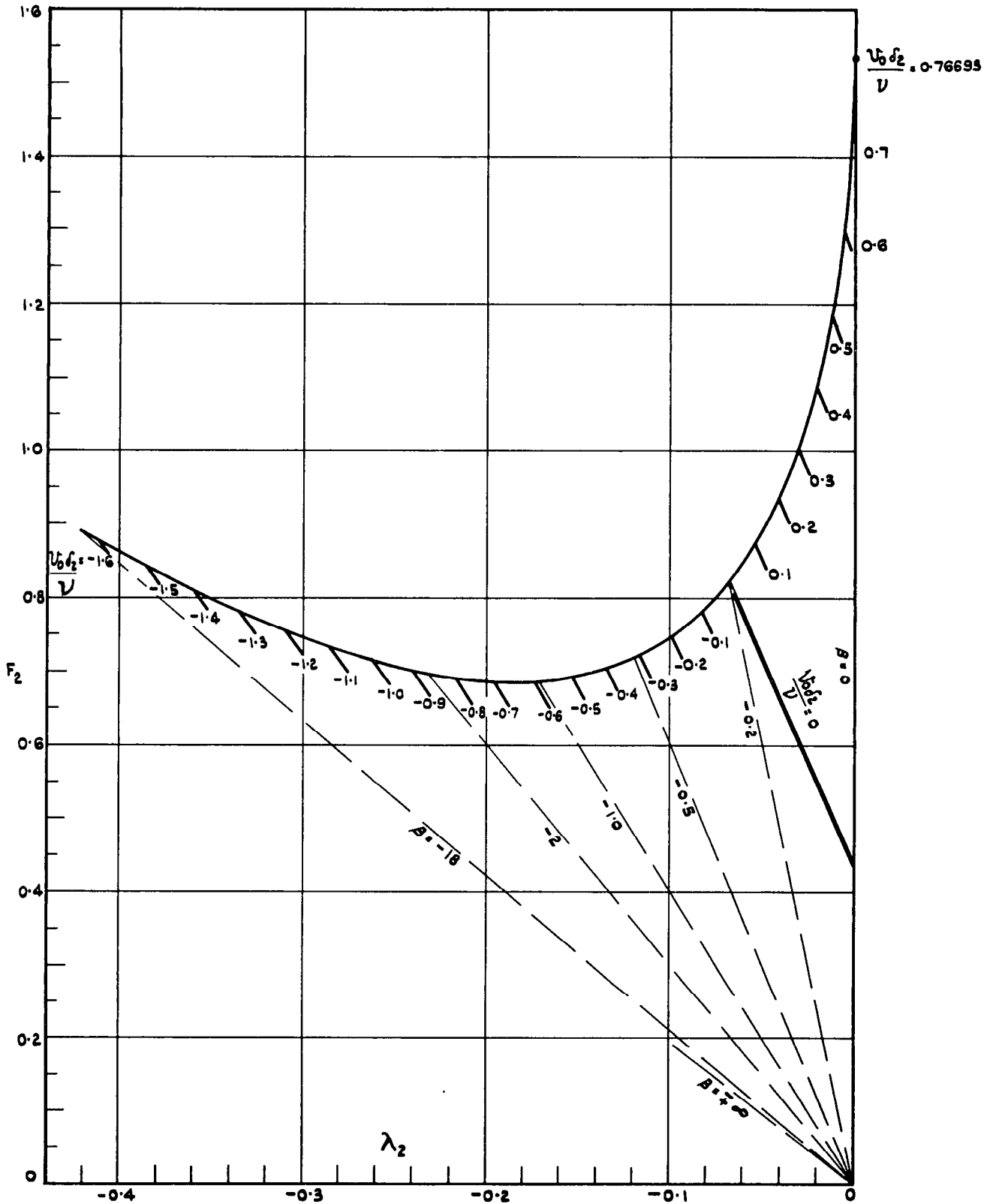
Variation of F_2 with λ_2 for the separation solutions. The short lines indicate where the curves of specified $(v_0 \delta_2 / v)$ intercept the separation line.

FIG. 4
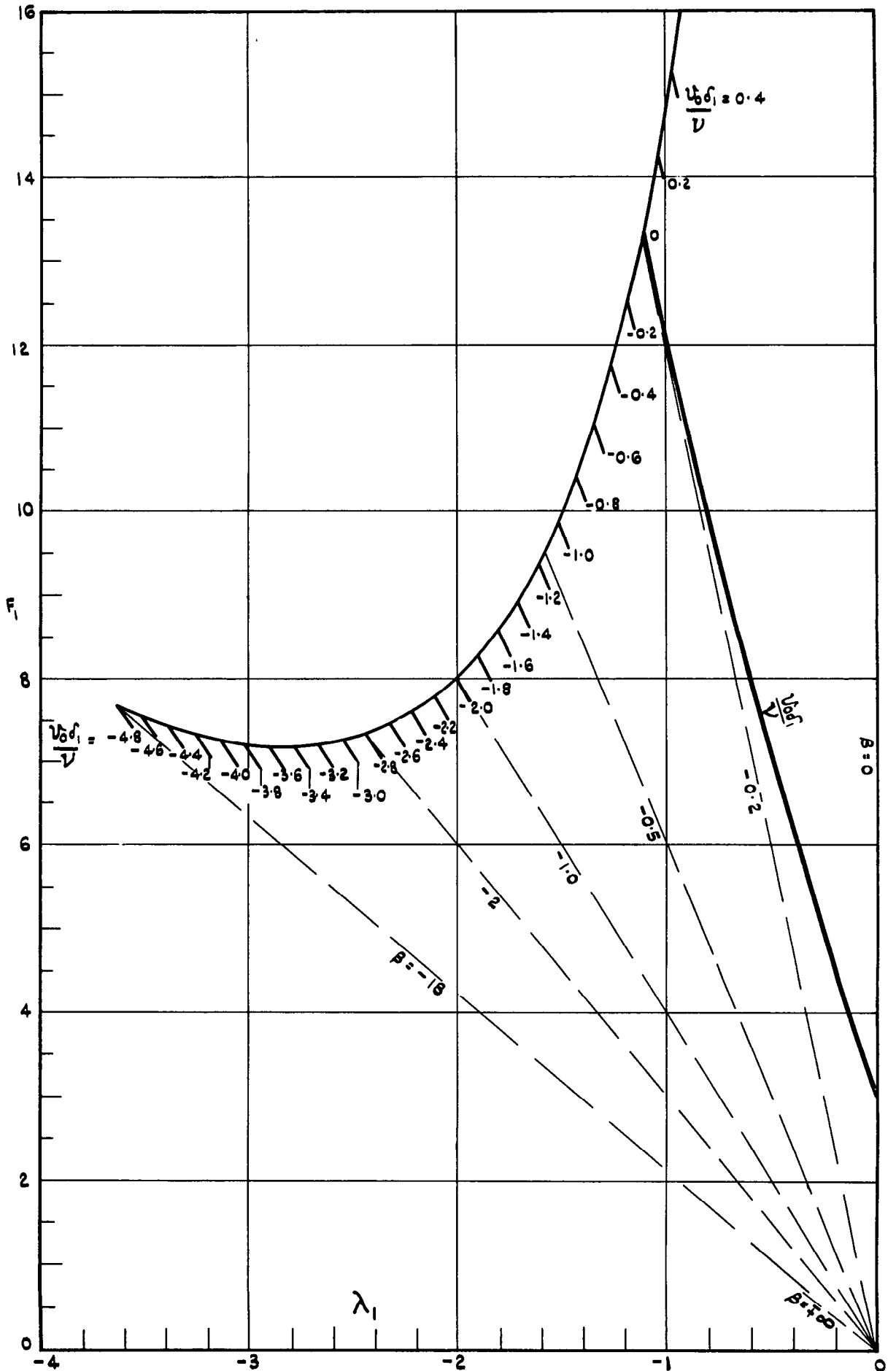
Variation of F_1 with λ_1 for the separation solutions. The intercepts of the lines of specified $(v_0 \, \delta_1/v)$ with the separation line are also indicated

FIG. 5

POINT
SINK.

A_1

υ_0

U.G

x

BOUNDARY
LAYER.

POROUS WALL.
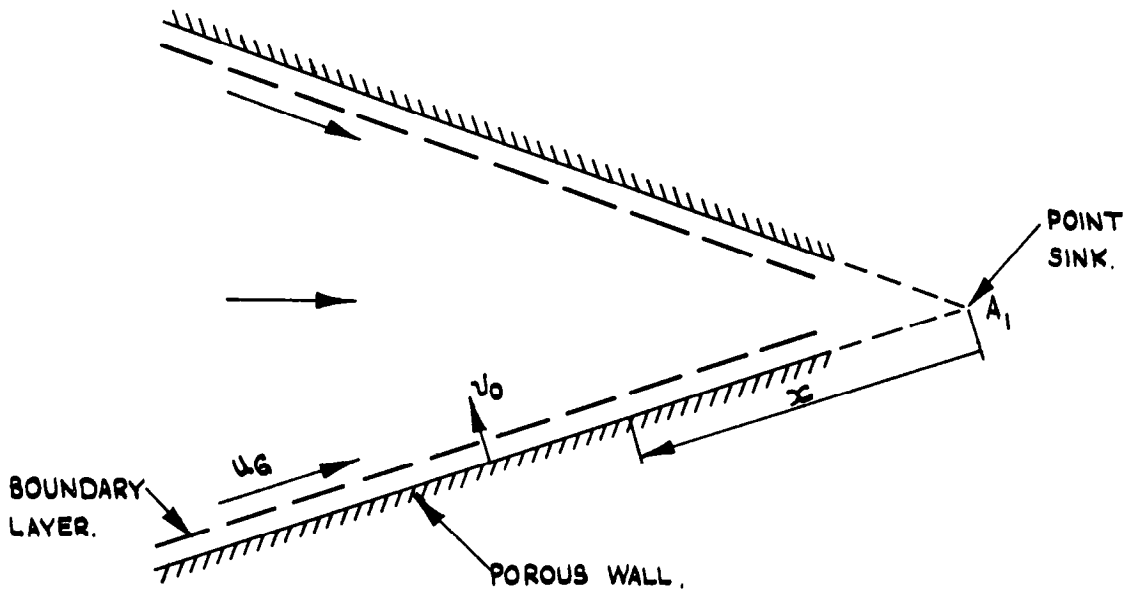
Diagrammatic illustration of the similar flow associated with infinite β

when the variables are real

FIG. 6

POINT
SOURCE.

A_2

υ_0

U.G.

x

BOUNDARY
LAYER.

POROUS WALL.
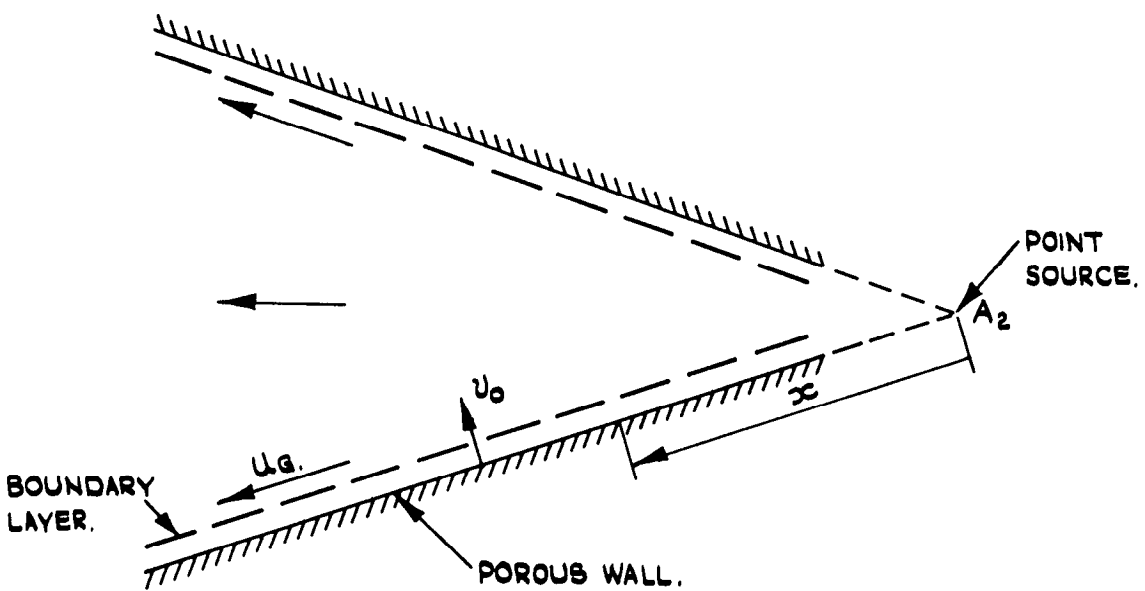
The similar flow associated with infinite β when the variables are

pure imaginary

FIG. 7
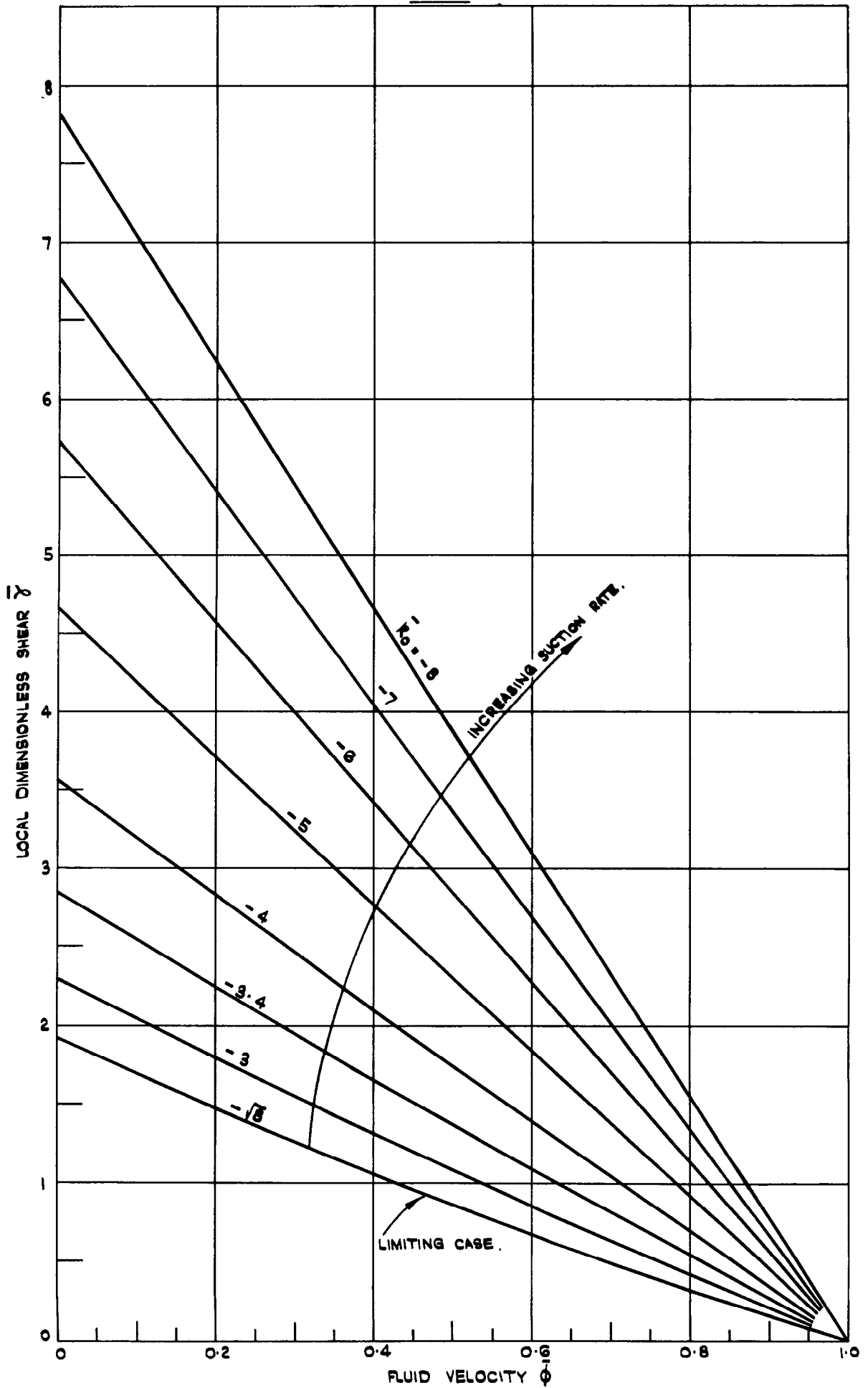
Solutions to equation (26) for various values of the mass transfer parameter $\bar{k}_o$

FIG. 8
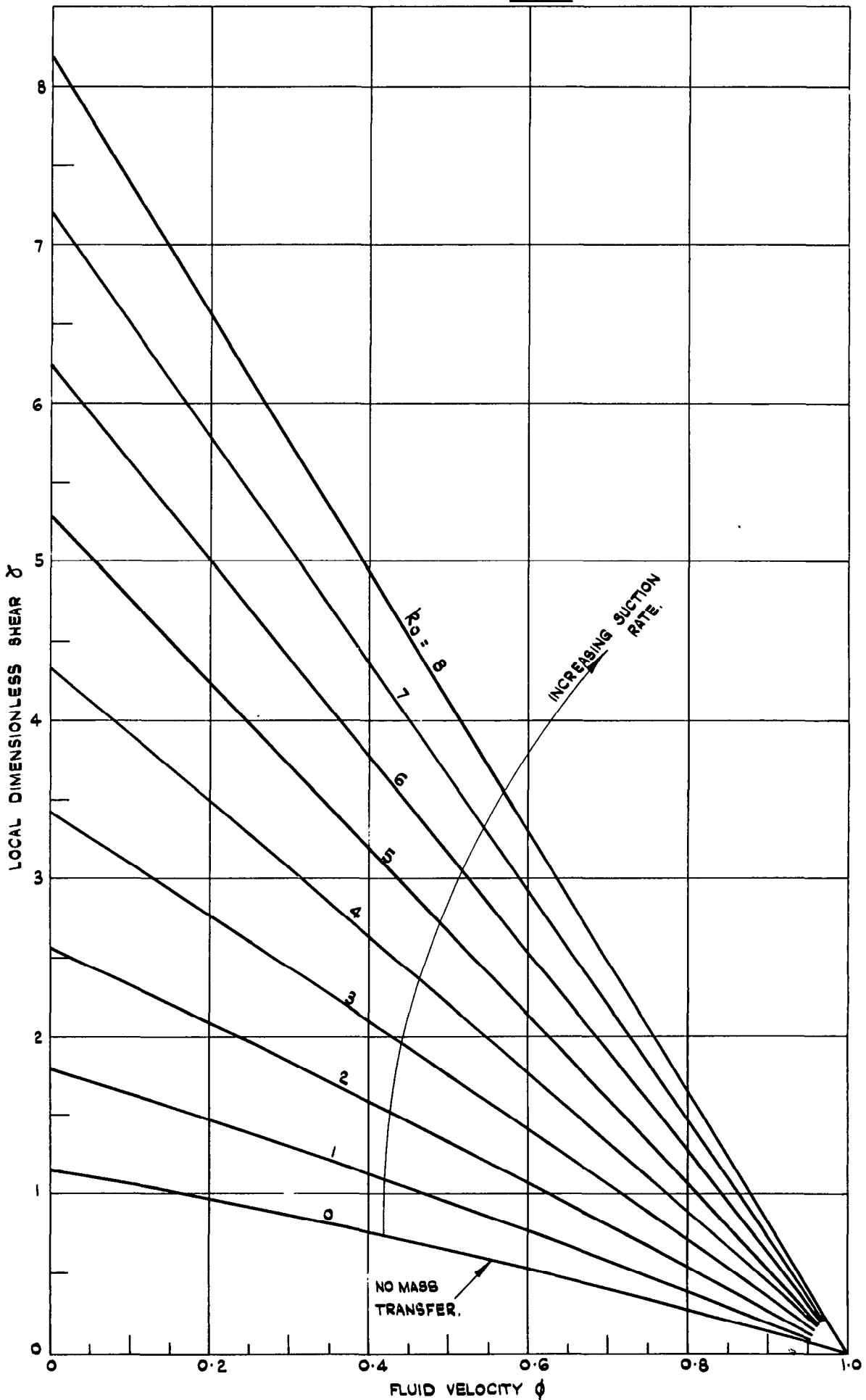
Solutions to equation (23) for various positive values of the mass

transfer parameter $\bar{k}_o$

FIG. 9
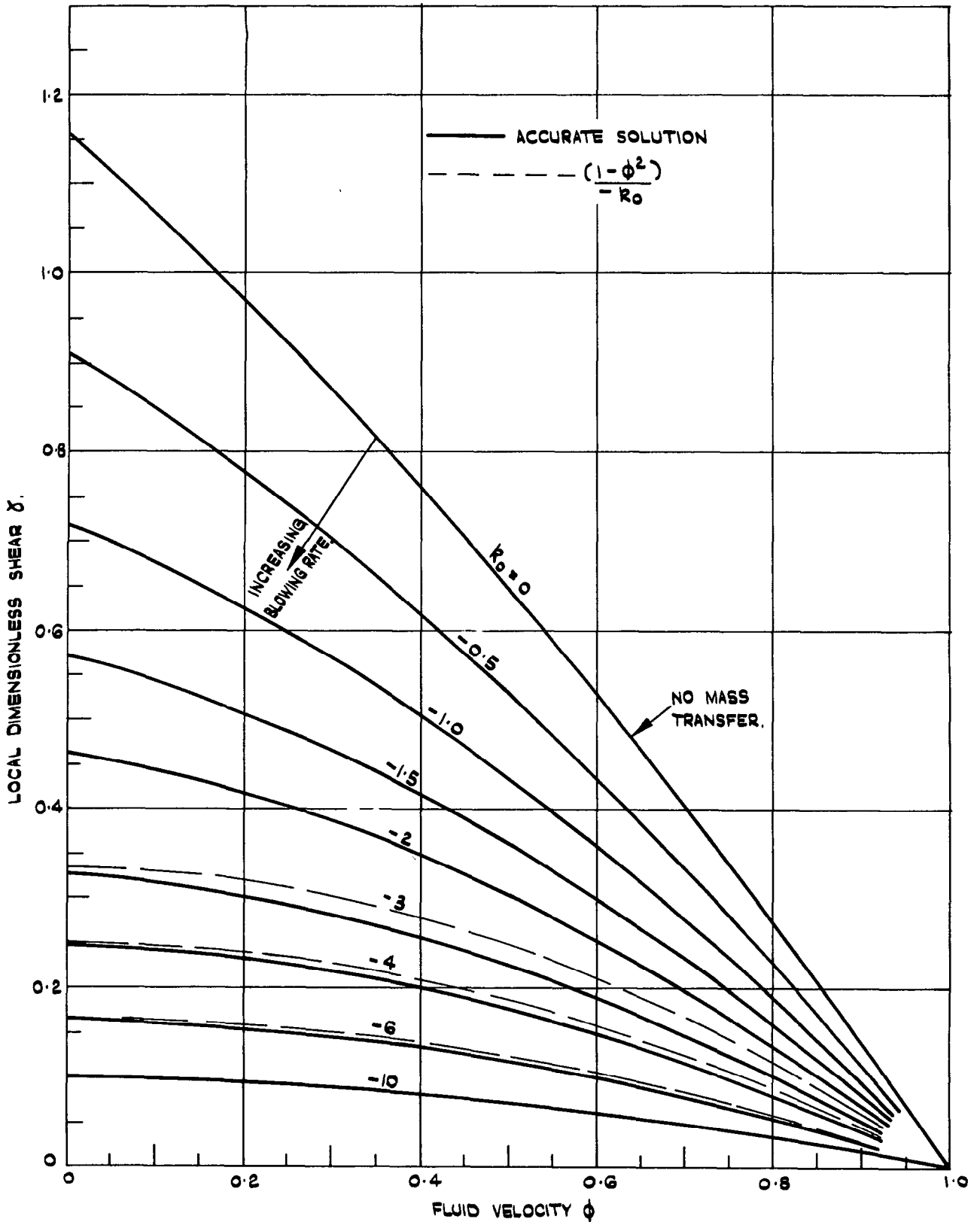
Solutions to equation (23) with blowing (k_o negative). The broken
lines show the asymptote for intensive blowing; to this scale the
asymptote coincides with the accurate solution for $k_o = -10$.
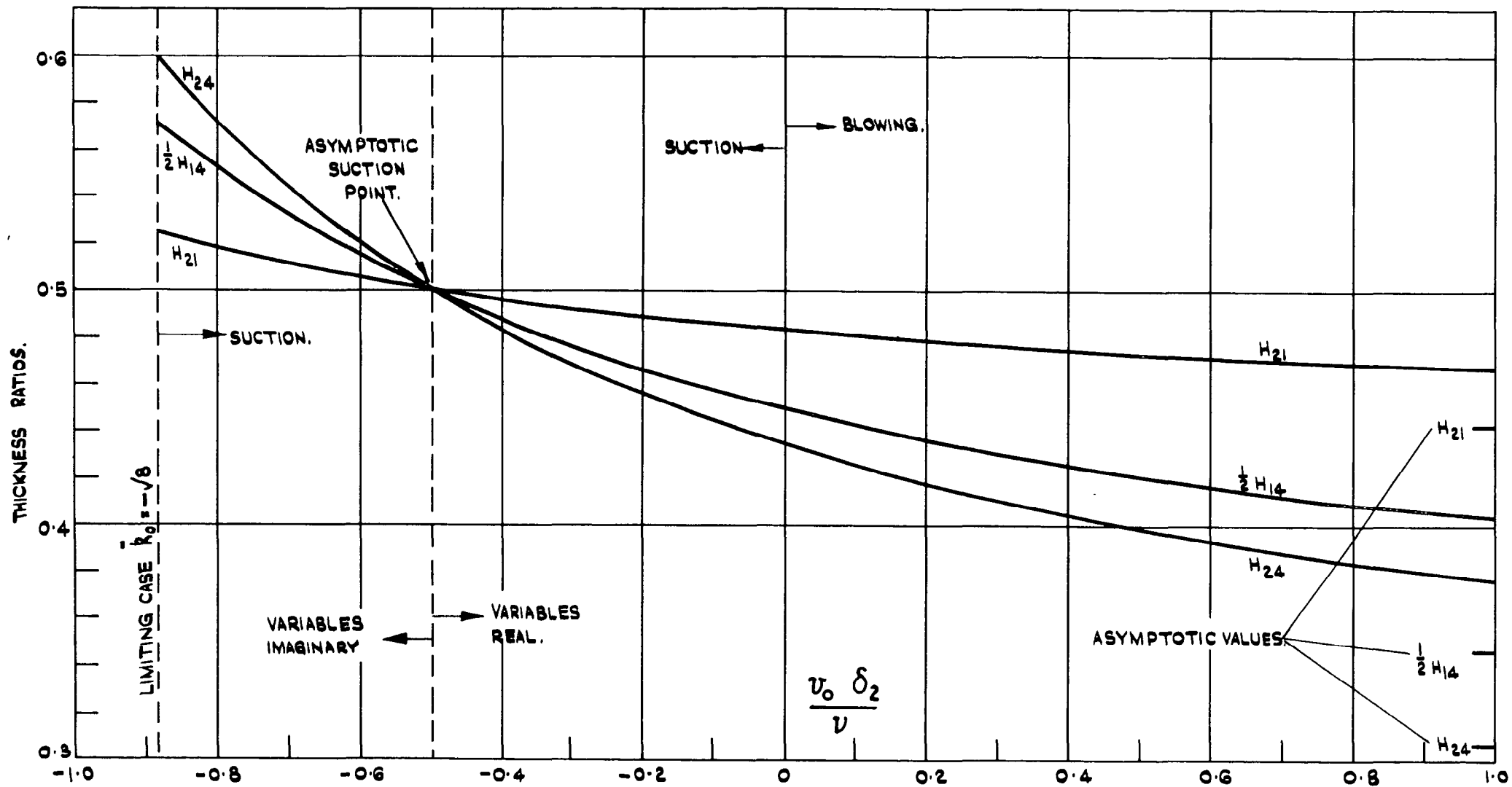
Variation of thickness ratios for $\beta = \pm\infty$ with suction and moderate blowing

FIG. 10

FIG. 11
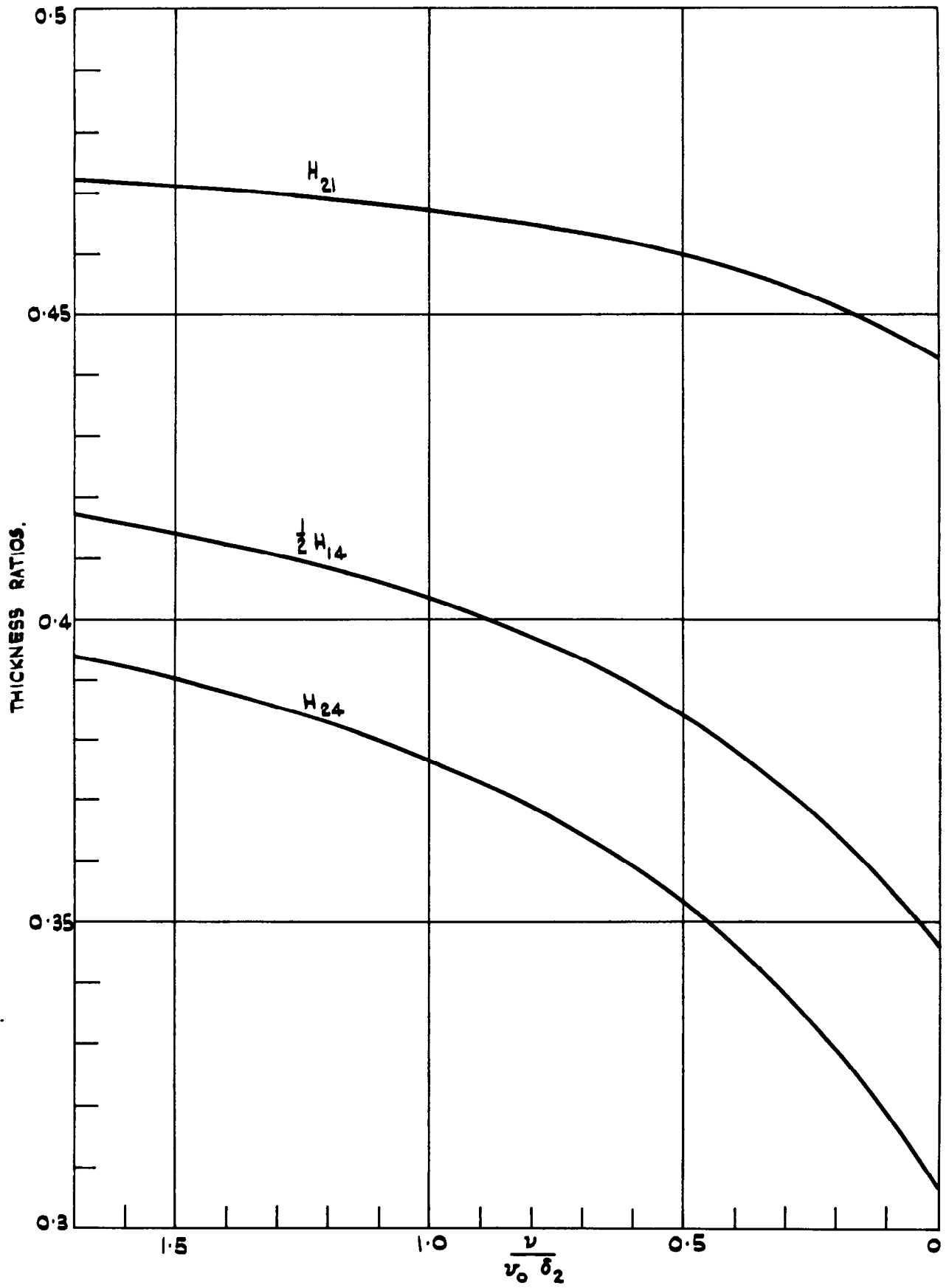
Variation of thickness ratios for $\beta = \pm\infty$ with intensive blowing
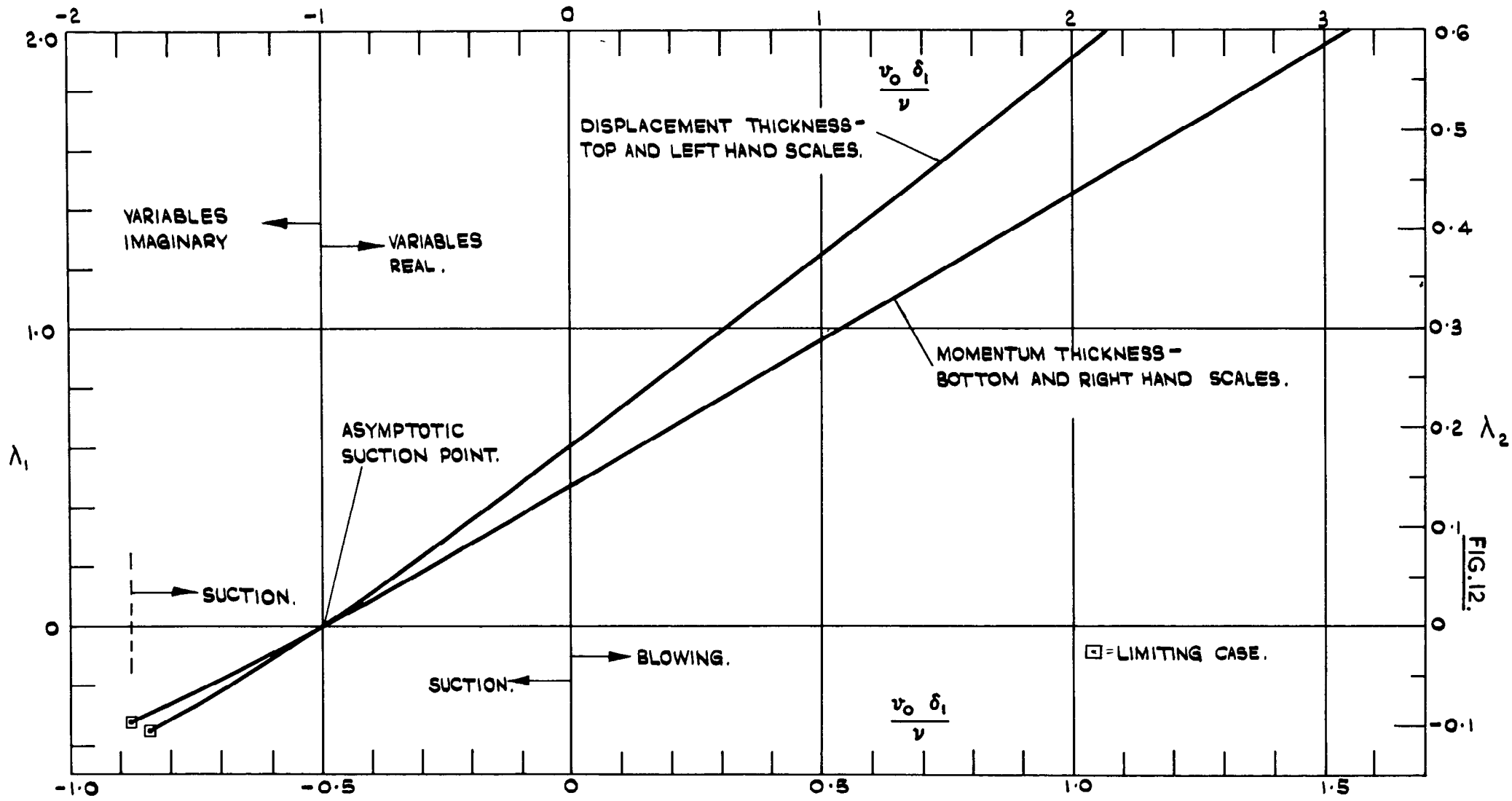
Pressure gradient parameters as functions of the associated mass transfer parameters for $\beta = \pm\infty$ with suction and moderate blowing
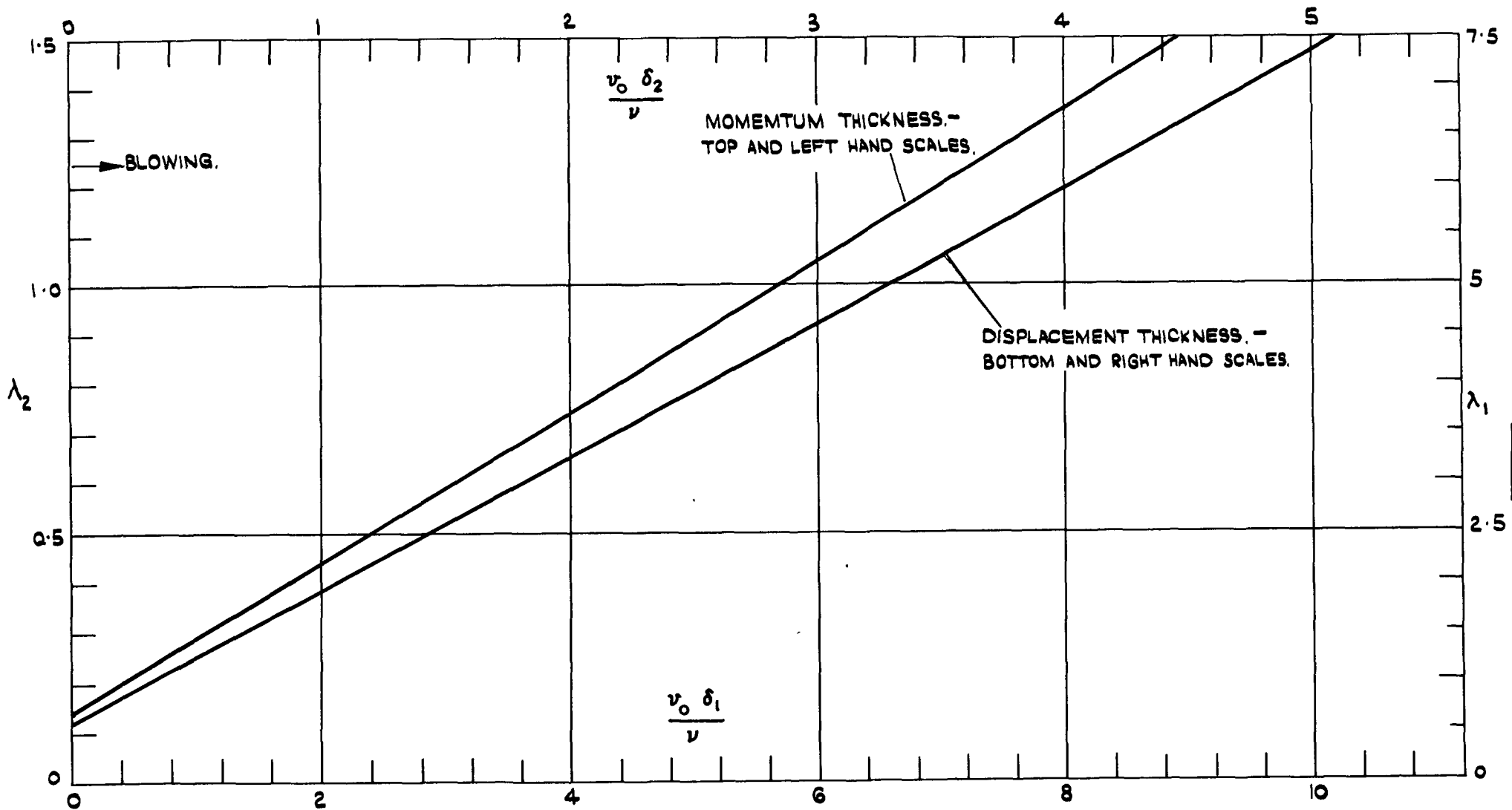
Pressure gradient parameters as functions of the associated mass transfer parameters for $\beta = \pm\infty$ with moderately

high blowing rates

FIG.14
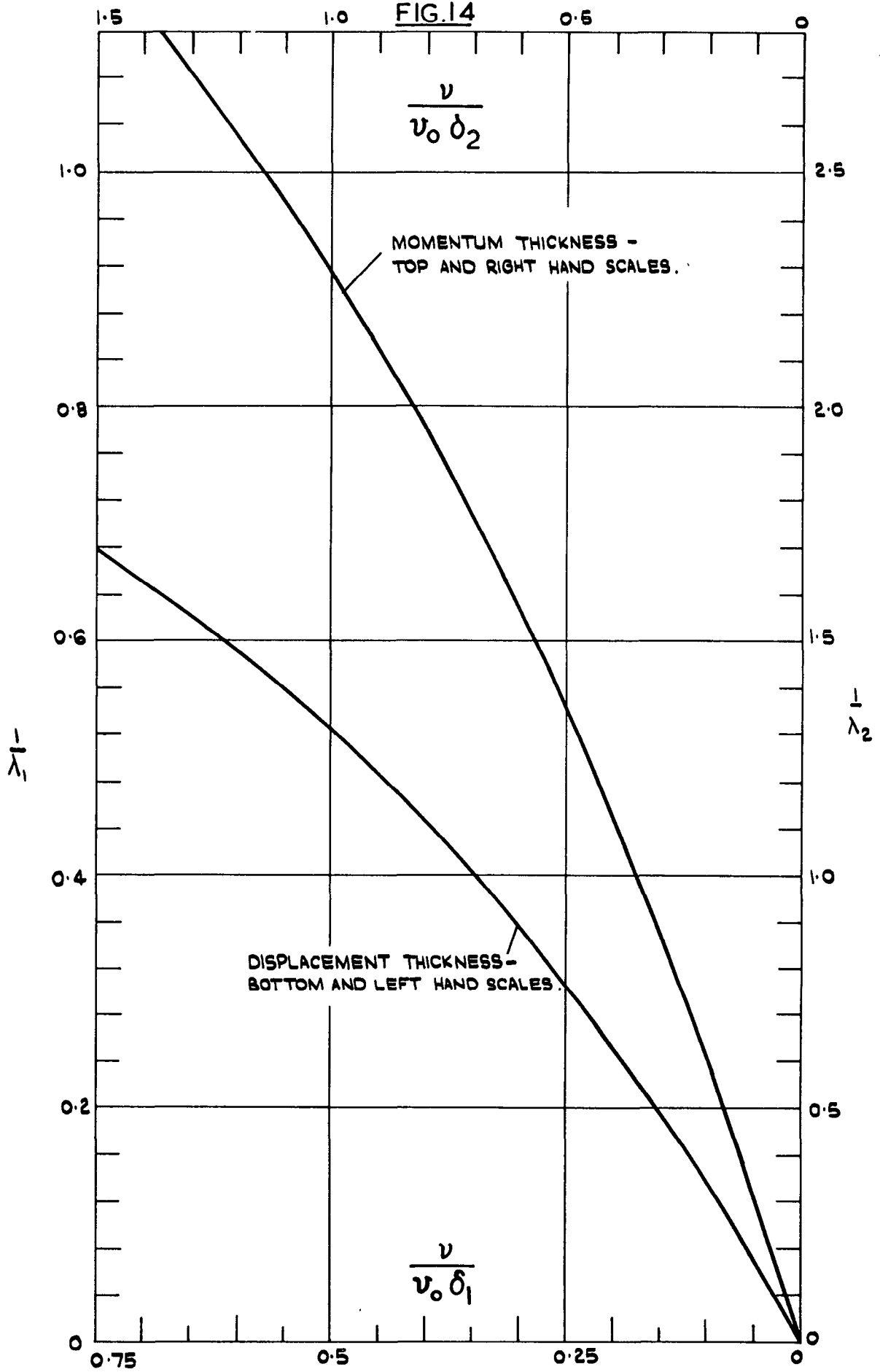
Pressure gradient parameters as a functions of the associated mass transfer parameters for $\beta = \pm \infty$ with intensive blowing

FIG 15
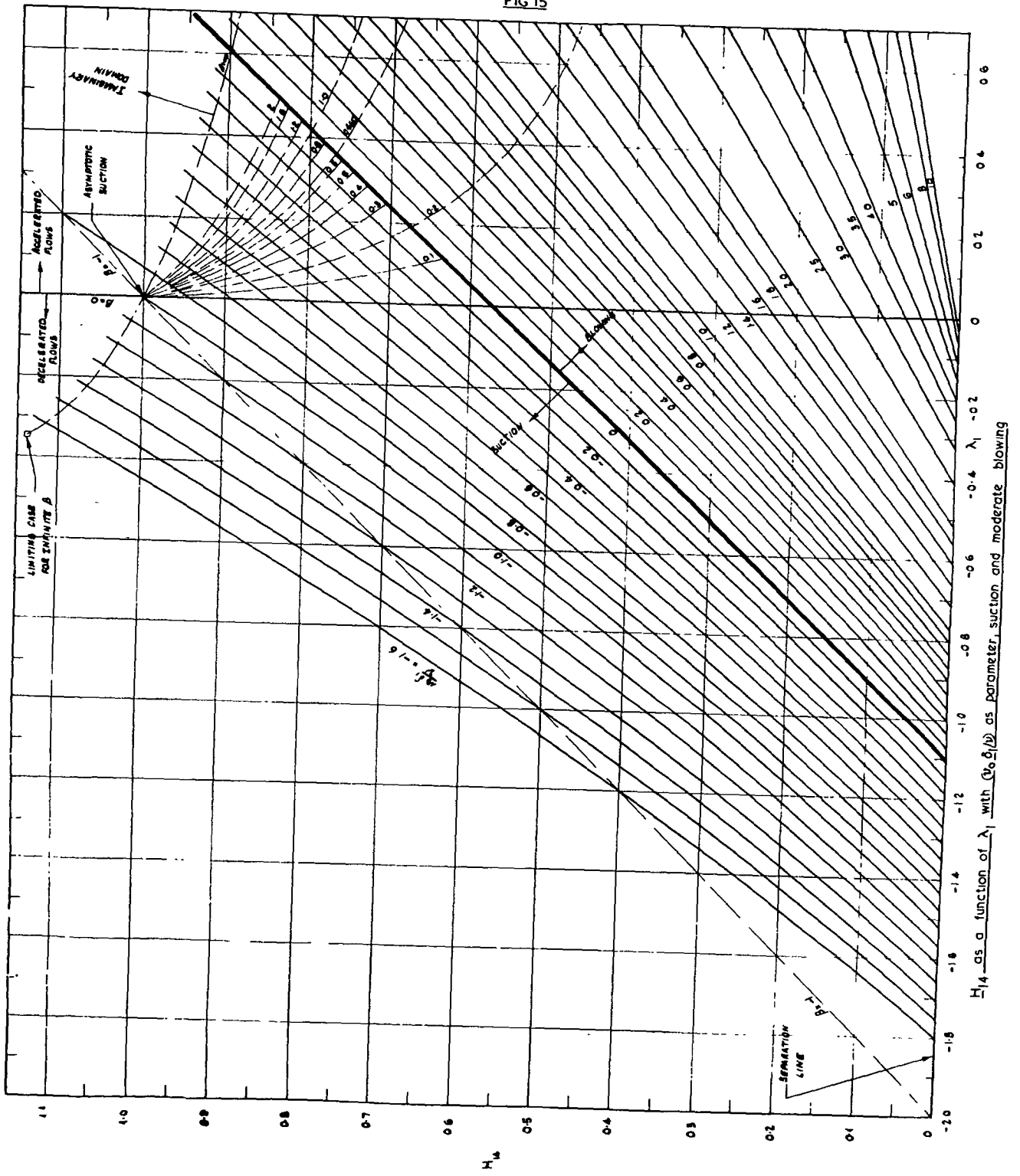
H_{14} as a function of λ_1 with $(v_0\,\delta_1/\nu)$ as parameter, suction and moderate blowing

FIG 16

H_{14} as a function of λ_1 with $(v_0 \delta_1 / v)$ as parameter, intensive blowing Circles denote known solution with values of $(v_0 \delta_1 / v)$ given alongside

FIG 17
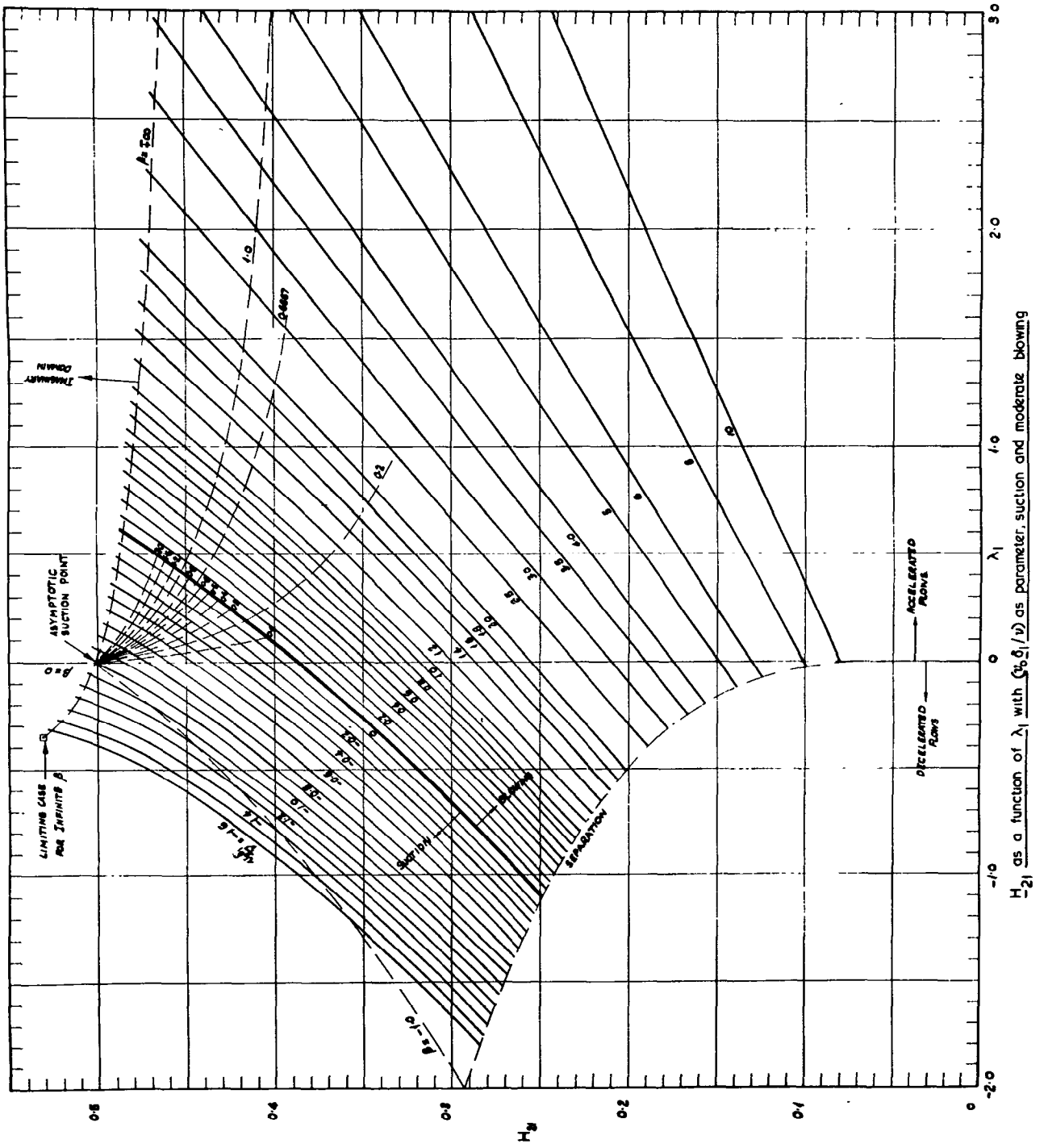
H_{21} as a function of λ_1 with $(v_0 \delta_{21}/\nu)$ as parameter, suction and moderate blowing

FIG 18
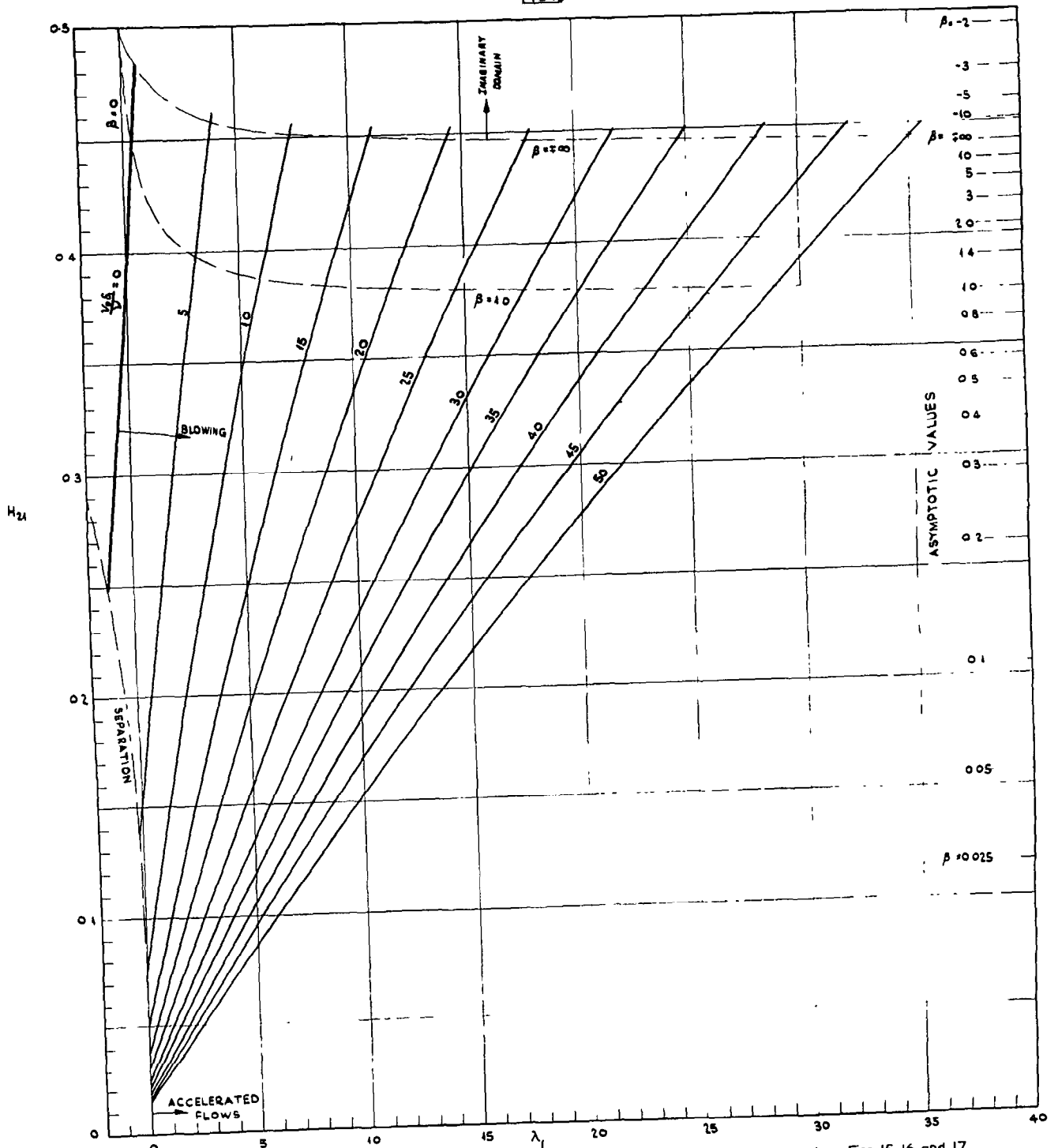
$\underline{H}_{21}$ as a function of λ_1 with $(y_o \delta_1 / v)$ as parameter This figure is less accurate then Figs 15,16 and 17

FIG 19

F_1 as a function of λ_1 with $(v_0 \delta_1 / v)$ as parameter, suction and moderate blowing

FIG 20
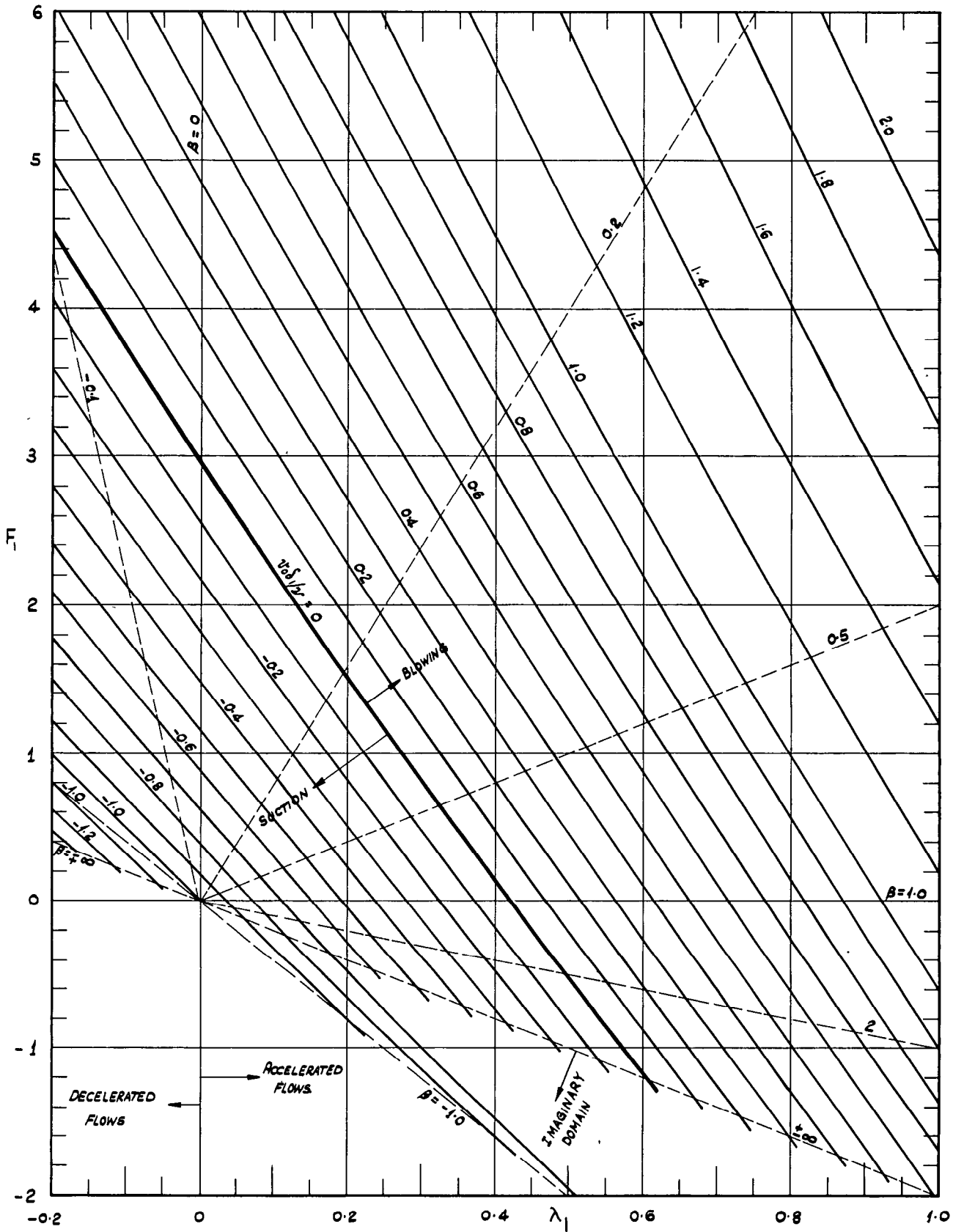
Part of Fig. 19 drawn to a larger scale

FIG. 21
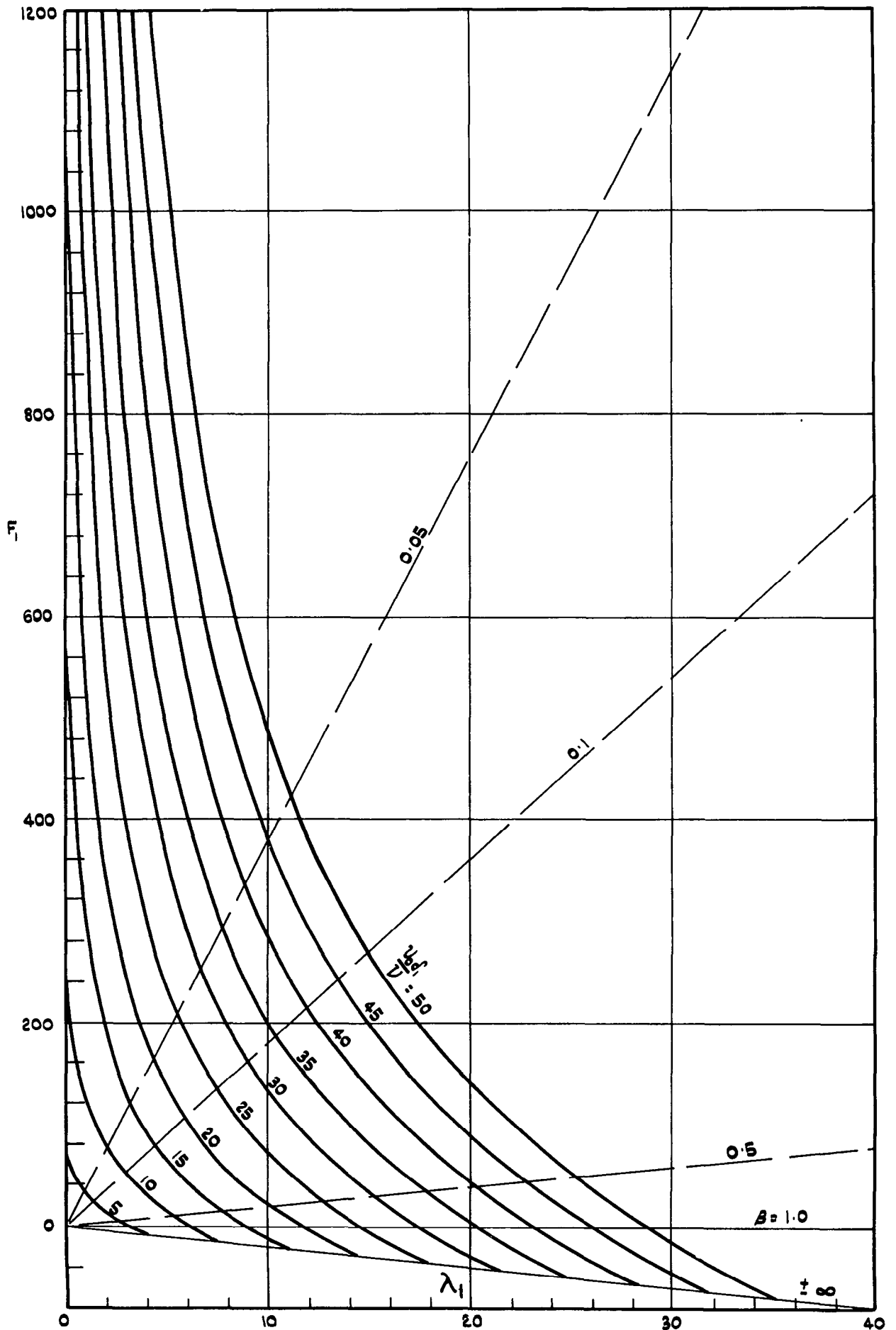
F_1 as a function of λ_1 with $(v_0 \delta_1 / v)$ as a parameter; intensive blowing.

Like Fig.18 this figure is not very accurate

FIG 22
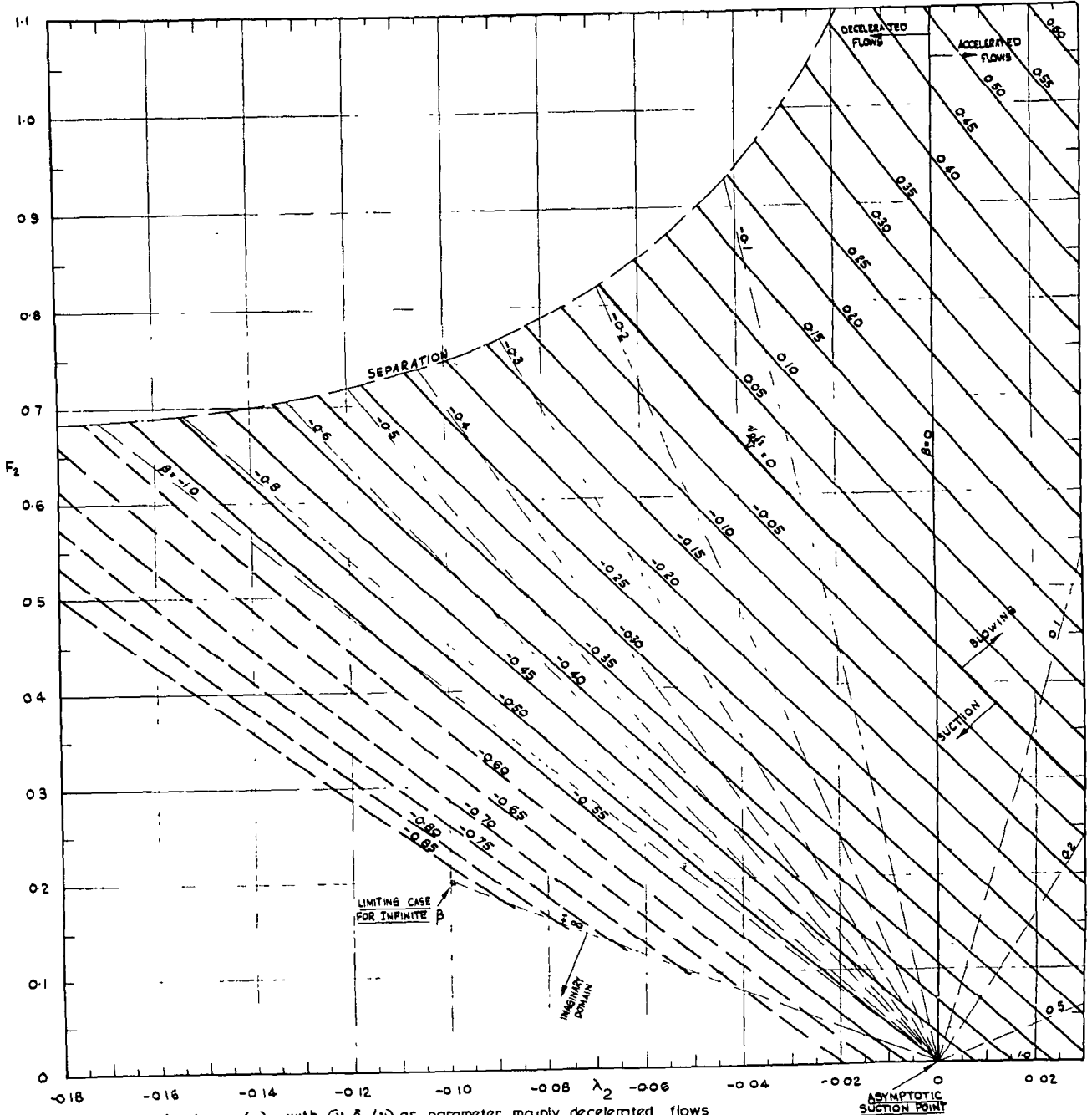
F_2 as a function of λ_2 with $(v_0 \delta_2/v)$ as parameter, mainly decelerated flows

FIG 23

H_{24} as a function of λ_2 with $(v_0 \delta_2/v)$ as parameter, mainly decelerated flow

FIG 24
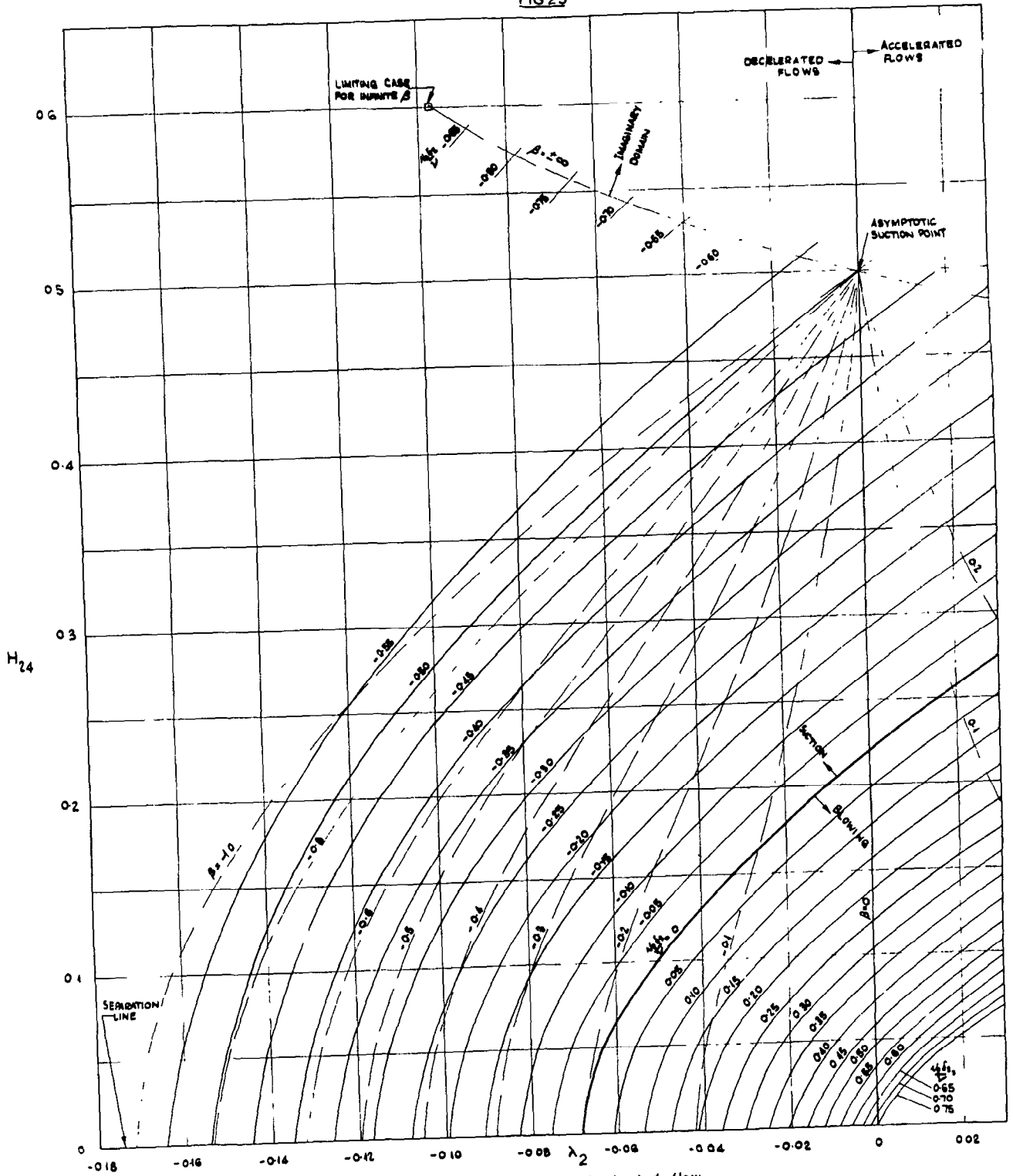
Intensive suction, F_2 as a function of λ_2 with $(v_0 \delta_2/v)$ as parameter

FIG 25
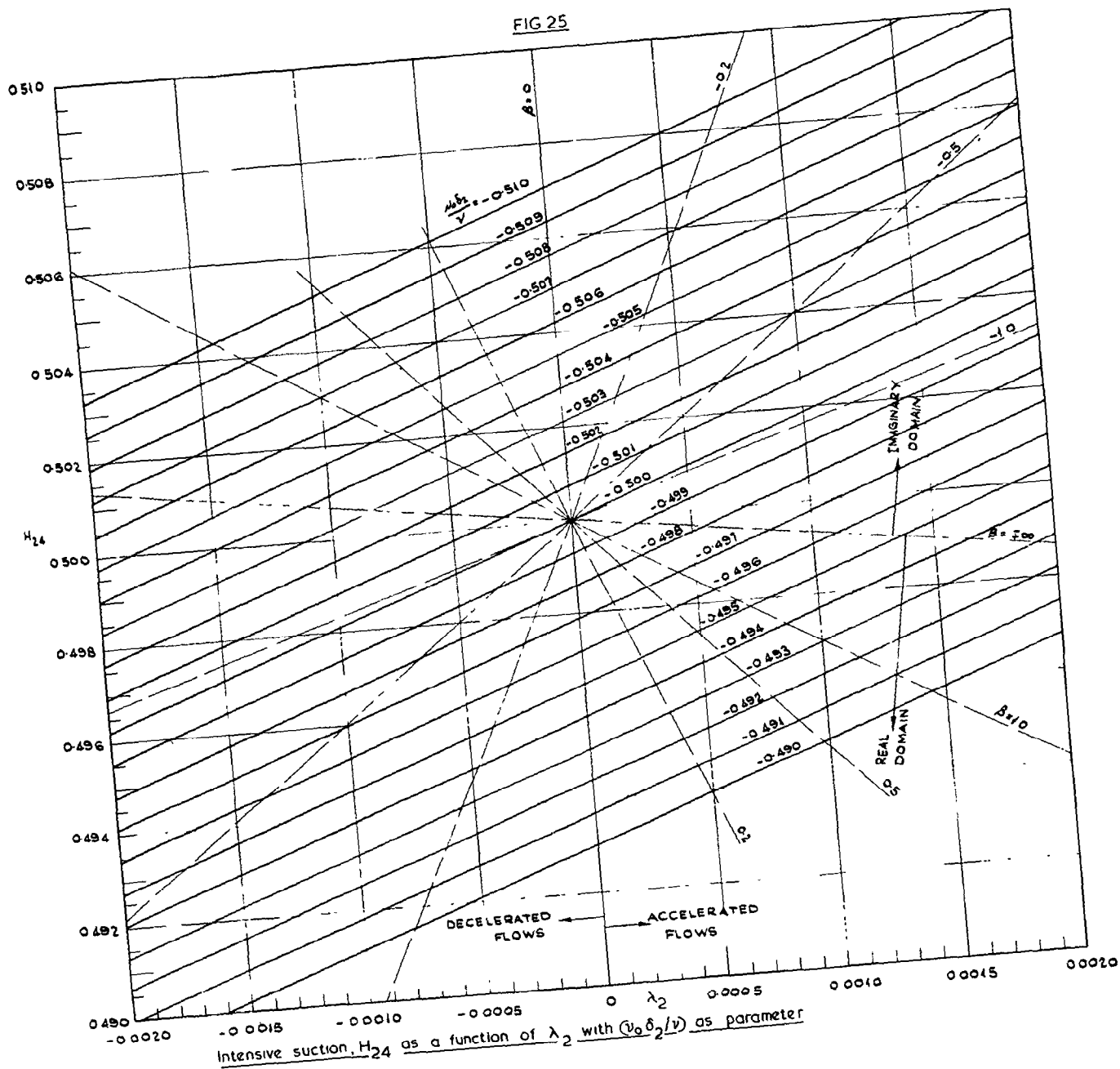
Intensive suction, H_{24} as a function of λ_2 with $(v_0 \delta_2/v)$ as parameter

FIG 26

Intensive suction, F_1 as a function of $(v_0\,\delta_1/v)$ as parameter.
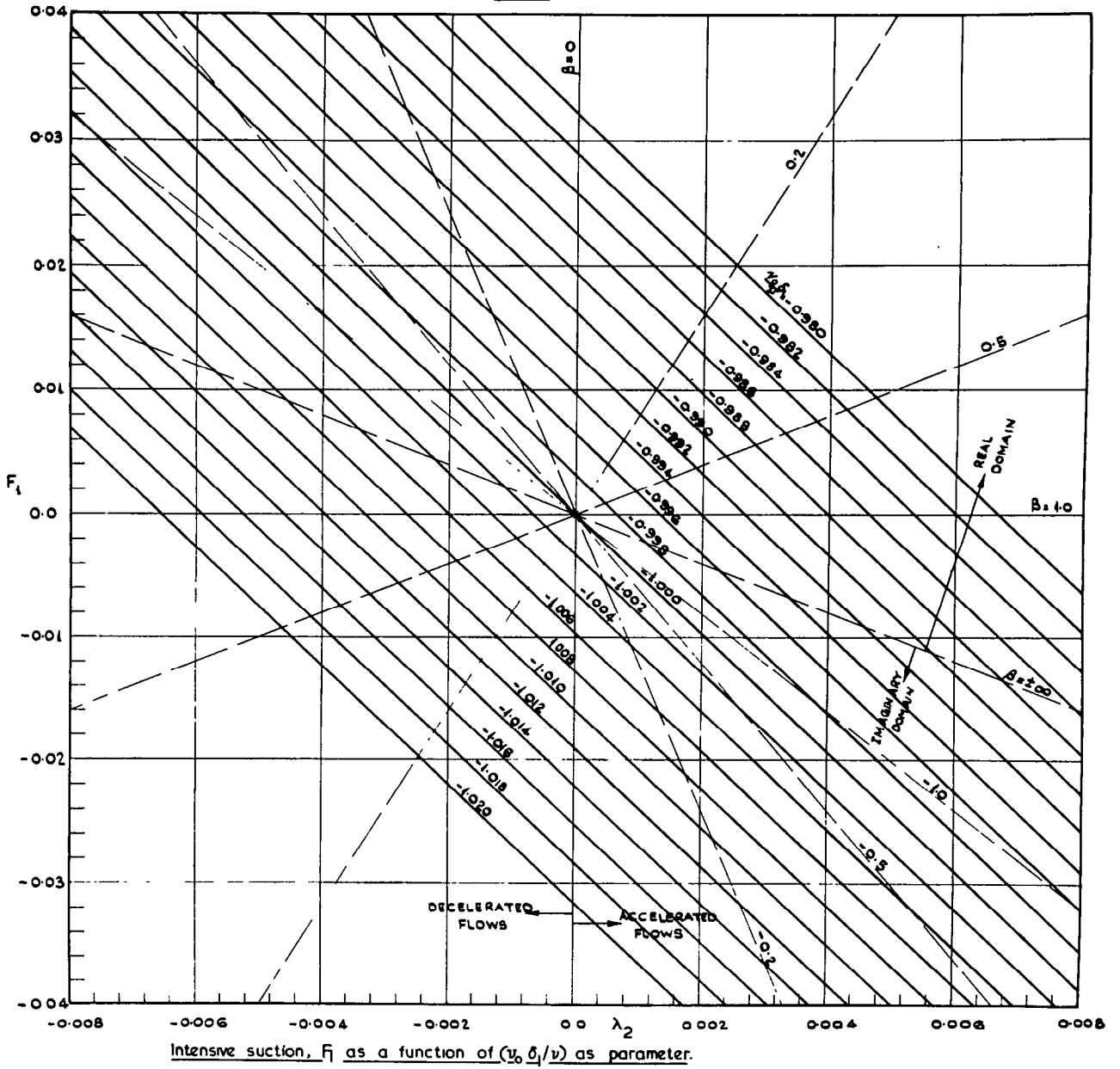
FIG 27
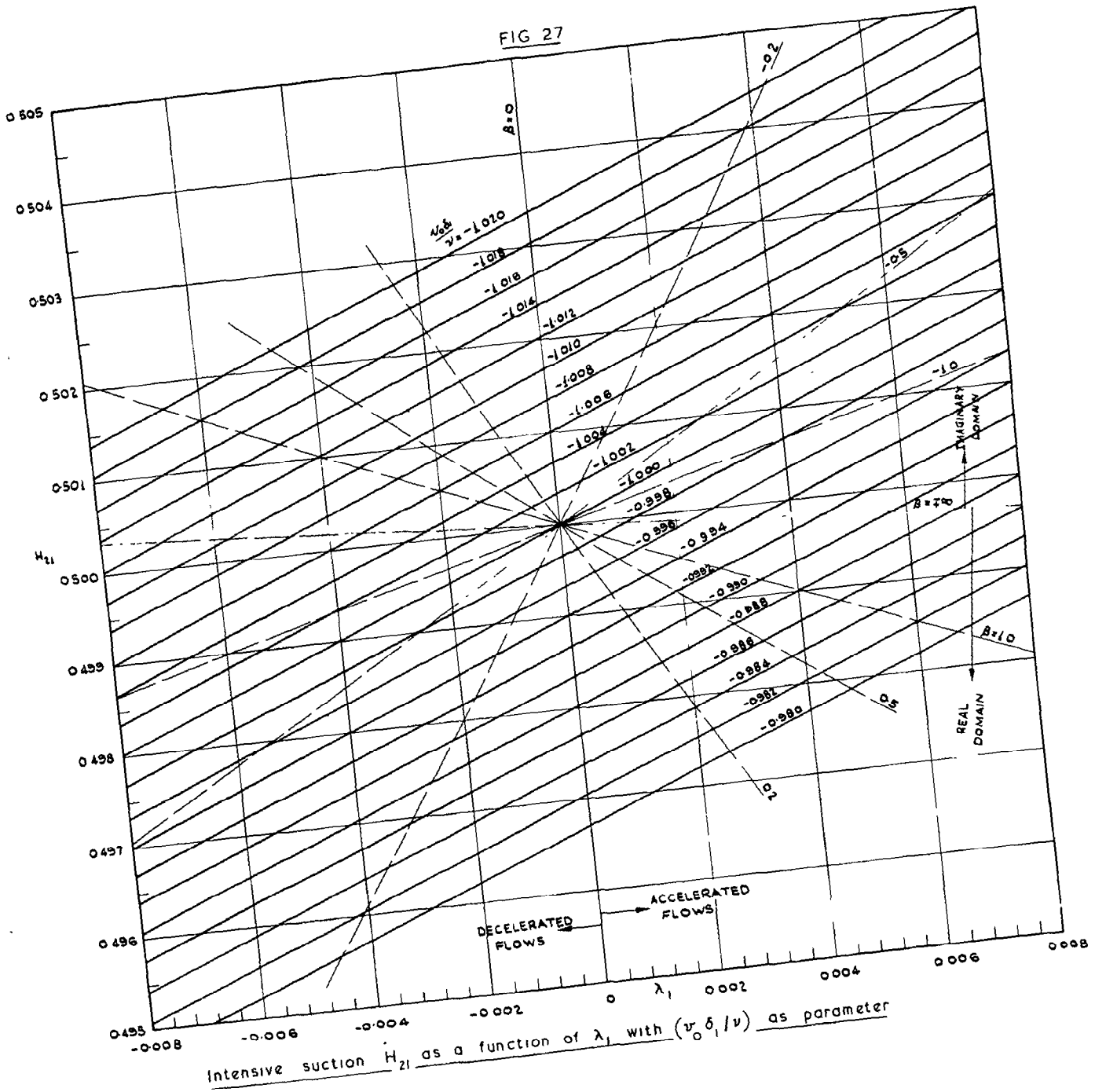
Intensive suction H_{21} as a function of λ_1 with $(v_o \delta_1/\nu)$ as parameter

FIG 28
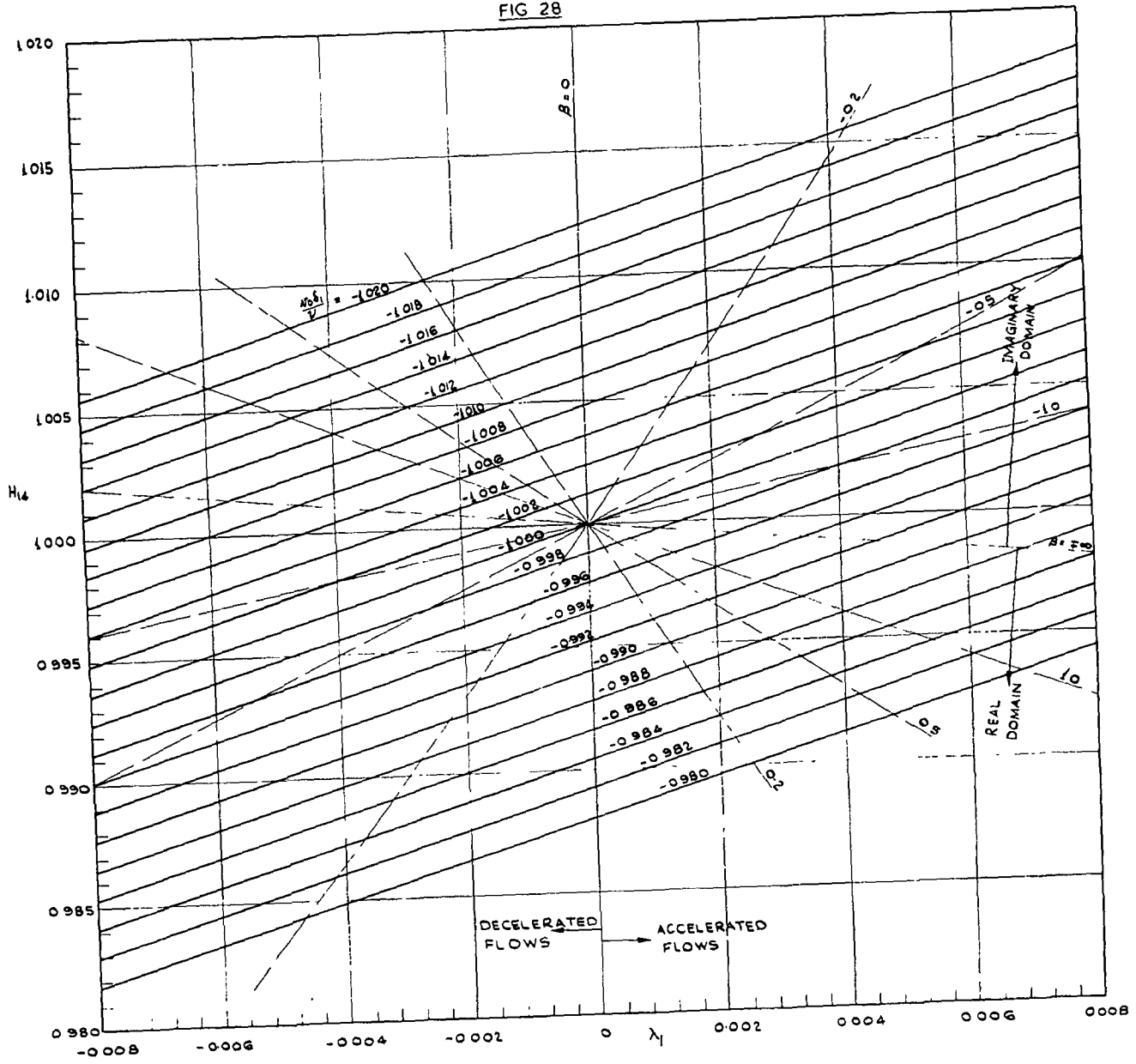
Intensive suction, H_{14} as a function of λ_1 with $(v_0 \delta_1/v)$ as parameter

FIG. 29
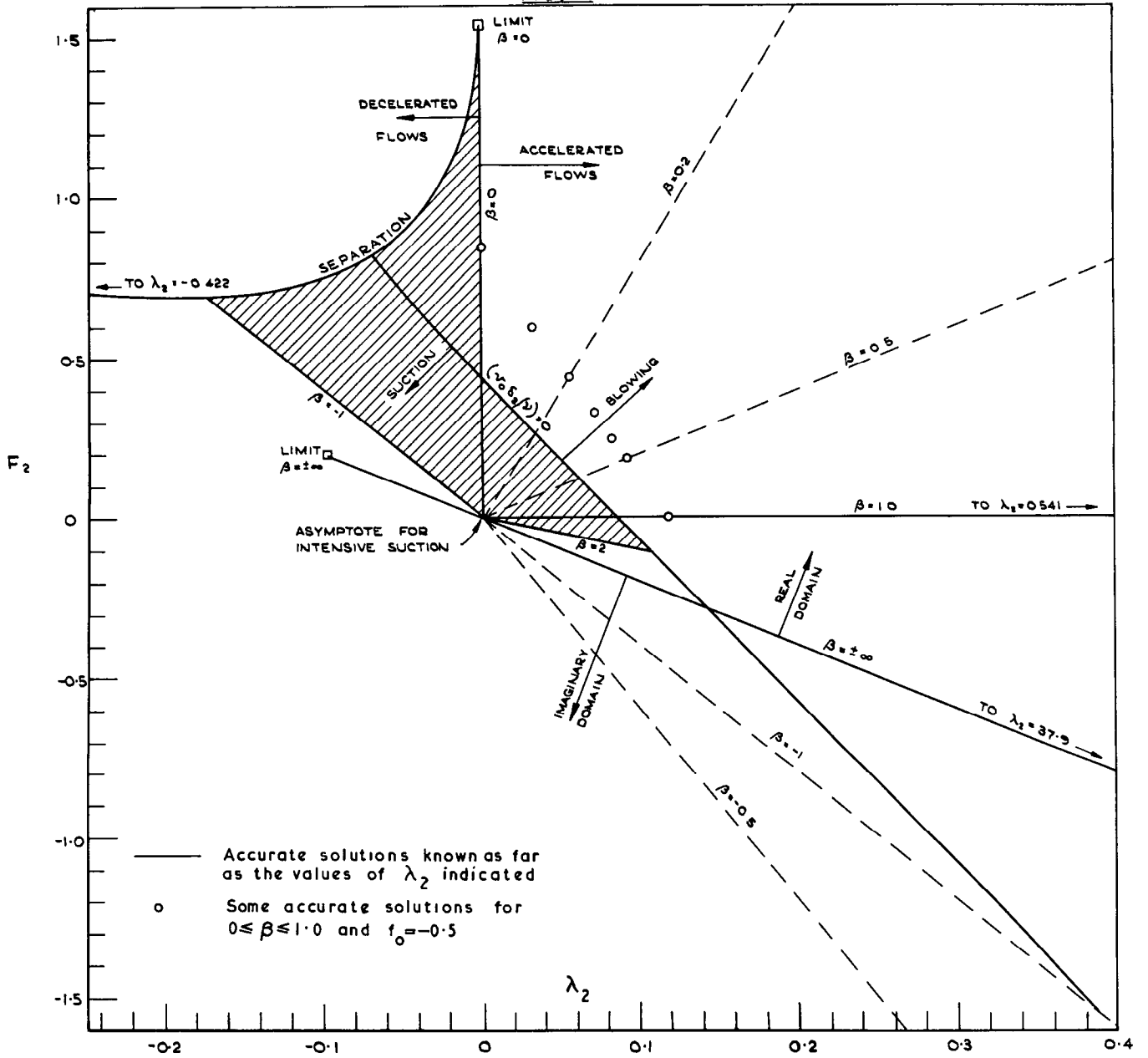
Showing diagrammatically the known accurate solutions to equation (12). Shaded region contains many accurate solutions

A.R.C. C.P. No.857
September, 1964
H. L. Evans, Imperial College

LAMINAR BOUNDARY LAYERS WITH UNIFORM FLUID PROPERTIES.
SIMILAR SOLUTIONS TO THE VELOCITY EQUATION
INVOLVING MASS TRANSFER

The report discusses solutions to the equation:
$$f''' + ff'' + \beta(1-f'^2) = 0$$
subject to the boundary conditions $f = f_0$, $f' = 0$ at $\eta = 0$ and $f' \to 1$ as $\eta \to \infty$. Numerical solutions are tabulated for wide ranges in the pressure gradient parameter β and mass transfer parameter f_0. Some related topics discussed are (i) the asymptotic behaviour of solutions for intensive mass transfer, (ii) the ranges of β and f_0 for which acceptable solutions exist and (iii) the application of these "similar" solutions to problems involving non-similar flows.